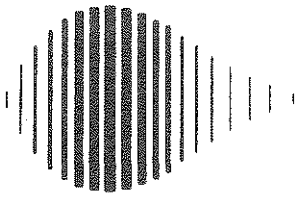

NATIONAL CENTER FOR EARTHQUAKE
ENGINEERING RESEARCH
State University of New York at Buffalo

EXPERIMENTAL STUDY AND ANALYTICAL PREDICTION OF EARTHQUAKE RESPONSE OF A SLIDING ISOLATION SYSTEM WITH A SPHERICAL SURFACE

by

A. S. Mokha, M. C. Constantinou and A. M. Reinhorn
Department of Civil Engineering
State University of New York at Buffalo
Buffalo, New York 14260

Technical Report NCEER-90-0020

October 11, 1990

This research was conducted at the State University of New York at Buffalo and was partially supported by the National Science Foundation under Grant No. ECE 86-07591.

NOTICE

This report was prepared by the State University of New York at Buffalo as a result of research sponsored by the National Center for Earthquake Engineering Research (NCEER). Neither NCEER, associates of NCEER, its sponsors, State University of New York at Buffalo, nor any person acting on their behalf:

a. makes any warranty, express or implied, with respect to the use of any information, apparatus, method, or process disclosed in this report or that such use may not infringe upon privately owned rights; or

b. assumes any liabilities of whatsoever kind with respect to the use of, or the damage resulting from the use of, any information, apparatus, method or process disclosed in this report.

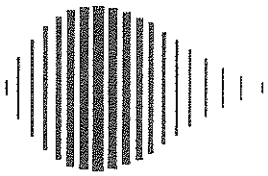

EXPERIMENTAL STUDY AND ANALYTICAL PREDICTION OF EARTHQUAKE RESPONSE OF A SLIDING ISOLATION SYSTEM WITH A SPHERICAL SURFACE

by

A.S. Mokha[1], M.C. Constantinou[2] and A.M. Reinhorn[3]

October 11, 1990

Technical Report NCEER-90-0020

NCEER Project Number 88-2002A

NSF Master Contract Number ECE 86-07591

1 Structural Engineer, Skimore, Owings and Merill, San Francisco, California, 94104. Formerly Research Assistant, Dept. of Civil Engineering, State University of New York at Buffalo

2 Associate Professor, Dept. of Civil Engineering, State University of New York at Buffalo

3 Professor, Dept. of Civil Engineering, State University of New York at Buffalo

NATIONAL CENTER FOR EARTHQUAKE ENGINEERING RESEARCH
State University of New York at Buffalo
Red Jacket Quadrangle, Buffalo, NY 14261

PREFACE

The National Center for Earthquake Engineering Research (NCEER) is devoted to the expansion and dissemination of knowledge about earthquakes, the improvement of earthquake-resistant design, and the implementation of seismic hazard mitigation procedures to minimize loss of lives and property. The emphasis is on structures and lifelines that are found in zones of moderate to high seismicity throughout the United States.

NCEER's research is being carried out in an integrated and coordinated manner following a structured program. The current research program comprises four main areas:

- Existing and New Structures
- Secondary and Protective Systems
- Lifeline Systems
- Disaster Research and Planning

This technical report pertains to Program 2, Secondary and Protective Systems, and more specifically, to protective systems. Protective Systems are devices or systems which, when incorporated into a structure, help to improve the structure's ability to withstand seismic or other environmental loads. These systems can be passive, such as base isolators or viscoelastic dampers; or active, such as active tendons or active mass dampers; or combined passive-active systems.

Passive protective systems constitute one of the important areas of research. Current research activities, as shown schematically in the figure below, include the following:

1. Compilation and evaluation of available data.
2. Development of comprehensive analytical models.
3. Development of performance criteria and standardized testing procedures.
4. Development of simplified, code-type methods for analysis and design.

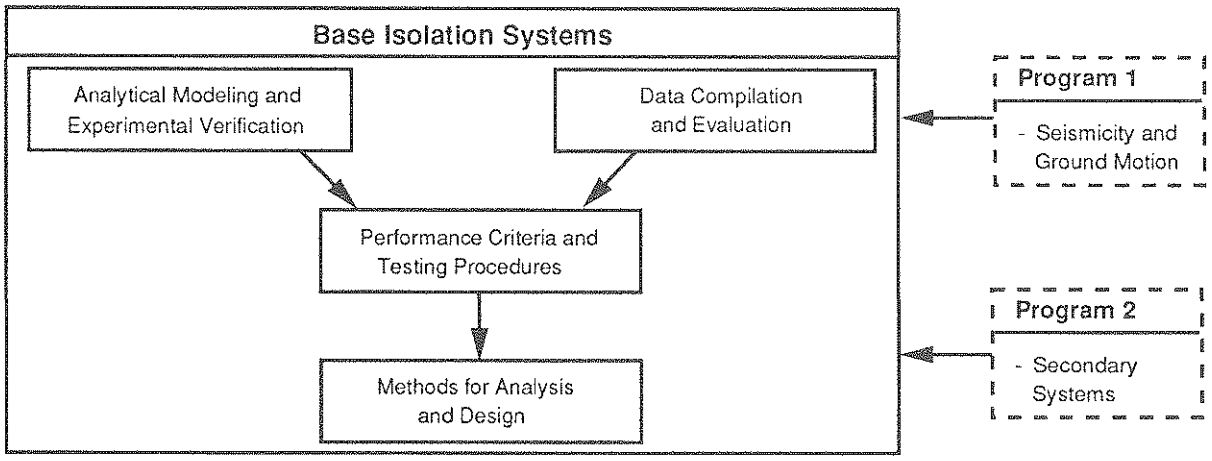

This report presents an evaluation of a sliding isolation system with a spherical surface. The study is part of a series of experimental and analytical investigations being carried out at the University at Buffalo on a variety of base isolation systems. The isolation system was tested in a six-story quarter-scale model structure on the shake table at the University at Buffalo. Test results showed an increased capacity of the structure to withstand earthquake forces while remaining undamaged. Experimental results confirmed that system response could be predicted by analytical techniques.

ABSTRACT

This report describes the results of an experimental study of the behavior of a sliding isolation system with a spherical surface installed in a flexible structure with large aspect ratio. A series of shake table tests was conducted and the results show a marked increase in the capacity of the structure to withstand earthquake forces, while undamaged, in comparison to the conventionally founded structure. Analytical techniques are used to predict the dynamic response of the system and the obtained results are in very good agreement with the experimental results.

ACKNOWLEDGEMENTS

The research reported herein was supported by the National Center for Earthquake Engineering Research under contract No. 88-2002A, the National Science Foundation under Grant No. CES-8857080 and by Earthquake Protection Systems, Inc.

TABLE OF CONTENTS

LIST OF ILLUSTRATIONS

LIST OF TABLES

SECTION 1
INTRODUCTION

Base isolation is a design technique for reducing the effects of earthquake motions on structures. This technique is becoming widely accepted. Currently, as many as ten building and bridge structures in the United States and forty buildings in Japan have been constructed or are under construction on some form of isolation system (Buckle 1986, Kelly 1988). Furthermore, several base-isolated structures have been constructed in New Zealand (Buckle 1986). Most of these structures utilize elastomeric isolation systems for earthquake protection. A 50,000 gallon emergency fire water tank in California and three buildings in Japan are protected by sliding isolation systems.

Sliding isolation systems utilize sliding interfaces (usually Teflon-steel interfaces) to support the weight of the structure. These interfaces provide little resistance to lateral loading by virtue of their low friction. Recentering capability is provided by a separate mechanism. In the three sliding isolated structures in Japan, this mechanism takes the form of cylindrical rubber springs (Mokha et al 1988 and 1990, Kelly 1988). In the isolated water tank in California, the sliding and recentering mechanisms are integrated in one unit in which the sliding surface takes a spherical shape. One isolation system with spherical surface carries the name **Friction Pendulum System (or FPS)** (Zayas et al 1987). It is the subject of the experimental study reported herein.

In the Friction Pendulum System, the isolated structure is supported by bearings. Each bearing consists of an articulated slider on a spherical concave chrome surface. The slider is faced with a bearing material which, when in contact with the polished chrome surface, results in a maximum sliding friction coefficient of the order of 0.1 or less at high velocity of sliding and a minimum friction coefficient of the order of 0.05 or less at very slow

velocity of sliding. This dependency of the coefficient of friction on velocity is a characteristic of Teflon type materials as described by Mokha et al, 1988 and 1990. The FPS bearing acts like a fuse which is activated only when the earthquake forces overcome the static value of friction. When set in motion, the bearing develops a lateral force equal to the combination of the mobilized frictional force and the restoring force which develops as a result of the induced rising of the structure along the spherical surface. This restoring force is proportional to the displacement and the weight carried by the bearing and is inversely proportional to the radius of curvature of the spherical surface. Accordingly, the system has the following important properties:

(1) Rigidity for forces up to the static value of coefficient of friction times the weight.

(2) Lateral force which is proportional to the weight carried by the bearing. As a result of this significant property the resultant lateral force develops at the center of mass, thus eliminating eccentricities. This property has been confirmed in shake table tests by Zayas et al, 1987.

(3) Period of vibration in the sliding mode which is independent of the mass of the structure and related only to the radius of curvature of the spherical surface.

In addition to the above mentioned properties, the Friction Pendulum System has other properties common to sliding isolation systems, like low sensitivity to the frequency content of excitation and high degree of stability (Mokha et al 1988, Constantinou et al 1990, Su et al 1989, Mostaghel and Khodaverdian 1987).

An experimental study of the Friction Pendulum System, reported by Zayas et al, 1987, has been carried out with a two-story model in which the bearings were mounted on top of the first story columns. The properties of the model structure were varied so that a wide

range of structural flexibilities and distribution of mass and stiffness were obtained. The results confirmed the theoretically predicted properties of the system.

The main purpose of the research reported in this report was to investigate the feasibility of the Friction Pendulum System in isolating taller buildings with large aspect ratio. For this purpose, shake table tests were performed on a 1/4-scale artificial mass simulation model of a six-story steel moment-resisting frame in which the ratio of height to maximum distance between bearings was 2.25. The model was subjected to several simulated earthquake motions of significantly different frequency content and of peak acceleration of up to 1g. In all tests, the model frame remained elastic with peak interstory drift restricted to values less than 0.005 times the story height. The same drift was obtained in fixed-base tests with peak table acceleration of only 0.1g.

In the conducted tests, two new bearing materials were used, a material called Techmet-B and a woven Teflon fabric composite. Both materials exhibit a coefficient of friction which depends on the velocity of sliding. This property appears to be important in theoretical predictions of the behavior of the system. A mathematical model of friction which is appropriate for these materials (Constantinou et al, 1990) is employed in the analysis of the tested system and the obtained results are in excellent agreement with the experimentally obtained results.

SECTION 2
TEST STRUCTURE

The shake table experiments were carried out with a model that represents a section in the weak direction of a typical steel moment-resisting frame at approximately quarter scale. The model is six-story with three bays (Figure 2-1). Concrete blocks were used to add mass as necessary for similitude requirements bringing the model weight to 51.4 Kips (229.2 kN). The distribution of weight was approximately as follows: 7.65 Kips (34.1 kN) at the sixth floor, 7.84 Kips (34.9 kN) at the fifth to first floor and 4.56 Kips (20.3 kN) at the base (W14 x 90 sections). The columns were bolted to two heavy W14x90 sections and the bearings were placed between these beams and the shake table.

The natural frequencies, damping ratios and mode shapes of the model structure under fixed base conditions were determined experimentally and are listed in Table 2-I. The identification tests were carried out on the shake table using as input a banded (0-50Hz) white noise of 0.04g peak acceleration. The structural parameters were identified from the absolute acceleration transfer functions of the six floors of the model using modal identification techniques (Reinhorn et al, 1989).

The model structure was analyzed using a commercial finite element program (GTSTRUDL). A three dimensional frame model was used which was subsequently condensed to one having only six degrees of freedom, corresponding to the displacement of each of the six floors of the structure. The analytically determined frequencies and mode shapes are listed in Table 2- I. These quantities compare quite closely with the experimental frequencies and mode shapes. In general, the analytical frequencies are lower than the experimental ones indicating that the structure is actually stiffer than the theory predicted.

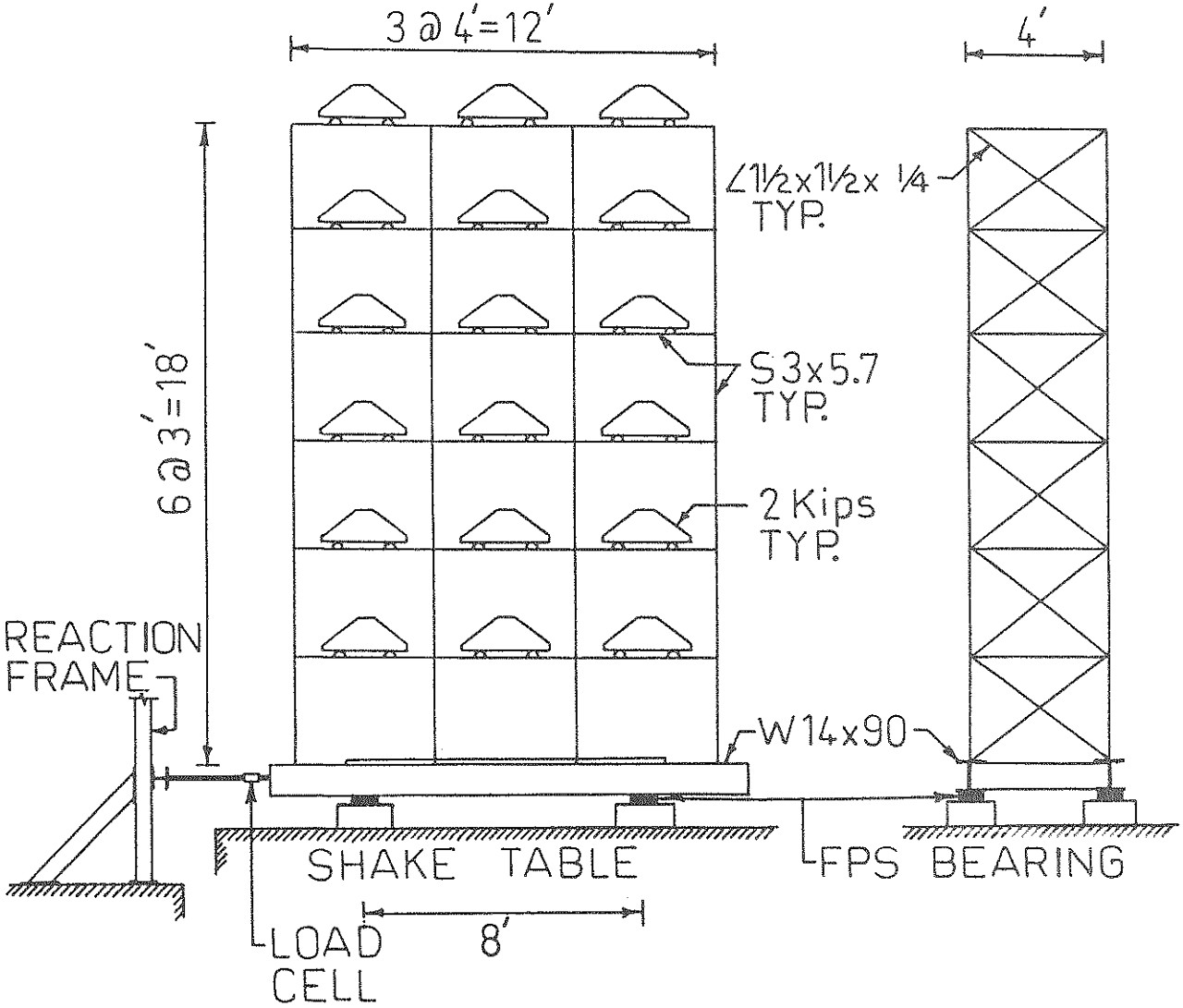

Figure 2-1 Six-Story Steel Test Structure (1ft = 304.8mm).

Table 2-I - Characteristics of Structure Under Fixed Base Conditions
(Value in Parenthesis is Analytical)

Mode (1)	Frequency Hz (2)	Damping Ratio (3)	Mode Shape (4)					
			Floor 1	Floor 2	Floor 3	Floor 4	Floor 5	Floor 6 (top)
1	2.34 (2.14)	0.0142	0.214 (0.164)	0.437 (0.395)	0.632 (0.611)	0.797 (0.791)	0.921 (0.923)	1 (1)
2	7.76 (7.72)	0.0204	0.563 (0.520)	1 (1)	0.900 (0.956)	0.326 (0.386)	-0.423 (-0.401)	-0.997 (-0.996)
3	13.28 (12.04)	0.0235	0.822 (0.804)	0.750 (0.863)	-0.248 (-0.230)	-1 (-1)	-0.435 (-0.383)	0.850 (0.817)
4	19.04 (17.98)	0.0155	1 (1)	-0.010 (0.104)	-0.827 (-0.996)	0.283 (0.240)	0.639 (0.908)	-0.461 (-0.619)
5	24.80 (24.02)	0.0059	0.739 (1)	-0.851 (-0.769)	0.229 (-0.027)	0.708 (0.805)	-1 (-0.946)	0.425 (0.397)
6	28.92 (28.82)	0.0086	0.515 (0.679)	-0.850 (-0.919)	1 (1)	-0.902 (-0.879)	0.605 (0.580)	-0.209 (-0.196)

SECTION 3
INSTRUMENTATION

The instrumentation consisted of accelerometers and sonic displacement transducers which were placed at each floor to measure the horizontal acceleration and displacement of that floor with respect to a stationary reference frame. At the sixth and third floors and at the base of the structure, accelerometers and displacement transducers were placed at both sides of the model in order to measure any torsional motion of the model. Accelerometers were also placed above the bearings, to measure vertical acceleration and help determine whether the model uplifted from its supports.

Figure 3-1 shows the instrumentation of the structure. All displacement transducers measure displacements of the model in the testing direction (longitudinal direction). Accelerometers were placed as shown in Figure 3-1 to measure longitudinal, transverse and vertical accelerations at selected points of the structure. A total of 35 channels of data were recorded of which 30 channels are shown in Figure 3-1 and another five channels (not shown) recorded the shake table motion. Furthermore, two more channels of data recorded forces in two load cells used in determining the properties of the isolation bearings as described in sequel.

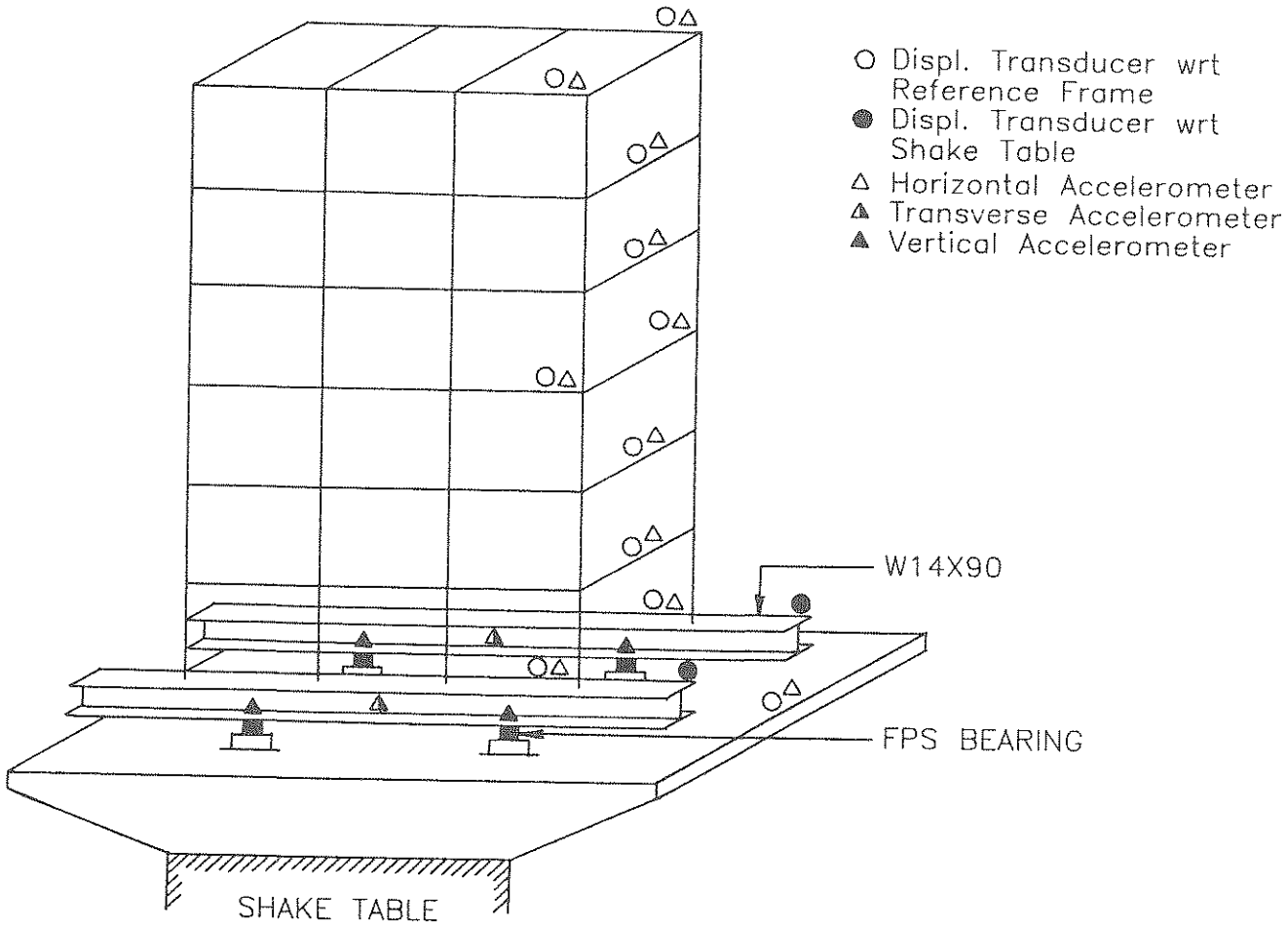

Figure 3-1 Instrumentation Diagram of Test Structure.

SECTION 4
ISOLATION SYSTEM

The isolation system consisted of four FPS bearings which were placed under the base of the model at 8 feet (2.44m) distance as shown in Figure 2-1. In this configuration, the aspect ratio of height of model to distance between bearings is 2.25.

The bearing design is shown in Figure 4-1. The bearing consists of an articulated slider on a polished chrome concave surface of radius of curvature, R, equal to 9.75 inches (247.65mm). The spherical cavity housing the articulated slider is faced with a low friction material. The side of the slider in contact with the polished concave surface is faced with a bearing material. Two different bearing materials were used:

(1) A material which carries the trade name Techmet-B (product of Oiles Industry Co., Japan). Average pressure at the sliding interface was about 7 Ksi (48.3 MPa). Under these conditions, this material exhibited a higher coefficient of friction than the high load woven Teflon fabric.

(2) A form of woven Teflon with reinforcing fibers to provide high load carrying capacity. In this case, the Teflon fabric was backed by a thin steel plate of smaller dimensions than the slider (which has a diameter of 1.5 inches or 38.1 mm) so that the average pressure at the interface under the load of the model was about 20 Ksi (138 MPa).

Figure 4-2 shows a photograph of the FPS bearing with material Techmet-B prior to installation. Figure 4-2a shows the two parts of the bearing (spherical surface at right and articulated slider at left) and Figure 4-2b shows in more detail the bearing material facing the articulated slider. The material was bonded to a thin metal plate and screwed to the slider.

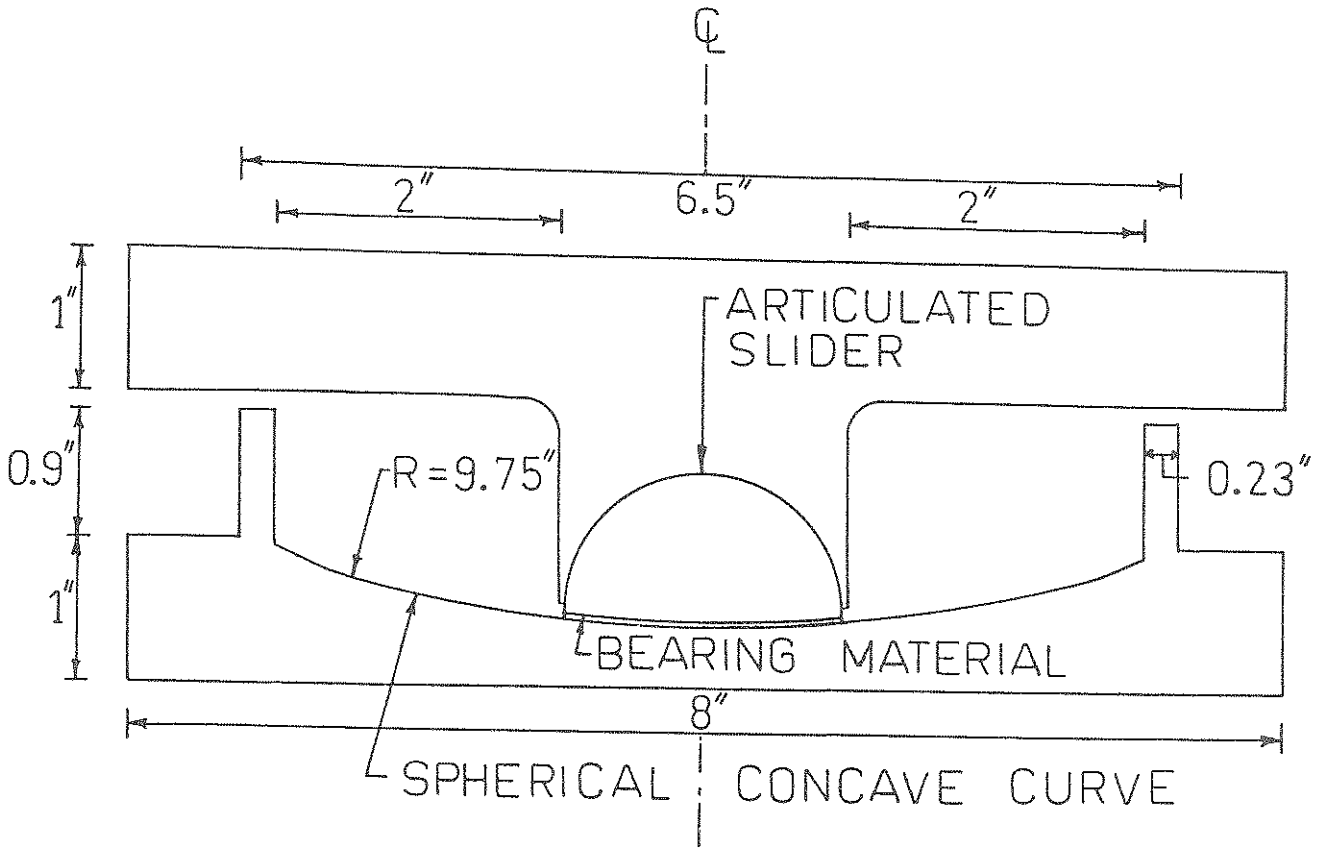

Figure 4-1 Friction Pendulum System Bearing Design (1 inch = 25.4mm).

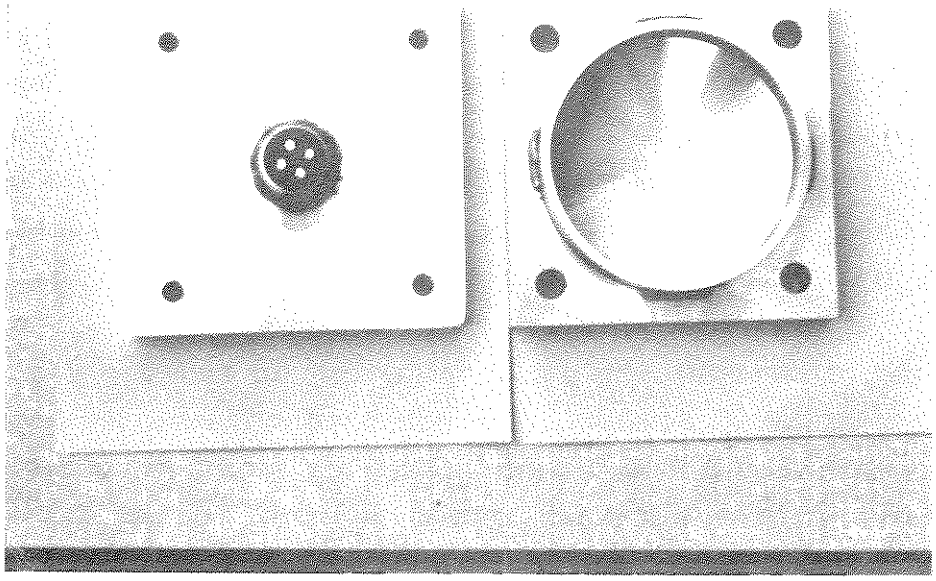

4a

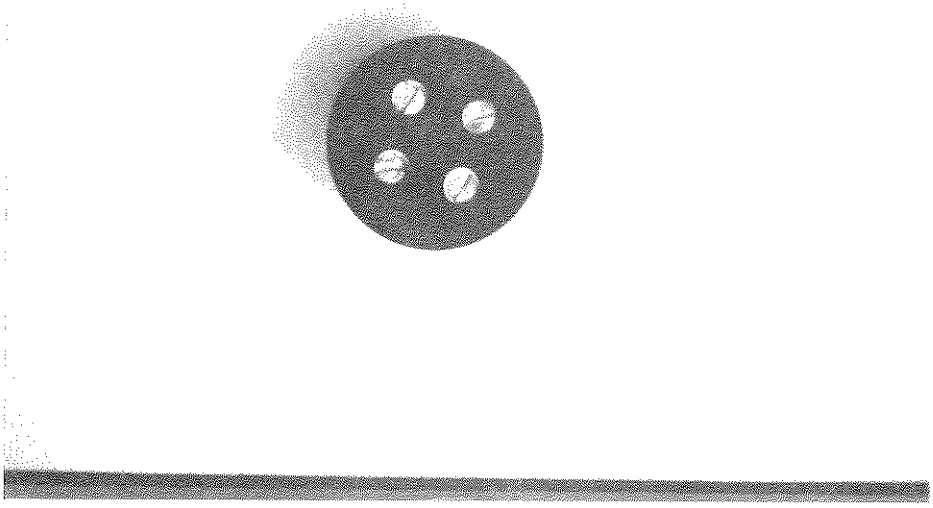

4b

Figure 4-2 Photograph of FPS Bearing and Detail of Articulated Slider. Material Techmet-B is Screwed on Slider.

An interesting complication developed as a result of the high stiffness of the beams (W14x90 sections) forming the base of the model. Prior to testing the FPS system, another isolation system consisting of flat sliders, was tested. The flat sliders were placed on top of axial load cells which were raised with a system of leveling plates and bolts until all four sliders were subjected to the same load. In this position the load cells were bolted to the shake table and grouted. The load cells were flexible in the horizontal direction and plates were welded all around, reducing them to simple pedestals as shown in Figure 2-1. To install the FPS bearings, the model was locally jacked up and the flat sliders were replaced two at a time. The sliding concave surface of the FPS bearings was leveled and then bolted and grouted to the pedestal below. However, the beams of the base were too stiff to adjust themselves by deforming and accommodate small variations in the straightness of the beams and the support pedestals. This resulted in uneven distribution of load to the four bearings. This was discovered at the conclusion of the tests when the bearings were removed and found that only three of them experienced wear. The model was essentially riding on three supports. Despite this, the model moved only in the testing direction without any torsional movement.

The properties of the isolation system were determined by the following test. The base of the model was connected to a reaction frame by two stiff rods which were instrumented with load cells as shown in Figure 2-1. The shake table was driven in displacement control mode with specified frequency and displacement amplitude. The force recorded by the load cells represents the force mobilized at the isolation system, provided that the structure above remains motionless. Force-displacement loops recorded for the woven Teflon bearing material are shown in Figure 4-3. Evidently, the mobilized force depends on the velocity of sliding as a result of the velocity dependence of the coefficient of sliding friction (Mokha et al 1988 and 1990).

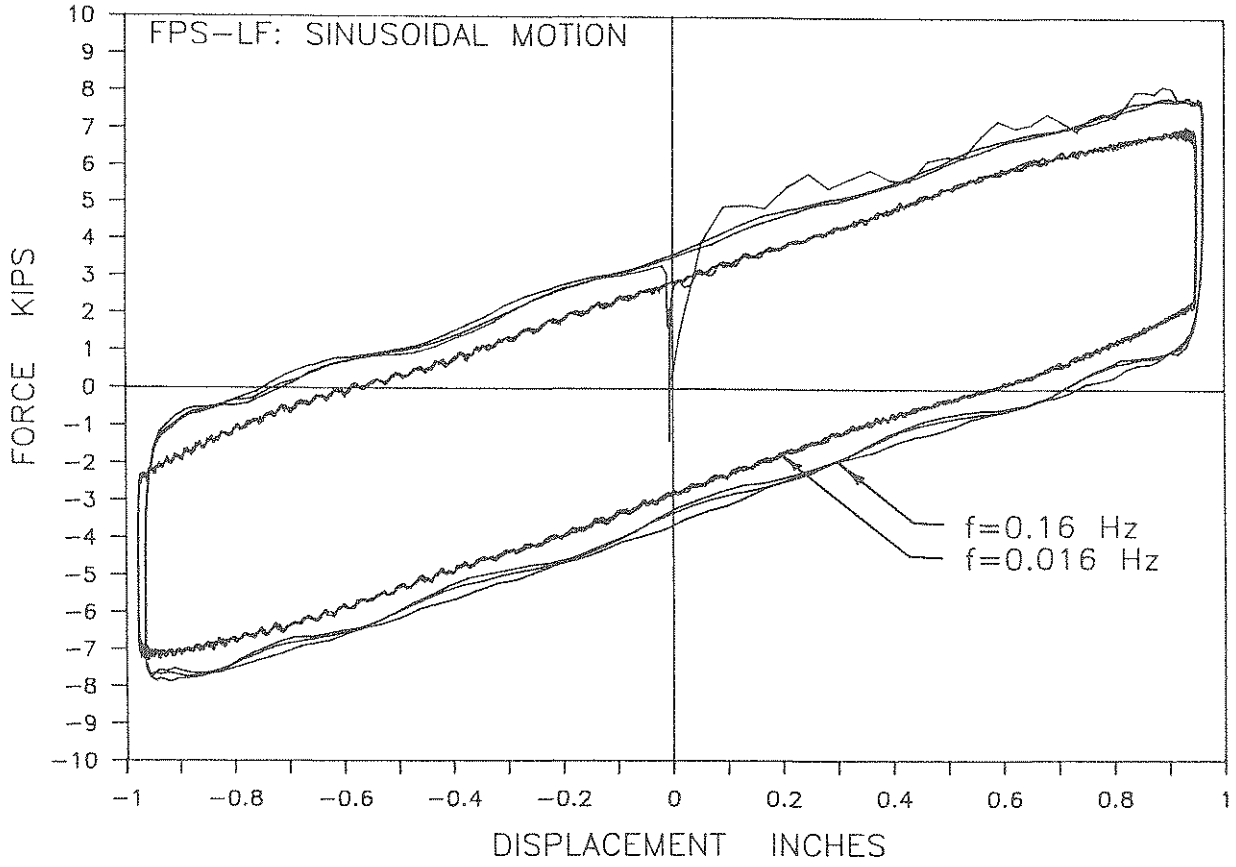

Figure 4-3 Force-Displacement Loops of Isolation System (Woven Teflon Material) Determined in Sinusoidal Motion Tests (1 inch = 25.4mm, 1 Kip = 4.46kN).

The lateral force at the isolation level follows with excellent accuracy the following relationship:

$$F_b = \left(\frac{W}{R}\right) U_b + \mu(\dot{U}_b) W sgn(\dot{U}_b) \qquad (4.1)$$

in which W is the weight of the model, R is the radius of curvature of the bearings, μ is the coefficient of friction mobilized during sliding and U_b is the bearing displacement. The first term in Eq. (4.1) corresponds to the stabilizing tendency of pendulum action of the FPS bearings with the quantity W/R representing the slope of the force-displacement relationship (see Figure 4-3). Accordingly, the period of vibration of the structure in its rigid body condition is:

$$T = 2\pi\left(\frac{R}{g}\right)^{1/2} \qquad (4.2)$$

where g is the gravitational acceleration. This of course is the natural period of a pendulum of length R which shows that the fundamental concept of the system is based on principles of pendulum motion (Zayas et al, 1987). The radius of curvature of the bearings was 9.75 inches (247.65mm) resulting in a period of 1 sec (2 secs in the prototype scale).

From force-displacement loops, like those depicted in Figure 4-3, the coefficient of friction was determined from the recorded force at zero displacement and found to follow the following relation which was proposed by Constantinou et al, 1990:

$$\mu(\dot{U}_b) = f_{max} - Df \ \exp(-a|\dot{U}_b|) \qquad (4.3)$$

in which f_{max} and (f_{max} - Df) are the maximum and minimum mobilized coefficients of friction, respectively, and a is a parameter that controls the variation of the coefficient with the velocity of sliding. For the bearings with woven Teflon these parameters were f_{max} = 0.075, Df = 0.035 and a = 1.1 sec/inch (43.3 sec/m), whereas for the bearings with material Techmet-B these parameters were f_{max} = 0.095, Df = 0.045 and a = 0.9 sec/inch (35.4 sec/m).

SECTION 5
TEST PROGRAM

The isolated model was tested with six different earthquake motions and one sinusoidal motion of 2.4 Hz frequency. This frequency coincides with the fundamental frequency of the six-story model superstructure. The characteristics of the earthquake motions are listed in Table 5-I. The records have significantly different frequency content with the Hachinohe and Mexico City being long period motions. The records were time scaled by a factor of two to satisfy similitude requirements of the quarter scale model. The time scaled Mexico City motion has a frequency content almost entirely at 1 Hz which coincides with the rigid body mode frequency of the isolated model.

Plots of time histories of some of the earthquake motions used in this program are given in Figure 5-1. These motions are shown in scaled time as recorded by the accelerometers monitoring the shake table during testing. All motions except those of Mexico City and sinusoidal wave at 2.4Hz were recorded in the tests with Techmet-B bearing material. The Mexico City and sinusoidal wave motions were recorded in tests with woven Teflon bearing material. Certain designations are shown in Figure 5-1 which help identify the record and test. HF stands for the Higher Friction Techmet-B material, whereas LF stands for the Lower Friction woven Teflon material. The shown records were normalized with respect to the peak acceleration of the actual record by the percentage shown in the figures. For example, the designation 50% implies that the record shown in Figure 5-1 has a peak acceleration about equal to 50% of the peak acceleration of the actual (historic) record.

Figure 5-2 gives the Fourier amplitude spectra of the motions in Figure 5-1, shown in scaled frequency. These spectra clearly demonstrate the significant differences in frequency content of the earthquake motions used in the testing program. It should be noted

Table 5 -I - Earthquake Motions Used in Test Program

Notation (1)	Record (2)	Peak Accel. g (3)	Predominant Freq. Range - Hz (4)	Magnitude (5)
El Centro S00E	Imperial Valley, May 18, 1940 Component S00E	0.34	1 - 4	6.7
Taft N21E	Kern County, July 21, 1952 Component N21E	0.16	0.5 - 5	7.2
Pacoima S74W	San Fernando, February 9, 1971 Component S74W	1.08	0.25 - 2	6.4
Pacoima S16E	San Fernando, February 9, 1971 Component S16E	1.17	0.25 - 6	6.4
Miyagi-Ken-Oki	Tohoku Univ., Sendai, Japan, June 12, 1978 Component EW	0.16	0.5 - 5	7.4
Hachinohe	Tokachi-Oki Earthq., Japan, May 16, 1968 Component NS	0.23	0.25 - 1.5	7.9
Mexico City	SCT Building, Sept. 19, 1985 Component N90W	0.17	0.5	8.1

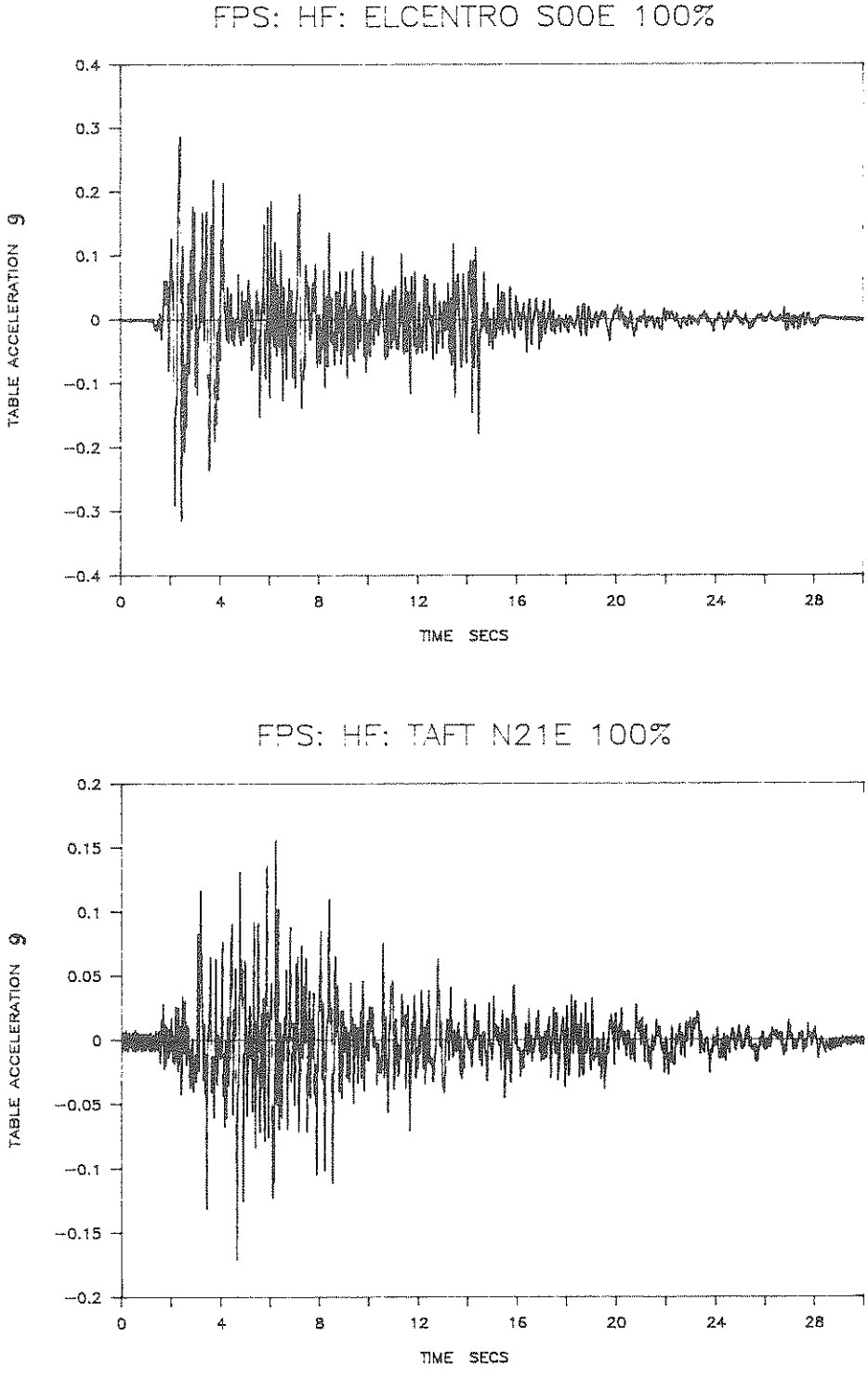

Figure 5-1 Recorded Time Histories of Shake Table Acceleration. HF Stands for Techmet-B Material. LF Stands for Woven Teflon Material.

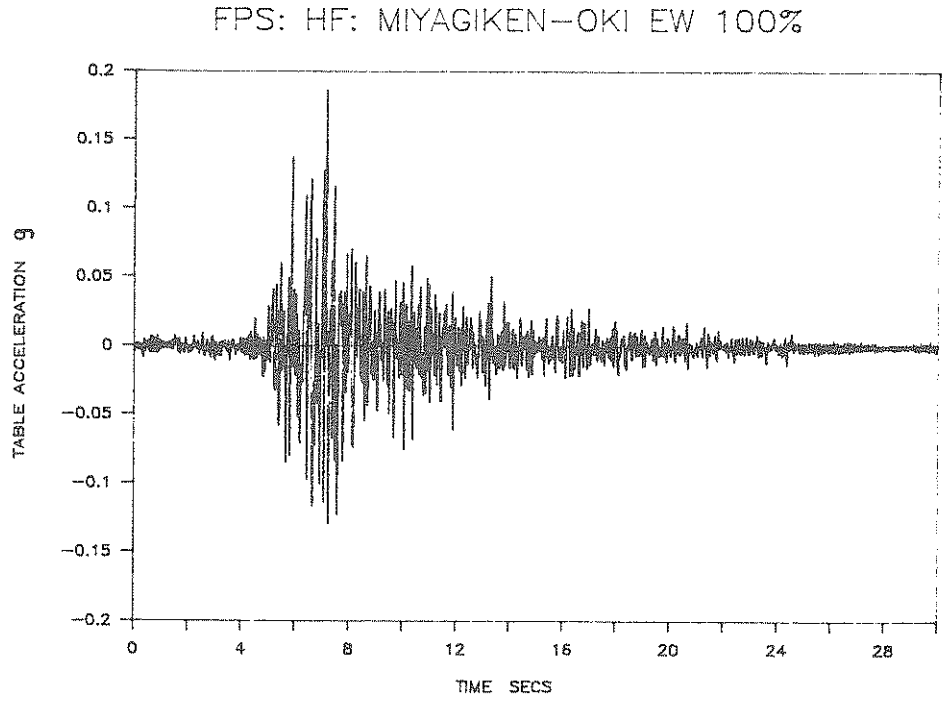

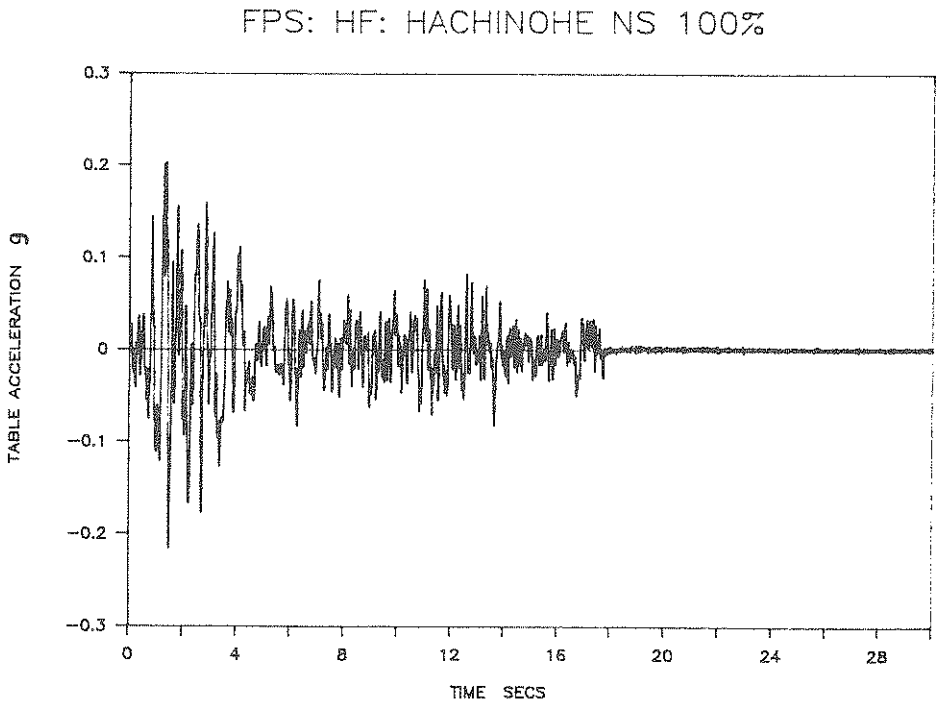

Figure 5-1 Recorded Time Histories of Shake Table Acceleration. HF Stands for Techmet-B Material. LF Stands for Woven Teflon Material (continued).

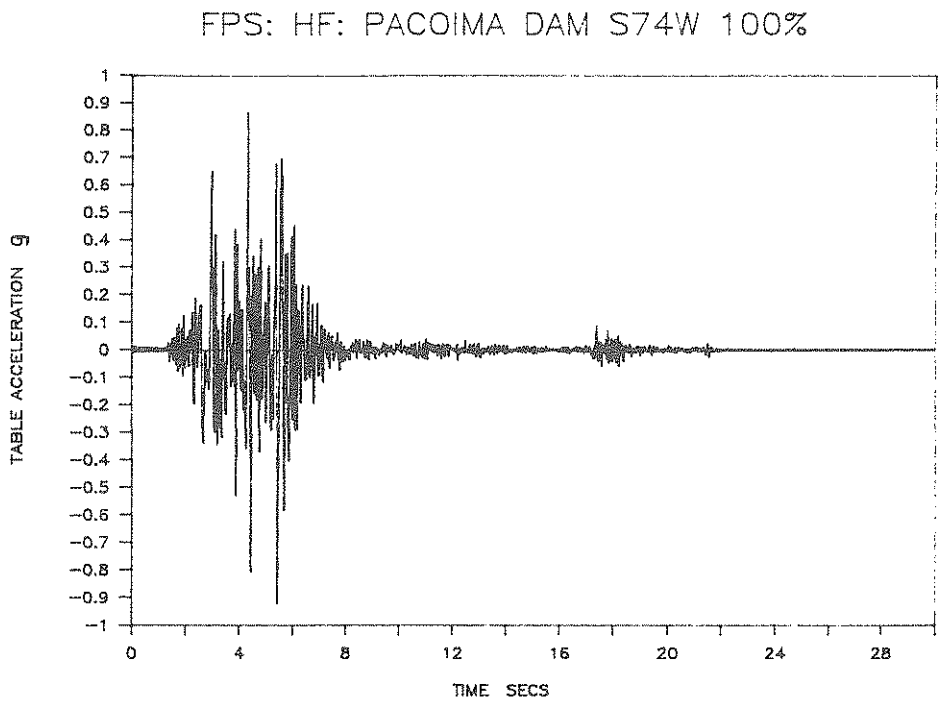

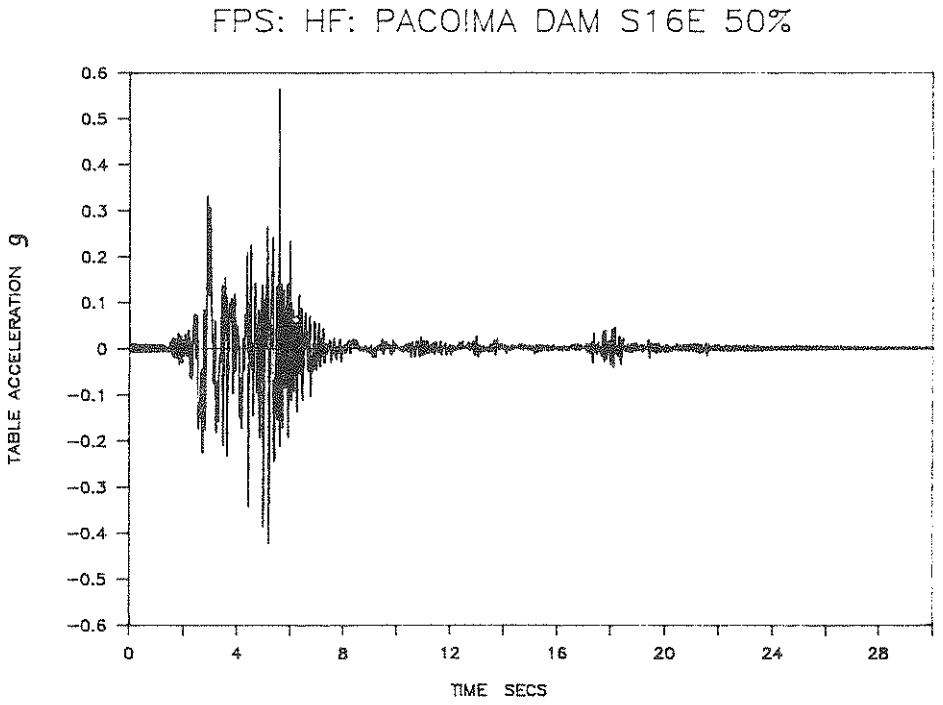

Figure 5-1 Recorded Time Histories of Shake Table Acceleration. HF Stands for Techmet-B Material. LF Stands for Woven Teflon Material (continued).

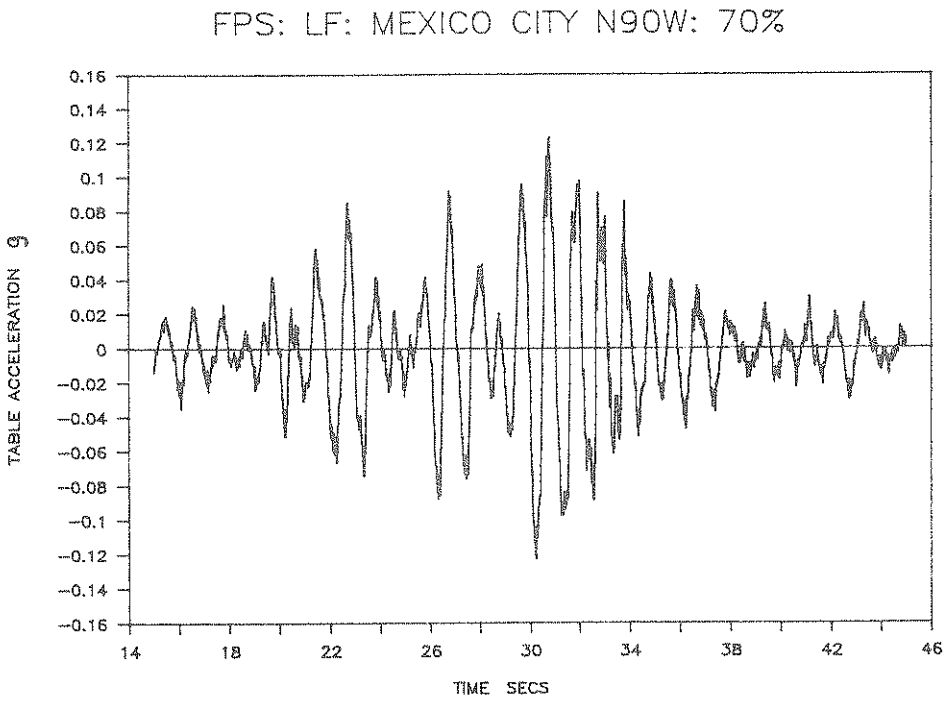

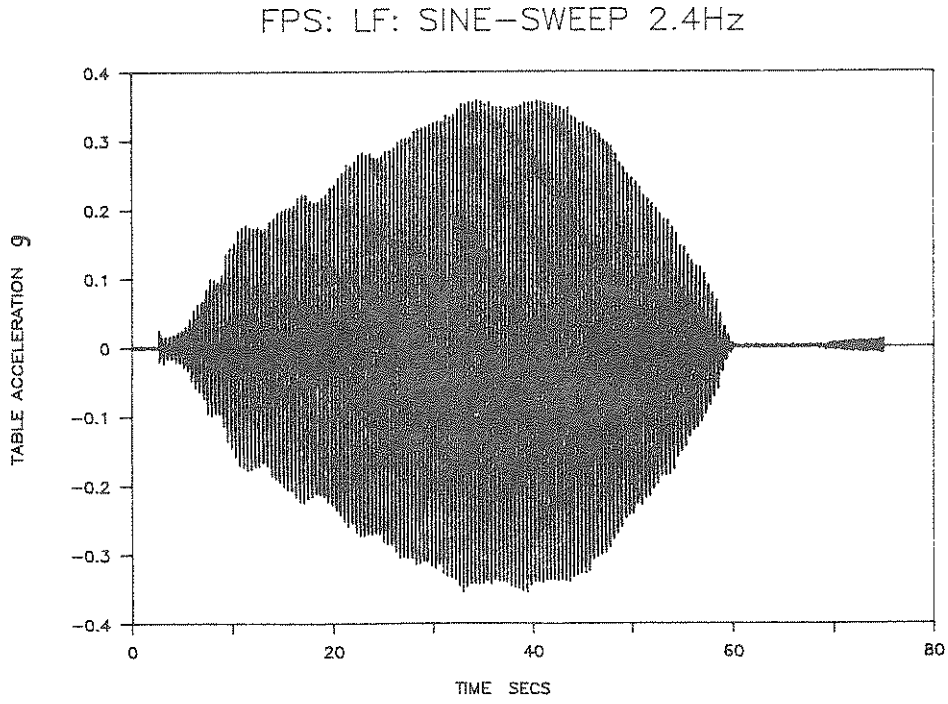

Figure 5-1 Recorded Time Histories of Shake Table Acceleration. HF Stands for Techmet-B Material. LF Stands for Woven Teflon Material (continued).

that none of the used records has been compensated and that some structure-table interaction occurred. This explains some differences observed in the peak values of acceleration and in the frequency content in different tests with the same earthquake and level of input.

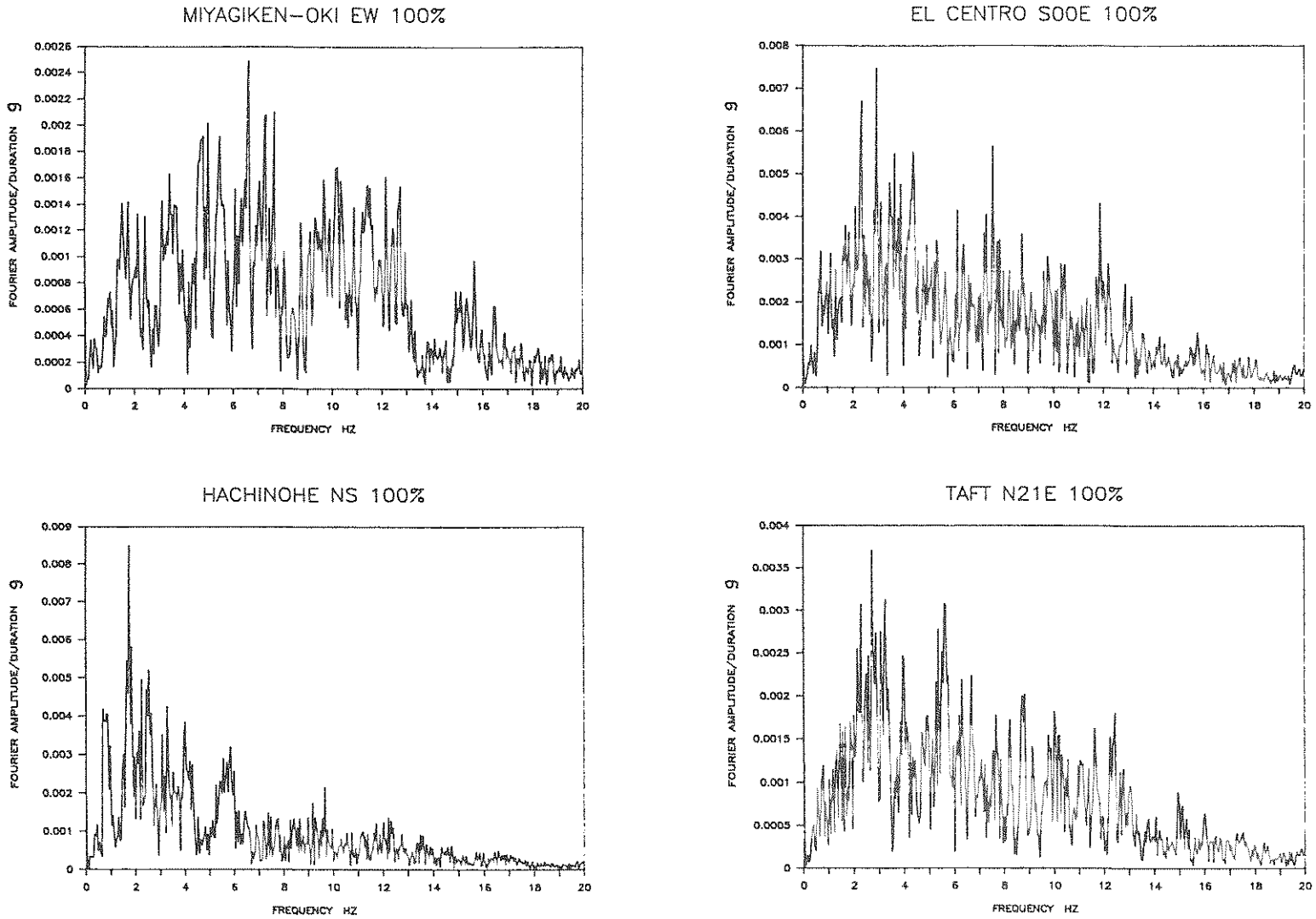

Figure 5-2 Fourier Amplitude Plots of Shake Table Acceleration Histories in Figure 5-1. Duration = 20.48 secs.

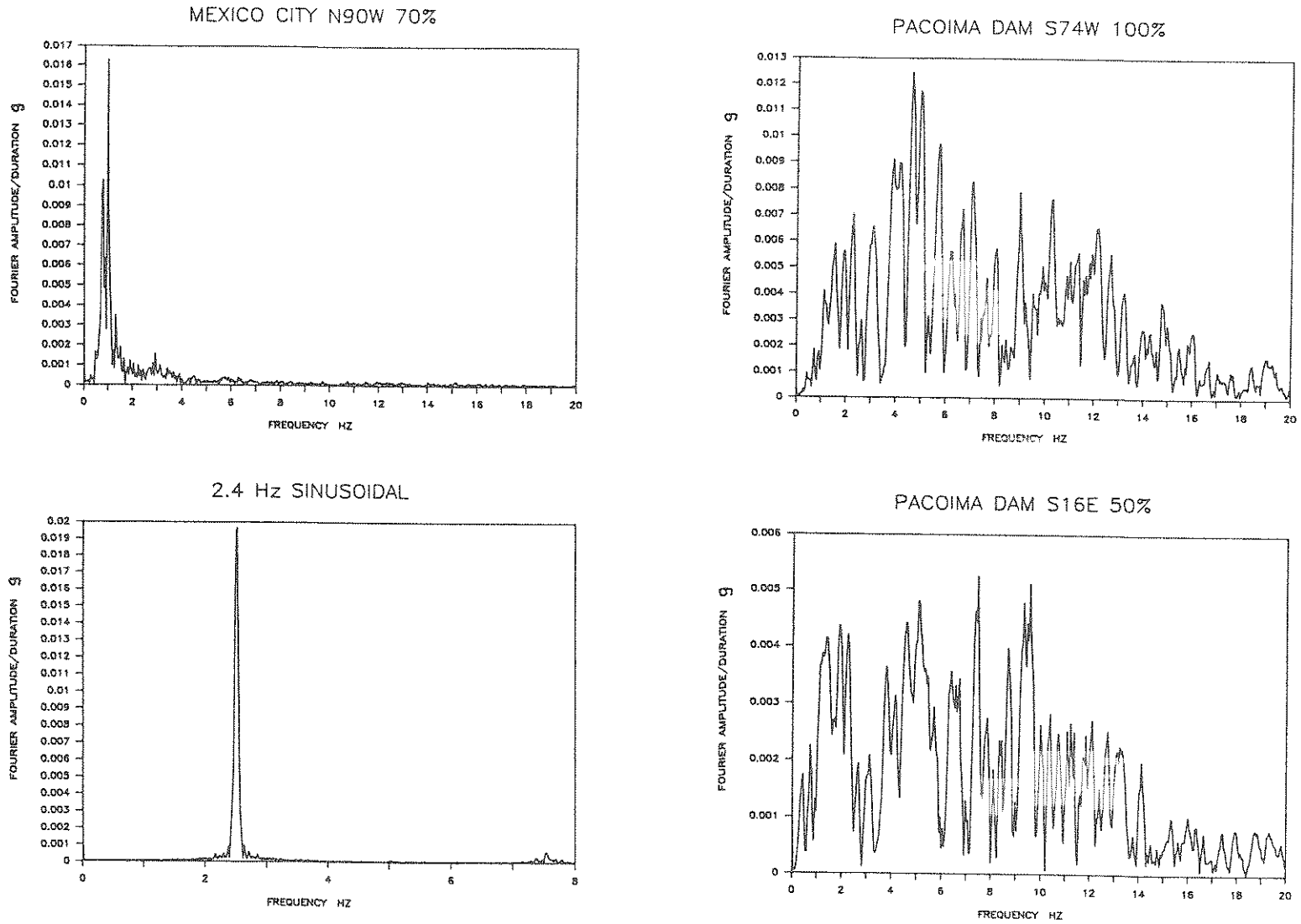

Figure 5-2 Fourier Amplitude Plots of Shake Table Acceleration Histories in Figure 5-1. Duration = 20.48 secs (continued).

SECTION 6
TEST RESULTS

The earthquake tests were performed at varying peak acceleration levels for each of the signals. Table 6-I lists the input signals in the test program, the isolation system condition, the peak table acceleration and the maximum response of the model in terms of base shear over weight (51.4 Kips) ratio, bearing displacement, floor acceleration, interstory drift and permanent displacement at the end of free vibration response. The base shear was computed from the floor and base acceleration records assuming that the mass of the model was concentrated at the level of the base and floors. The weight distribution used in the computation is: 7.65 Kips (34.1 kN) at 6th floor, 7.84 Kips (34.9 kN) at 5th to 1st floors and 4.56 Kips (20.3 kN) at the base.

Each earthquake signal was run at increasing levels of peak table acceleration (e.g. the case in Table 6-I of El Centro 200% corresponds to an increase of the actual peak acceleration by approximately a factor of 2) until the peak interstory drift reached approximately the value of 0.18 inches (4.57 mm) or 0.005 times the story height. This value has been analytically determined to be the limit of elastic behavior of the model structure.

It should be noted that the peak table acceleration in Table 6-I for the same earthquake and level of input varies in the two sets of tests with materials Techmet-B and woven Teflon. This is because the table motion has not been compensated and some structure-table interaction occurred.

The first important observation to be made from the results of Table 6-I is the effectiveness of the FPS bearings in reducing the interstory drift. Under fixed-base conditions the limit on drift was reached for a peak table acceleration of 0.1 g in the El Centro signal. In the isolated condition and for Techmet-B material the

Table 6-1 - Summary of Experimental Results

Excitation (1)	Isolation+ Condition (2)	Pk. Table Accel. (g) (3)	Bearing Displ. (in) (4)	Base Shear**/ Weight (5)	Pk. Model Base Accel. (g) (6)	Pk. Model* Floor Accel. (g) (7)	Pk. Model* Interstory Drift (inch) (8)	Permanent Displ. (inch) (9)
El Centro S00E 30%	Fixed	0.10	--	0.255	--	0.47 (6)	0.171 (2)	--
El Centro S00E 100%	FPS-HF	0.32	0.395	0.126	0.32	0.56 (6)	0.117 (2)	0.011
El Centro S00E 150%	FPS-HF	0.51	0.761	0.157	0.42	0.63 (6)	0.148 (2)	0
El Centro S00E 200%	FPS-HF	0.78	1.230	0.218	0.56	0.85 (6)	0.174 (3)	0.044
Taft N21E 100%	FPS-HF	0.17	0.112	0.101	0.23	0.37 (6)	0.077 (3)	0.022
Taft N21E 300%	FPS-HF	0.53	0.892	0.173	0.51	0.65 (6)	0.124 (3)	0
Miyagiken-OKI EW 100%	FPS-HF	0.19	0.076	0.096	0.18	0.31 (3,6)	0.072 (2)	0.008
Miyagiken-OKI EW 300%	FPS-HF	0.57	0.523	0.138	0.68	0.65 (6)	0.116 (3)	0.013
Hachinohe NS 100%	FPS-HF	0.22	0.568	0.152	0.40	0.40 (6)	0.090 (2)	0.027
Hachinohe NS 150%	FPS-HF	0.36	1.12	0.199	0.43	0.50 (6)	0.142 (2)	0
Sinusoidal 2.4 Hz	FPS-HF	0.17	0.230	0.106	0.22	0.39 (6)	0.078 (2)	0
Pacoima S74W 100%	FPS-HF	0.92	1.40	0.203	0.84	0.86 (6)	0.174 (3)	0.018
Pacoima S16E 50%	FPS-HF	0.56	1.11	0.198	0.47	0.63 (6)	0.163 (3)	0.036

*Quantity in parenthesis is story or floor at which maximum was recorded.
**Shear at bearing level. +HF: Techment B, LF: Woven Teflon. 1 inch = 25.4 mm

Table 6-I - (Continued) - Summary of Experimental Results

Excitation (1)	Isolation+ Condition (2)	Pk. Table Accel. (g) (3)	Bearing Displ. (in) (4)	Base Shear**/ Weight (5)	Pk. Model Base Accel. (g) (6)	Pk. Model* Floor Accel. (g) (7)	Pk. Model* Interstory Drift (inch) (8)	Permanent Displ. (inch) (9)
El Centro S00E 100%	FPS-LF	0.31	0.432	0.114	0.33	0.46 (6)	0.107 (2)	0
El Centro S00E 200%	FPS-LF	0.60	1.76	0.243	0.54	0.79 (6)	0.175 (2)	0.062
Taft N21E 100%	FPS-LF	0.17	0.136	0.090	0.22	0.35 (6)	0.070 (3)	0.013
Taft N21E 300%	FPS-LF	0.55	1.04	0.173	0.48	0.55 (6)	0.136 (3)	0
Miyagiken-OKI EW 100%	FPS-LF	0.19	0.090	0.088	0.19	0.32 (3)	0.065 (2)	0.007
Miyagiken-OKI EW 300%	FPS-LF	0.56	0.560	0.123	0.64	0.60 (6)	0.115 (2)	0.013
Hachinohe NS 100%	FPS-LF	0.22	0.588	0.126	0.35	0.36 (6)	0.092 (2)	0.031
Hachinohe NS 150%	FPS-LF	0.35	1.36	0.201	0.41	0.46 (6)	0.143 (2)	0
Pacoima S74W 100%	FPS-LF	0.92	1.52	0.198	0.83	0.80 (6)	0.167 (3)	0.011
Pacoima S16E 50%	FPS-LF	0.56	1.28	0.195	0.42	0.56 (6)	0.176 (3)	0.071
Sinusoidal 2.4 Hz	FPS-LF	0.36	0.530	0.115	0.34	0.48 (5)	0.075 (2)	0
Mexico N90W 40%	FPS-LF	0.07	0.044	0.087	0.08	0.12 (5, 6)	0.056 (2,3)	0.032
Mexico N90W 60%	FPS-LF	0.11	0.263	0.116	0.18	0.18 (6)	0.077 (2)	0.073
Mexico N90W 70%	FPS-LF	0.12	0.930	0.176	0.31	0.35 (6)	0.126 (3)	0.114

same limit is reached for a peak table acceleration of 0.78 g, indicating a eight-fold increase in the capacity of the super-structure to withstand this motion while remaining undamaged.

A more careful, however, investigation of the table acceleration records in the two cases revealed that the 0.78g peak value was merely a spike and that the record was effectively the original El Centro record increased by a factor of approximately two. Accordingly, the increase in capacity is about six-fold rather than eight-fold. The relative bearing displacement in this case is only 1.23 inches (31.2mm) or 4.92 inches in the prototype scale. It should be noted that this displacement is about half the bearing displacement recorded in tests with similar size and aspect ratio model but supported by elastomeric bearing isolation systems (Griffith et al, 1988).

Another important observation to be made is related to the peak model acceleration. The acceleration in most tests is larger than the peak table acceleration. Only in the case of the strongest signal (Pacoima S74W record) the table acceleration was de-amplified in the isolated model. The level of acceleration in the model is about 1.5 to 2 times that recorded in similar tests with elastomeric isolation systems (Griffith et al, 1988).

It has been common in the past to determine the effectiveness of an isolation system by the degree to which the table acceleration is reduced in the structure above the isolation system (e.g. Griffith et al, 1988). Indeed, in isolated structures in which all stories move in phase the accelerations must be low or otherwise the first story will be subjected to excessive shear, overturning moment and drift. However, in isolated structures in which the floor accelerations are out of phase (higher mode response) the reduction of the level of acceleration from that of the shake table is not a good measure of the effectiveness of the isolation system. In out of phase response the floor accelerations point in opposing

directions, thus leading to reduced story shear, overturning moment and drift. This is exactly the observed behavior of the tested system.

Evidence of this behavior is provided in Figures 6-1 to 6-4 which show acceleration and displacement profiles of the model at selected times for the case of the Techmet-B bearing material and for four excitations of significantly different frequency content: El Centro S00E 200% (peak table acceleration of 0.78g), Hachinohe NS 150% (peak table acceleration of 0.36g), Pacoima S74W 100% (peak table acceleration of 0.92g)and Miyagi-Ken-Oki EW 300% (peak table acceleration of 0.57g). The times at which the profiles are plotted correspond to the instances at which the peak model acceleration, peak base overturning moment, peak interstory drift, peak base shear and peak bearing displacement occur. These profiles clearly demonstrate that when the peak acceleration occurs the response is out of phase (second or third mode). Evidently, the effectiveness of the FPS bearings could not be assessed by the level of the model acceleration in comparison to that of the shake table. Rather the peak table acceleration at the limit of elastic behavior in comparison to the corresponding table acceleration under fixed base conditions could be used as a measure of the effectiveness of the isolation system in protecting the structural system above. Based on this criterion the tested system has been effective in protecting the structure above under extreme loading like the 1940 El Centro motion scaled to 0.78g. The tested system could also sustain, while elastic, other extreme loadings of significantly different frequency content like the 1971 Pacoima motion scaled to 0.92g, the 1978 Miyagi-Ken-Oki motion scaled to 0.57g and the 1968 long period Hachinohe motion scaled to 0.36g peak acceleration.

Similar behavior is observed in the case of the lower friction woven Teflon bearing material as demonstrated in Figures 6-5 to 6-8 which again show profiles of acceleration and displacement at selected times and for the same excitations as those in Figures 6-1 to 6-4. It should be noted that same earthquake and input level

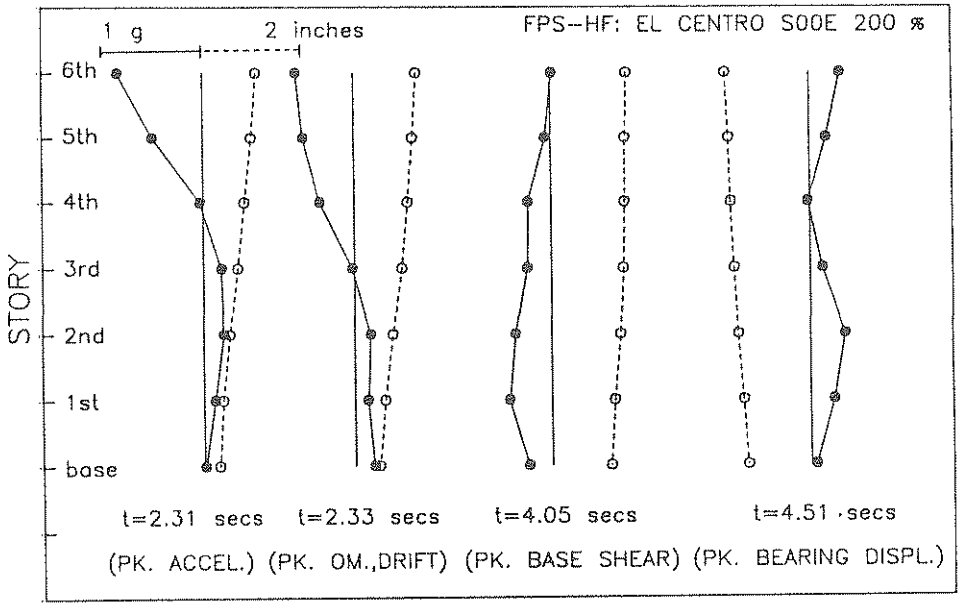

Figure 6-1 Profiles of Story Acceleration and Displacement in Case of Techmet-B Material and for El Centro Input (0.78g peak table acceleration). Profiles are shown at Times of Peak Model Acceleration, Peak Overturning Moment, Peak Interstory Drift, Peak Base Shear and Peak Bearing Displacement. Solid and Dashed Lines Represents Acceleration and Displacement Profiles, respectively.

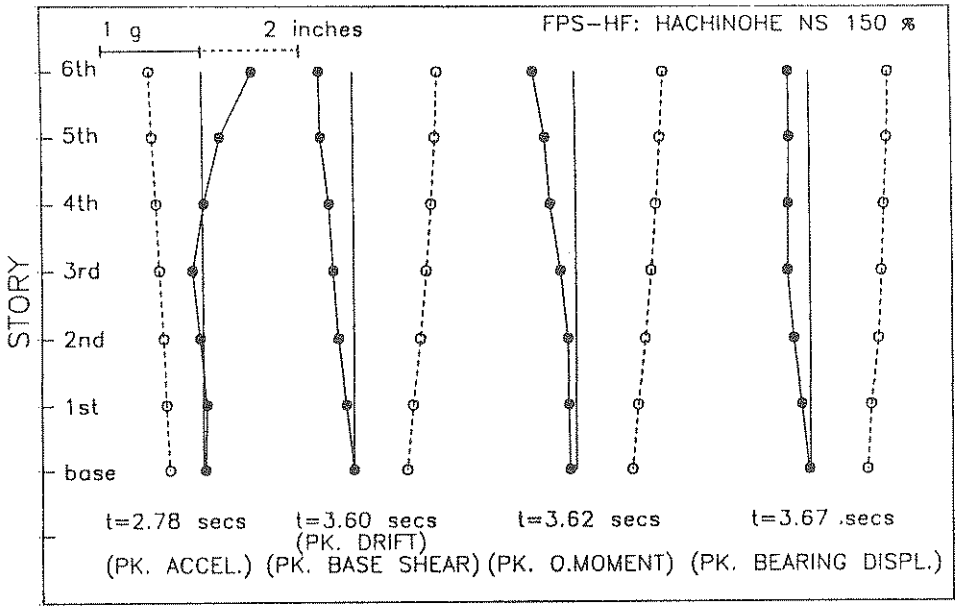

Figure 6-2 Profiles of Story Acceleration and Displacement in Case of Techmet-B Material and for Hachinohe Input (0.36g peak table acceleration).

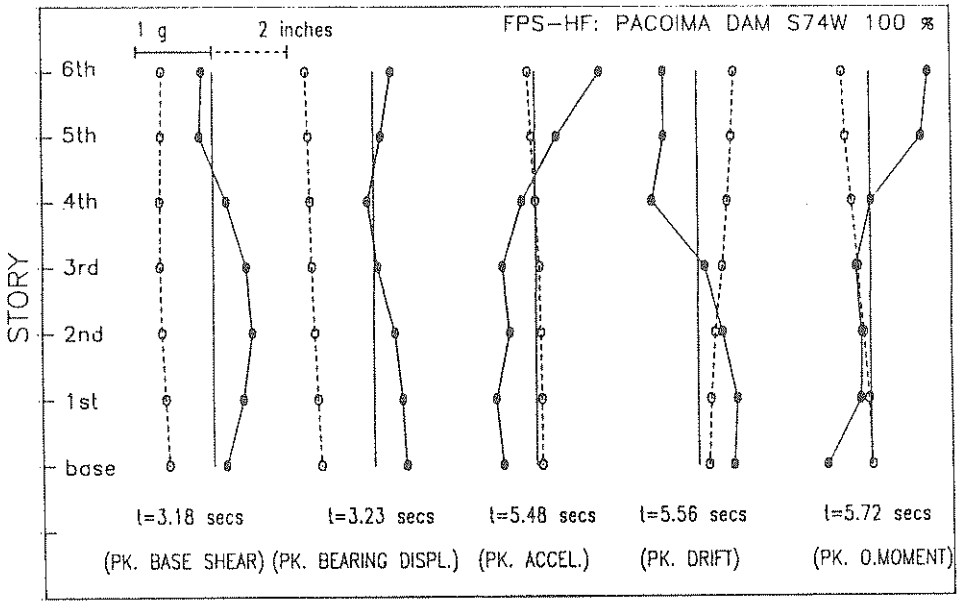

Figure 6-3 Profiles of Story Acceleration and Displacement in Case of Techmet-B Material and for Pacoima S74W Input (0.92g peak table acceleration).

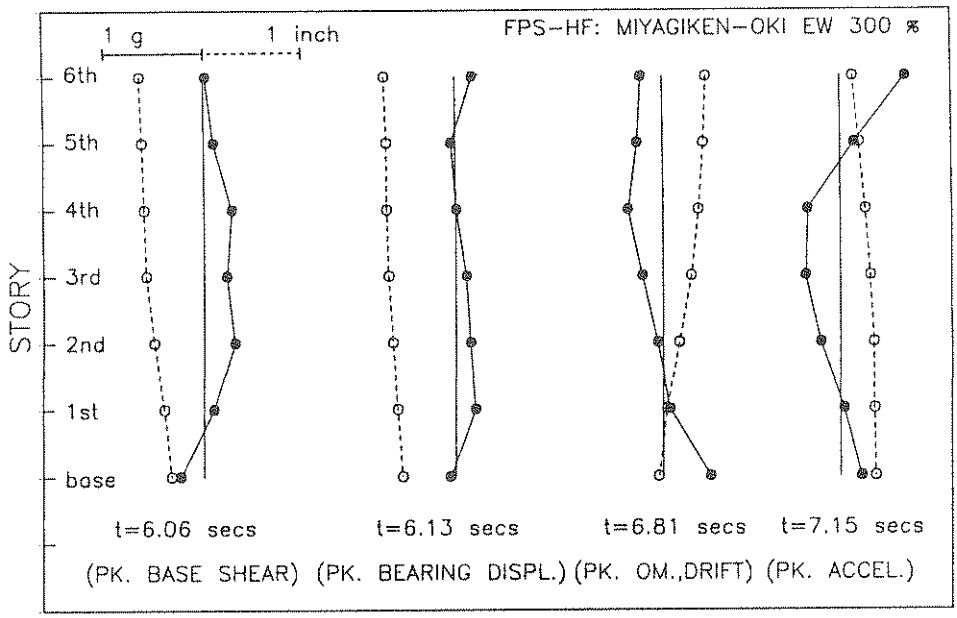

Figure 6-4 Profiles of Story Acceleration and Displacement in Case of Techmet-B Material and for Miyagiken-Oki Input (0.57g peak table acceleration).

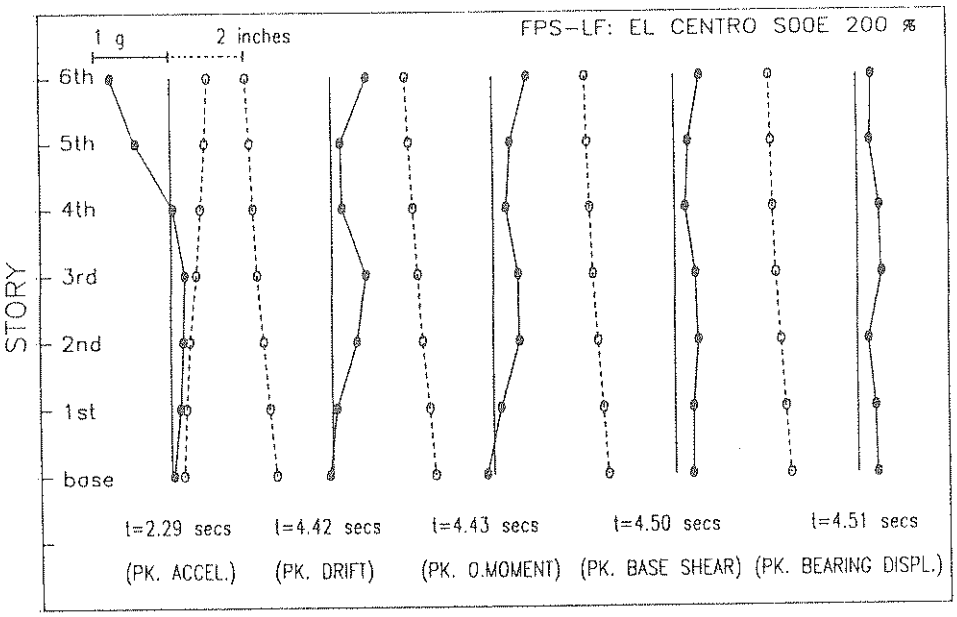

Figure 6-5 Profiles of Story Acceleration and Displacement in Case of Woven Teflon Material and for El Centro Input (0.60g peak table acceleration).

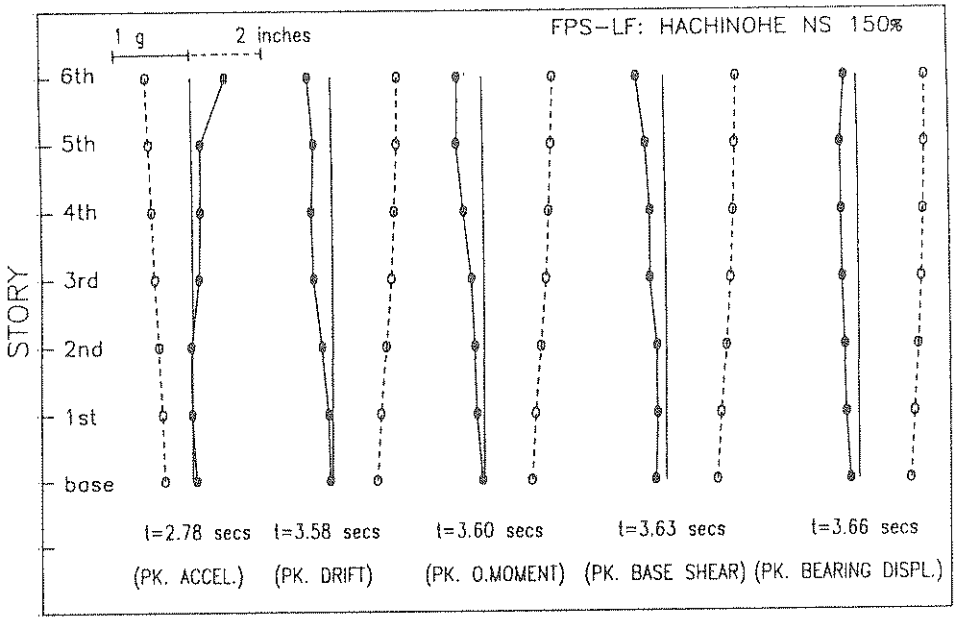

Figure 6-6 Profiles of Story Acceleration and Displacement in Case of Woven Teflon Material and for Hachinohe Input (0.35g peak table acceleration).

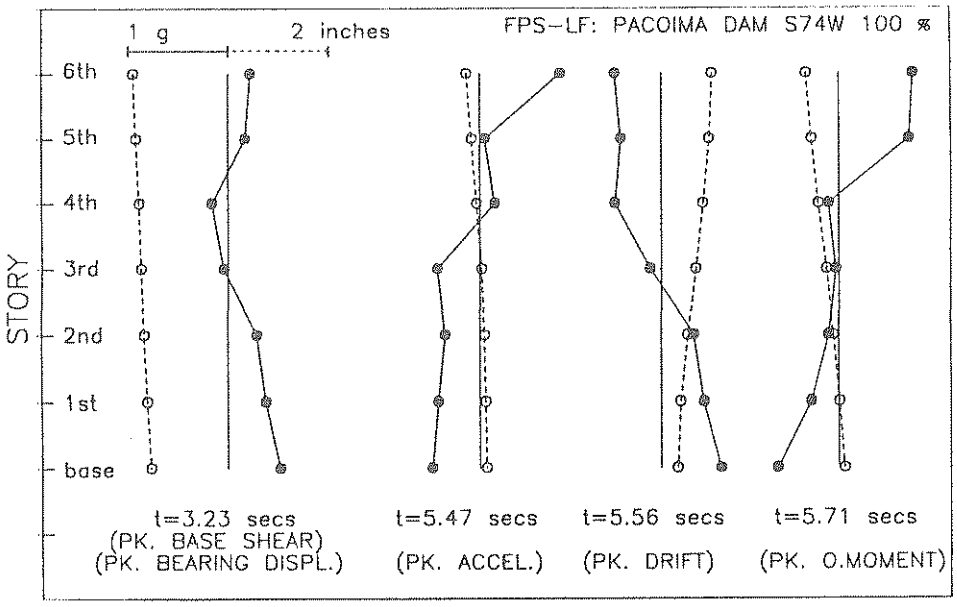

Figure 6-7 Profiles of Story Acceleration and Displacement in Case of Woven Teflon Material and for Pacoima S74W Input (0.92g peak table acceleration).

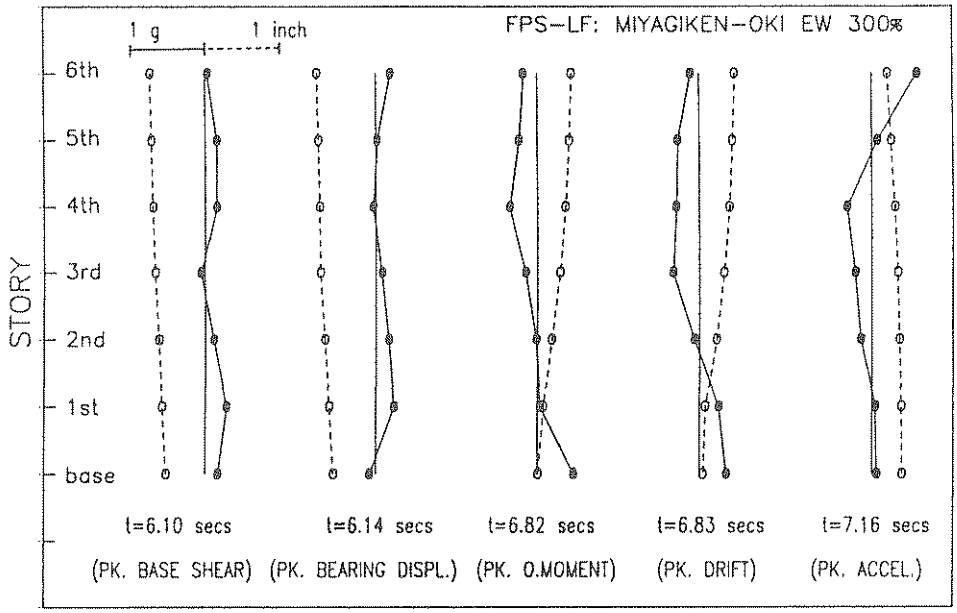

Figure 6-8 Profiles of Story Acceleration and Displacement in Case of Woven Teflon Material and for Miyagiken-Oki Input (0.56g peak table acceleration).

motions in the two cases of bearing material were actually slightly different in both peak acceleration values and frequency content. Despite these differences in the input and the difference in frictional properties, the profiles of acceleration and displacement in the two cases of bearing material are similar.

Of particular interest are the results of the sequence of tests with the Mexico City motion in the case of lower friction woven Teflon material. This motion is essentially a sinusoidal wave at the fundamental frequency of the isolation system. The results of Table 6-I show that the system was at resonance. For example in the test with 0.11g peak table acceleration, the bearing displacement was 0.263 inches (6.68 mm). A minor increase in acceleration (to 0.12g) resulted in an almost four-fold increase in displacement. This undesirable effect could be avoided by designing the bearings with higher friction so that the ratio of maximum coefficient of friction, f_{max}, to peak table acceleration in units of g is larger than the limit $\pi/4$. This remarkable property of sliding systems has been originally explained by Den Hartog, 1931 and very recently extended to velocity dependent frictional systems by Makris, 1989.

We now concentrate on specific aspects of the recorded response of the tested structure. Figure 6-9 shows time histories of the recorded sixth floor displacement and structural shear over weight ratio of the model in the fixed based test with El Centro motion of 0.1g peak acceleration (see Table 6-I for more details). The displacement is measured with respect to the table and the structural shear is the shear force at the first story. The total weight of the model, including the base, has been used in normalization (51.4 Kips). The shear force was not measured directly, but rather calculated from the floor acceleration records using the following weight distribution: 7.65 Kips (34.1 kN) for the sixth floor and 7.84 Kips (34.9 kN) for floors fifth to first. This test was conducted with the frame fixed to the shake table (the isolation system has been removed).

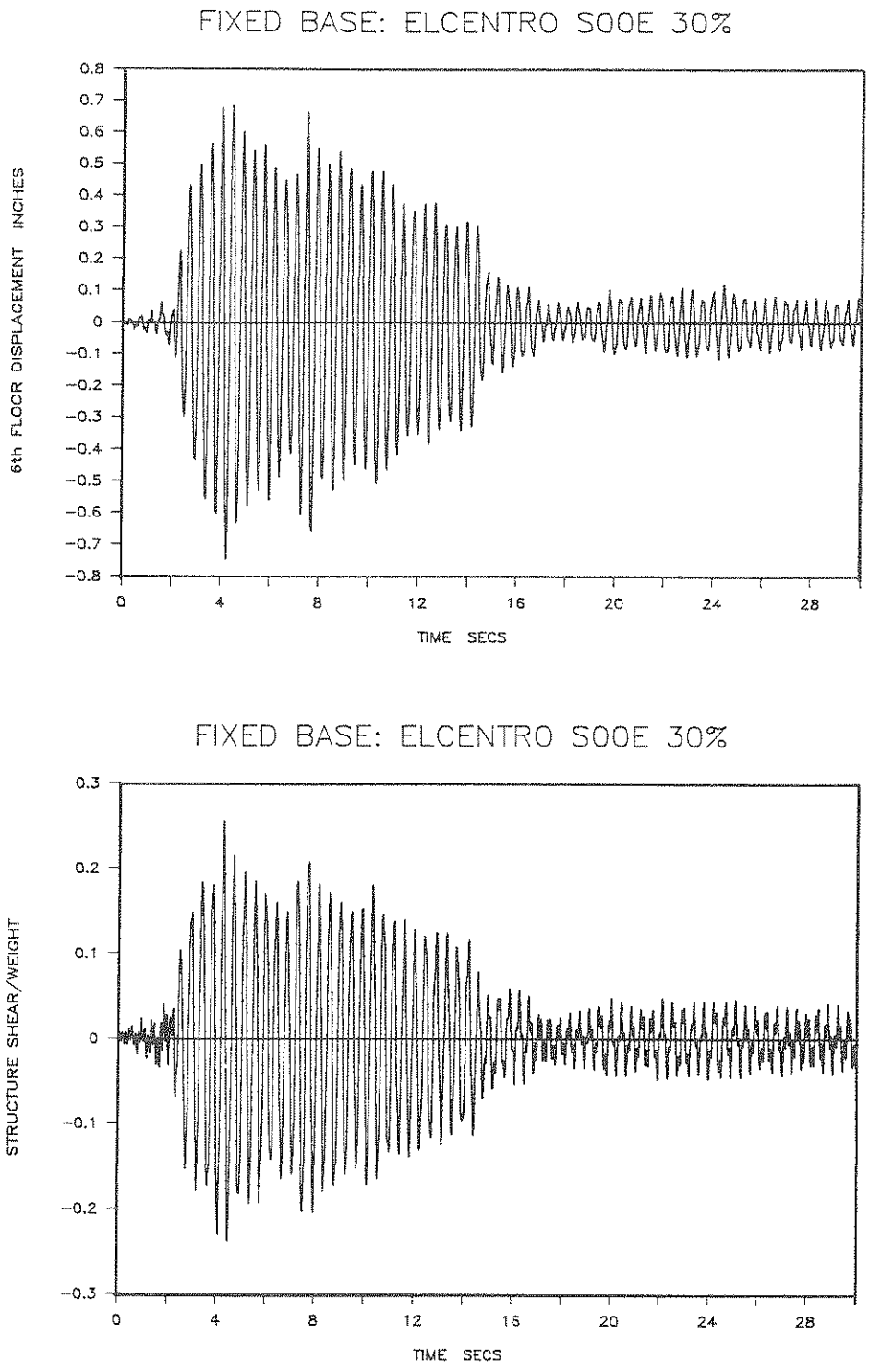

Figure 6-9 Experimental Time Histories of Sixth Floor Displacement with Respect to Base and Structure Shear Under Fixed Base Conditions and for El Centro Input (0.10 peak table acceleration). Structure Shear is Shear Force at First Story.

An inspection of the structural shear history in Figure 6-9 reveals a response almost entirely in the fundamental mode for times between 3 and 14 secs (strong portion of excitation). Actually a simple calculation using the recorded top floor acceleration of 0.47g and assuming response in the fundamental mode results in a structural shear over weight ratio of 0.285 rather than the exact 0.255.

Figures 6-10 to 6-35 present time histories of base (bearing) displacement, structural shear over weight (51.4 Kips) ratio and sixth floor displacement with respect to base and base shear (at bearing level) over weight ratio versus bearing displacement loop in tests of the isolated model. Again the designation HF in these figures stands for the Techmet-B bearing material, whereas the designation LF stands for the woven Teflon bearing material. It should be noted that the structural and base shear forces differ by the inertia force of the base of the model.

There are several observations to be made in these figures:

(1) The structural shear response contains higher mode frequencies. Of course this has been evident in the acceleration profiles presented in Figures 6-1 to 6-8. What is interesting is the differences in the frequency content of the structural shear history between the fixed base and isolated models in the case of El Centro input (Figures 6-9 to 6-12 and 6-21 to 6-22). Clearly the generation of high frequency response is associated with sticking in the FPS bearings as one can observe in the time histories of the bearing displacement.

(2) The shown hysteresis loops of the isolation system demonstrate increasing resistance with increasing displacement.

(3) The permanent displacement at the end of free vibration is very small. The permanent displacement in each of the tests is listed in Table 6-I. The maximum value was 0.114 inches (2.9mm) and was recorded in one of the tests with Mexico City input.

This value is less than six percent of the bearing design displacement of two inches (50.8mm). The performance of the FPS bearings in this respect was felt to be excellent.

(4) The resonance effects in the tests with Mexico City input are clearly evident in the bearing displacement histories of Figures 6-32 and 6-33.

(5) The results of Figures 6-34 and 6-35 for the 2.4Hz sinusoidal wave input are very interesting because a large number of cycles was completed (about 55 cycles in the case of Techmet-B material and 120 cycles in the case of woven Teflon material). The bearings completed this large number of cycles without any degradation.

(6) In the tests with the lower friction woven Teflon material the bearing displacement is more and the peak model acceleration is less than in the tests with the higher friction Techmet-B material. The lower peak model acceleration in the case of woven Teflon material does not necessarily result in lower peak interstory drift. The most notable example of this interesting phenomenon is in the case of El Centro 200% input. In the case of material Techmet-B the peak model acceleration was 0.85g and the peak interstory drift was 0.174 inches, whereas in the case of woven Teflon material these values were 0.79g and 0.175 inches, respectively (see Table 6-I). Explanation for this interesting behavior is provided by the acceleration profiles at the time of peak interstory drift which are shown in Figures 6-1 and 6-5 for the two cases. In the case of Techmet-B material (Figure 6-1) the response is out of phase and the top floor acceleration is 0.58g. In the case of woven Teflon material (Figure 6-5) the response is in phase and the top floor acceleration is 0.45g. In the out of phase response accelerations are larger, but they point in opposing directions, thus leading to reduced interstory drift.

Finally, we note that during the entire testing program no uplift occurred at the bearings and no torsional response was observed.

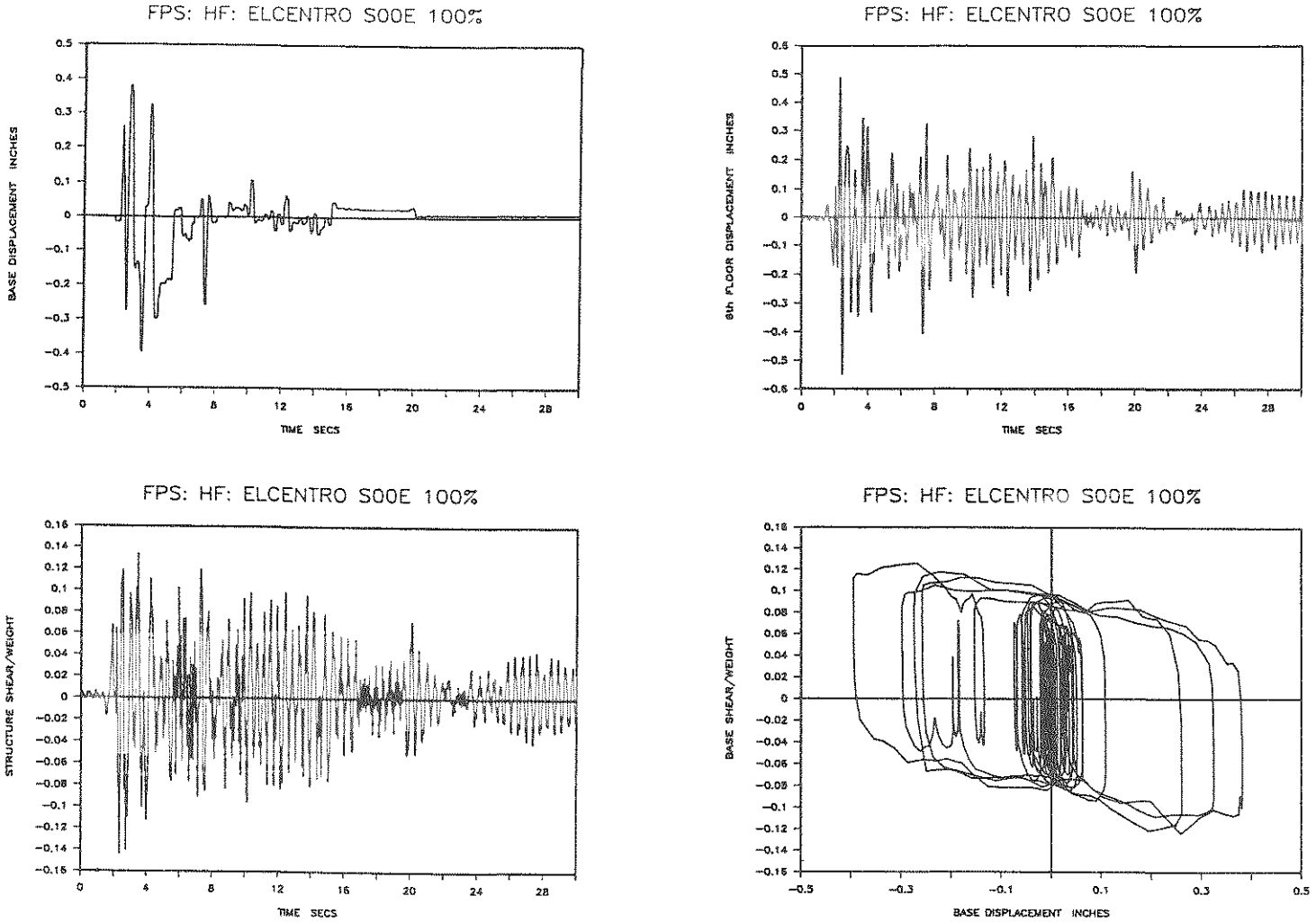

Figure 6-10 Experimental Time Histories of Base (Bearing) Displacement, Structure Shear and Sixth Floor Displacement with Respect to Base and Base Shear-Bearing Displacement Loop in Case of Techmet-B Material and for El Centro Input (0.32g peak table acceleration). Structure Shear is Shear at First Story. Base Shear is Shear at Bearing Level.

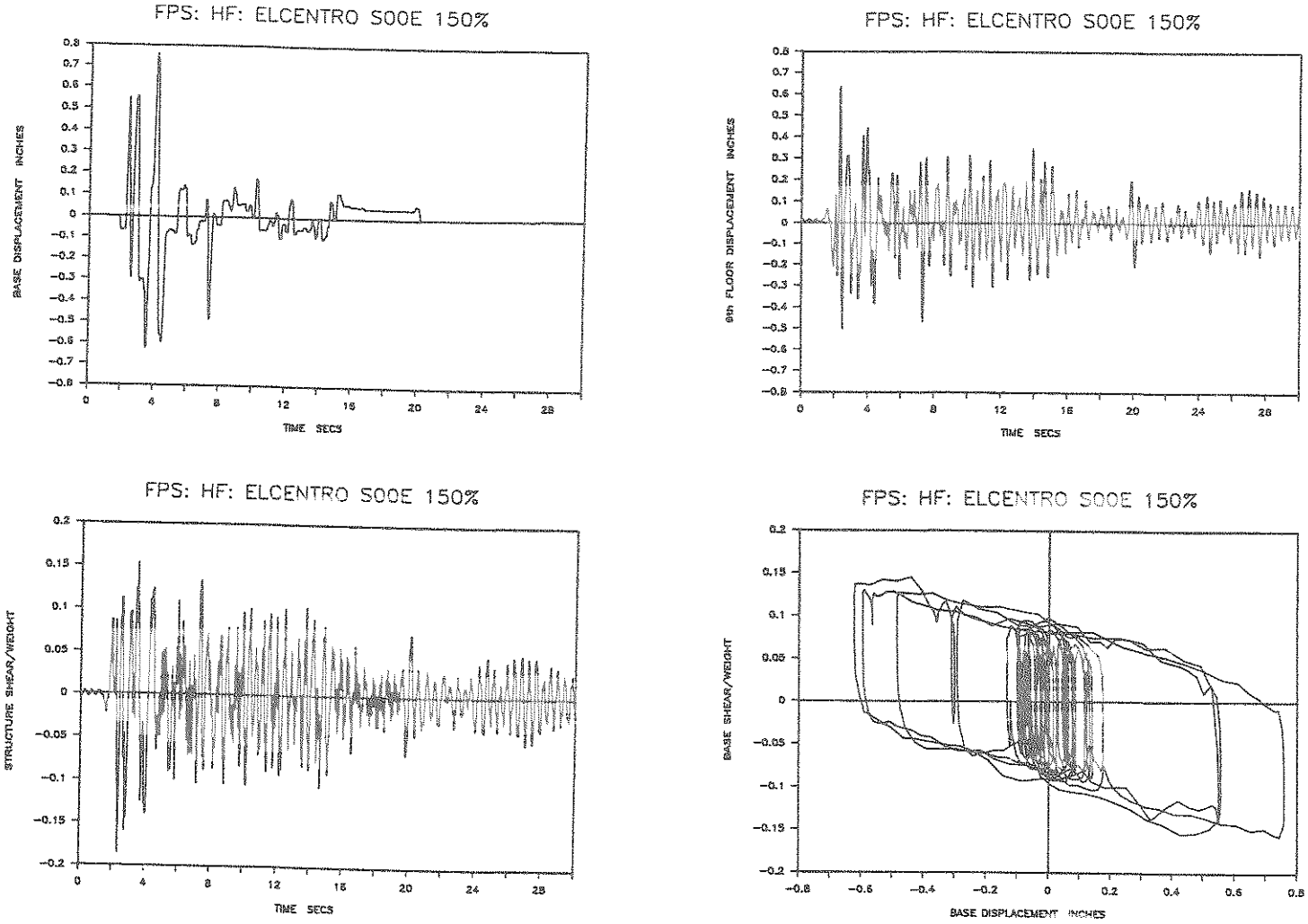

Figure 6-11 Experimental Time Histories of Base (Bearing) Displacement, Structure Shear and Sixth Floor Displacement with Respect to Base and Base Shear-Bearing Displacement Loop in Case of Techmet-B Material and for El Centro Input (0.51g peak table acceleration).

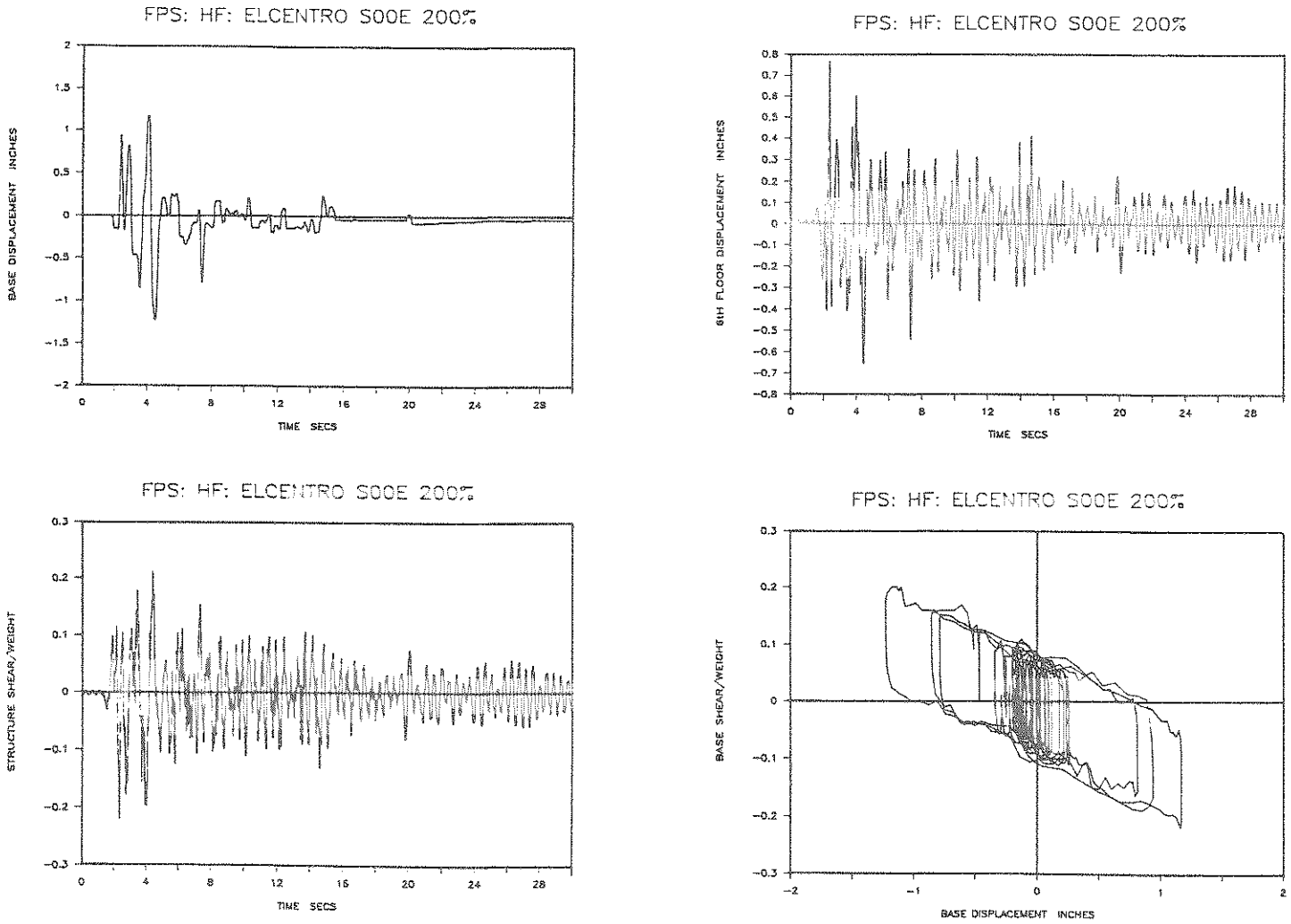

Figure 6-12 Experimental Time Histories of Base (Bearing) Displacement, Structure Shear and Sixth Floor Displacement with Respect to Base and Base Shear-Bearing Displacement Loop in Case of Techmet-B Material and for El Centro Input (0.78g peak table acceleration).

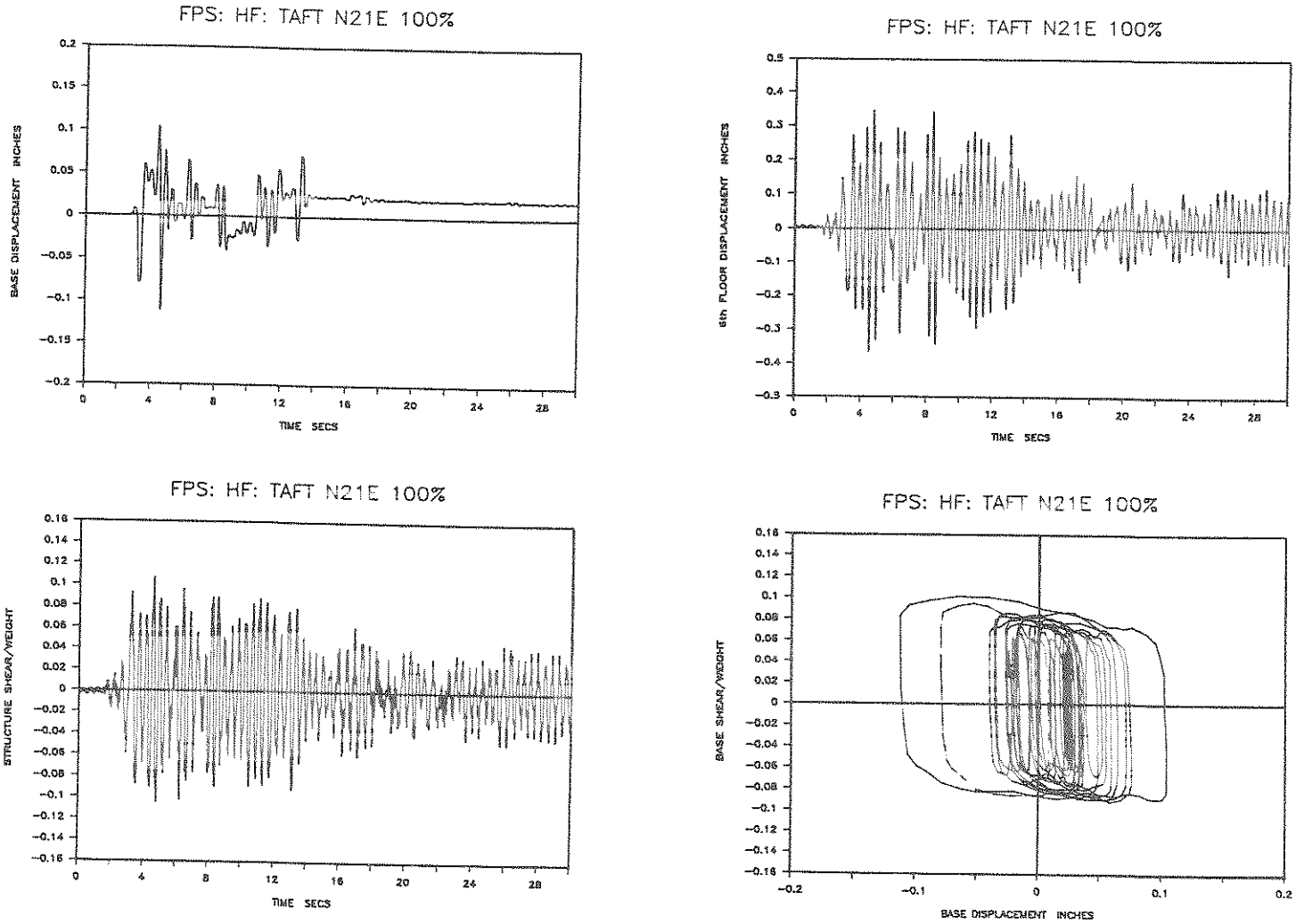

Figure 6-13 Experimental Time Histories of Base (Bearing) Displacement, Structure Shear and Sixth Floor Displacement with Respect to Base and Base Shear-Bearing Displacement Loop in Case of Techmet-B Material and for Taft Input (0.17g peak table acceleration).

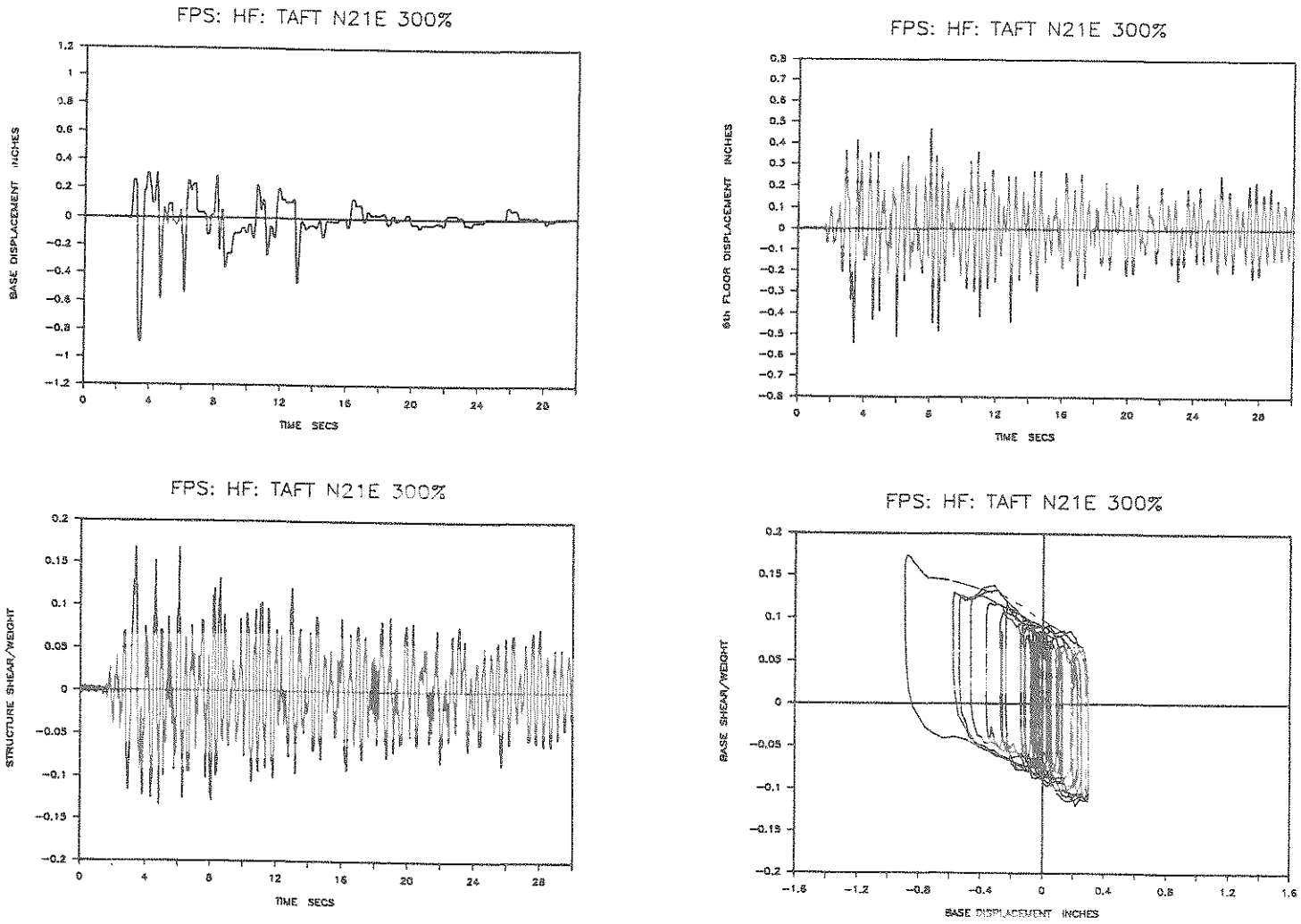

Figure 6-14 Experimental Time Histories of Base (Bearing) Displacement, Structure Shear and Sixth Floor Displacement with Respect to Base and Base Shear-Bearing Displacement Loop in Case of Techmet-B Material and for Taft Input (0.53g peak table acceleration).

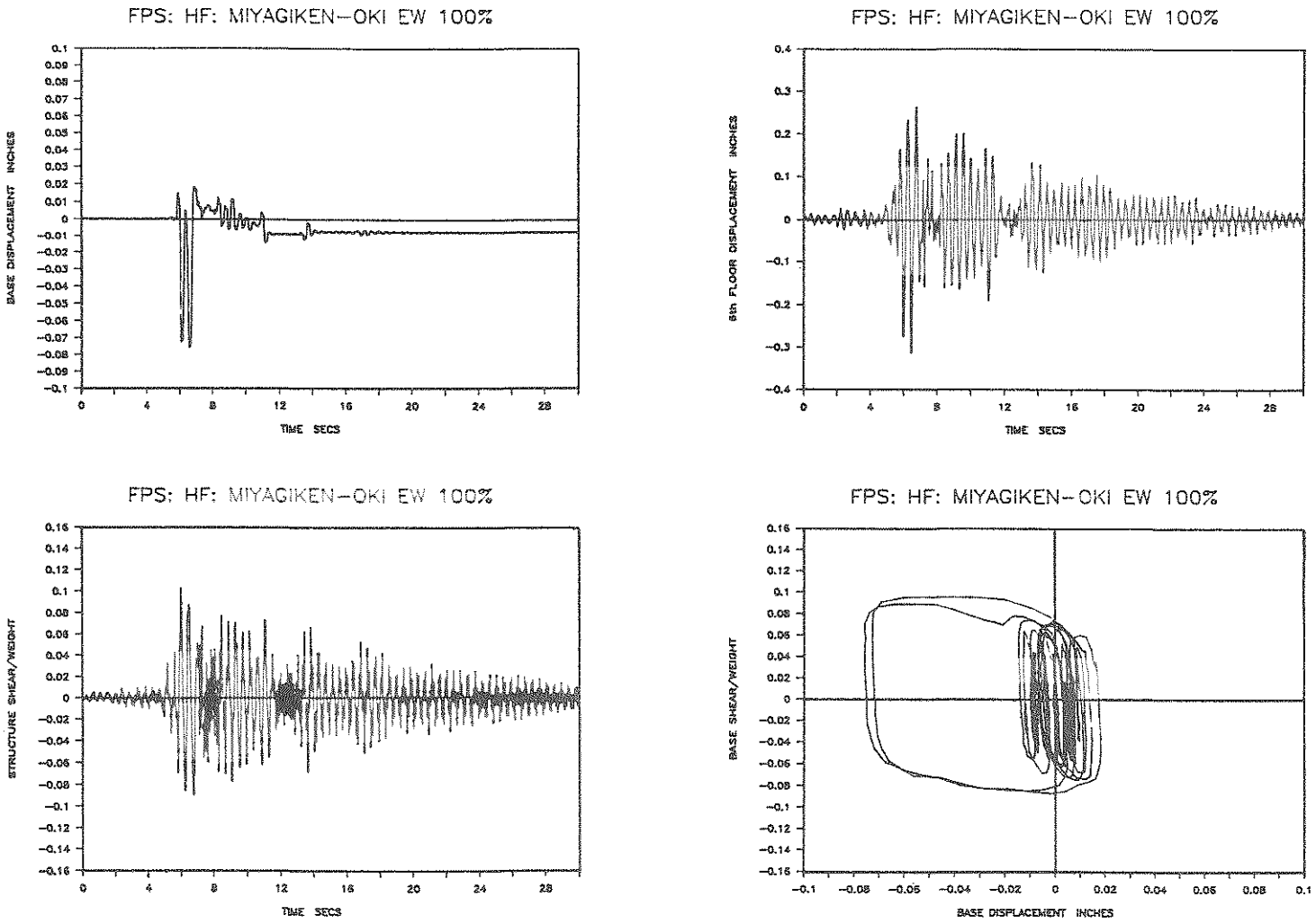

Figure 6-15 Experimental Time Histories of Base (Bearing) Displacement, Structure Shear and Sixth Floor Displacement with Respect to Base and Base Shear-Bearing Displacement Loop in Case of Techmet-B Material and for Miyagiken-Oki Input (0.19g peak table acceleration).

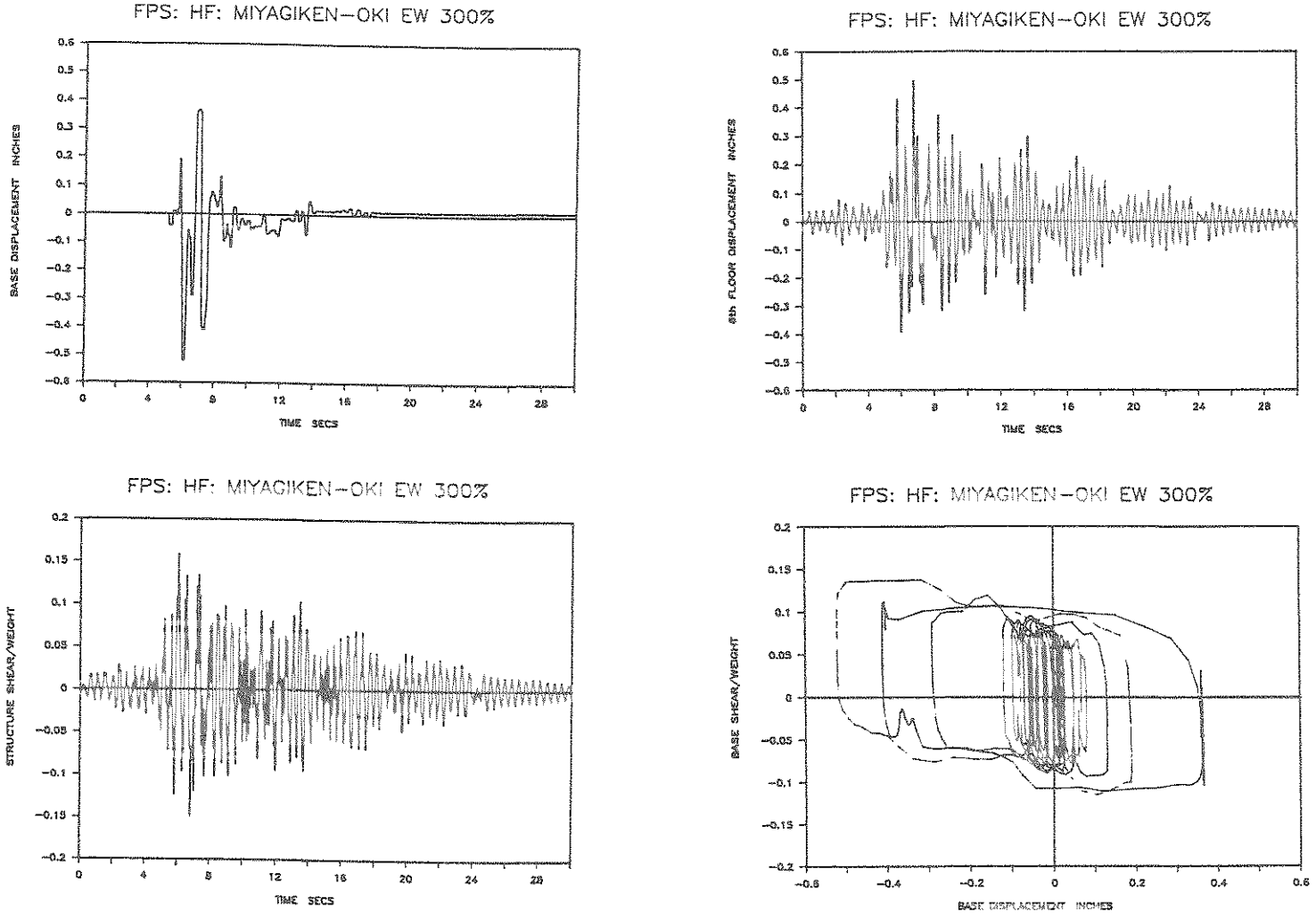

Figure 6-16 Experimental Time Histories of Base (Bearing) Displacement, Structure Shear and Sixth Floor Displacement with Respect to Base and Base Shear-Bearing Displacement Loop in Case of Techmet-B Material and for Miyagiken-Oki Input (0.57g peak table acceleration).

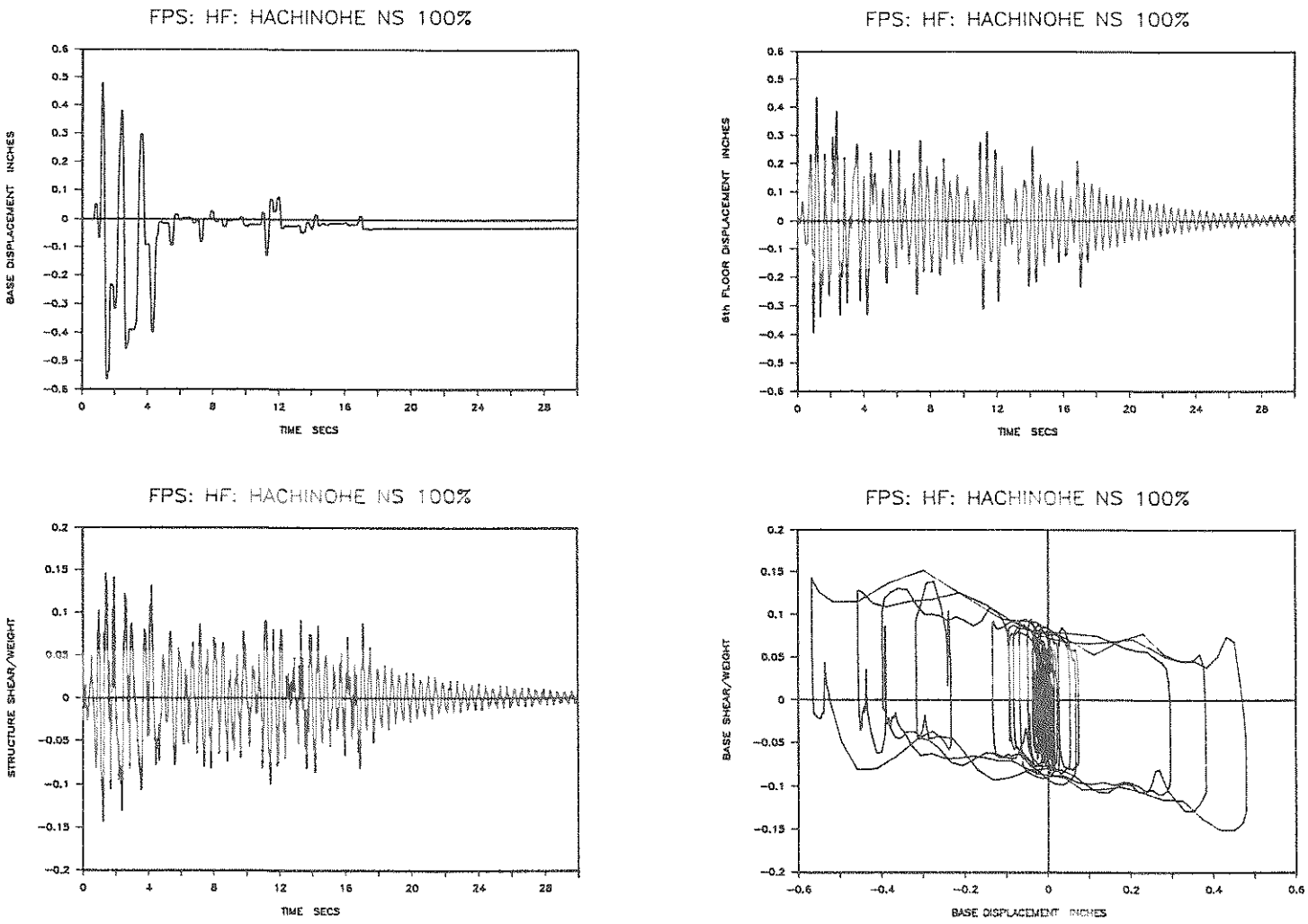

Figure 6-17 Experimental Time Histories of Base (Bearing) Displacement, Structure Shear and Sixth Floor Displacement with Respect to Base and Base Shear-Bearing Displacement Loop in Case of Techmet-B Material and for Hachinohe Input (0.22g peak table acceleration).

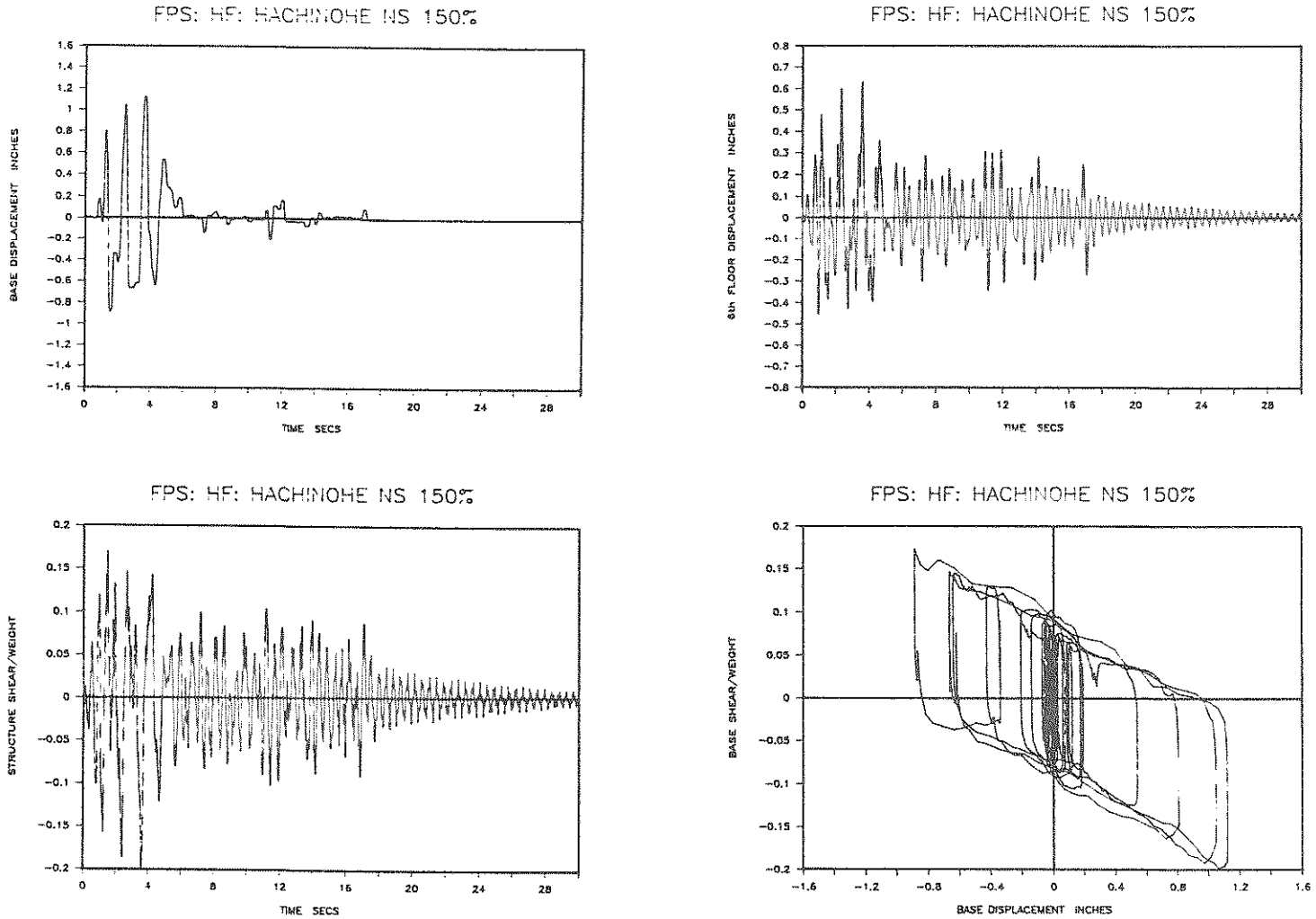

Figure 6-18 Experimental Time Histories of Base (Bearing) Displacement, Structure Shear and Sixth Floor Displacement with Respect to Base and Base Shear-Bearing Displacement Loop in Case of Techmet-B Material and for Hachinohe Input (0.36g peak table acceleration).

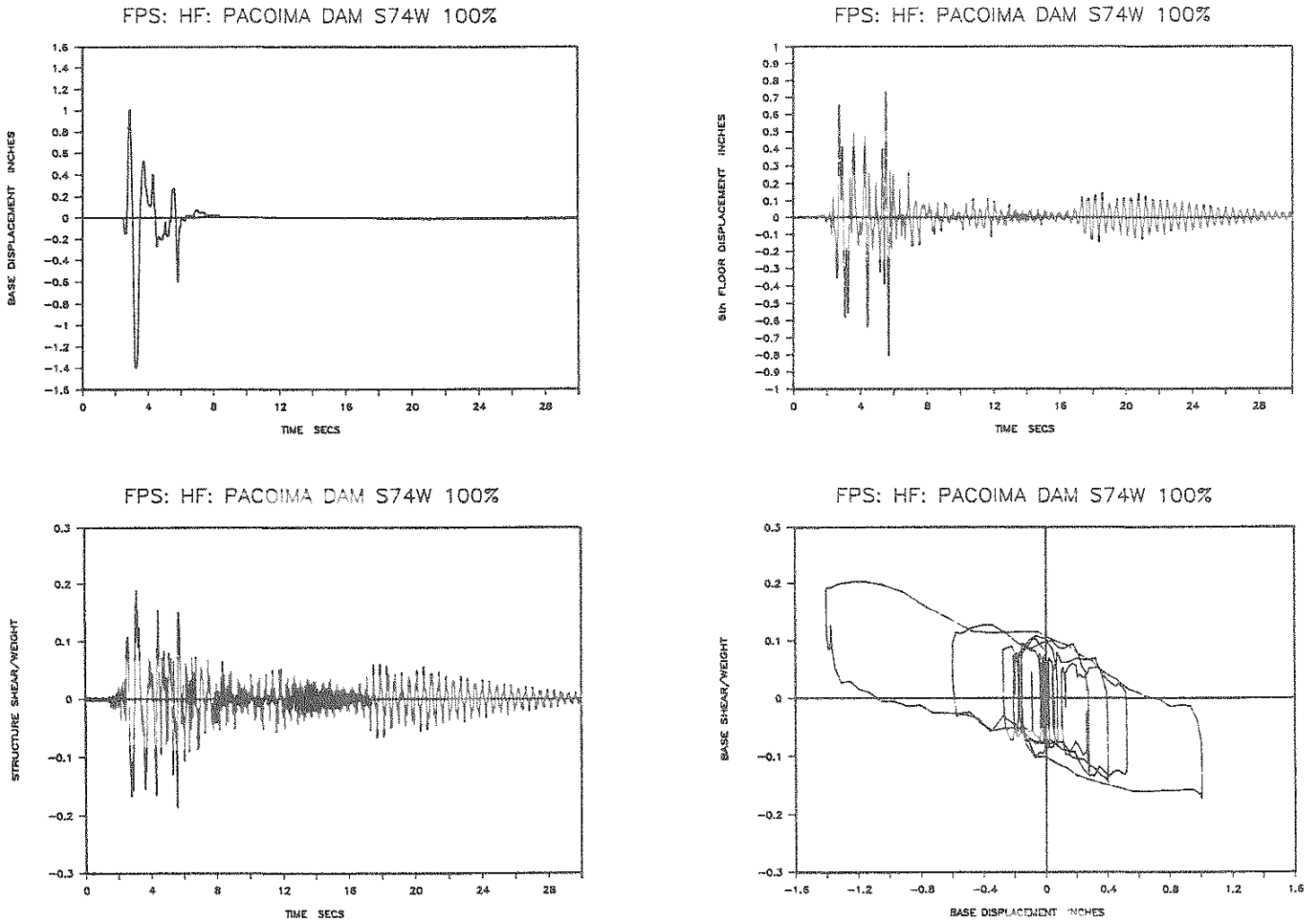

Figure 6-19 Experimental Time Histories of Base (Bearing) Displacement, Structure Shear and Sixth Floor Displacement with Respect to Base and Base Shear-Bearing Displacement Loop in Case of Techmet-B Material and for Pacoima S74W Input (0.92g peak table acceleration).

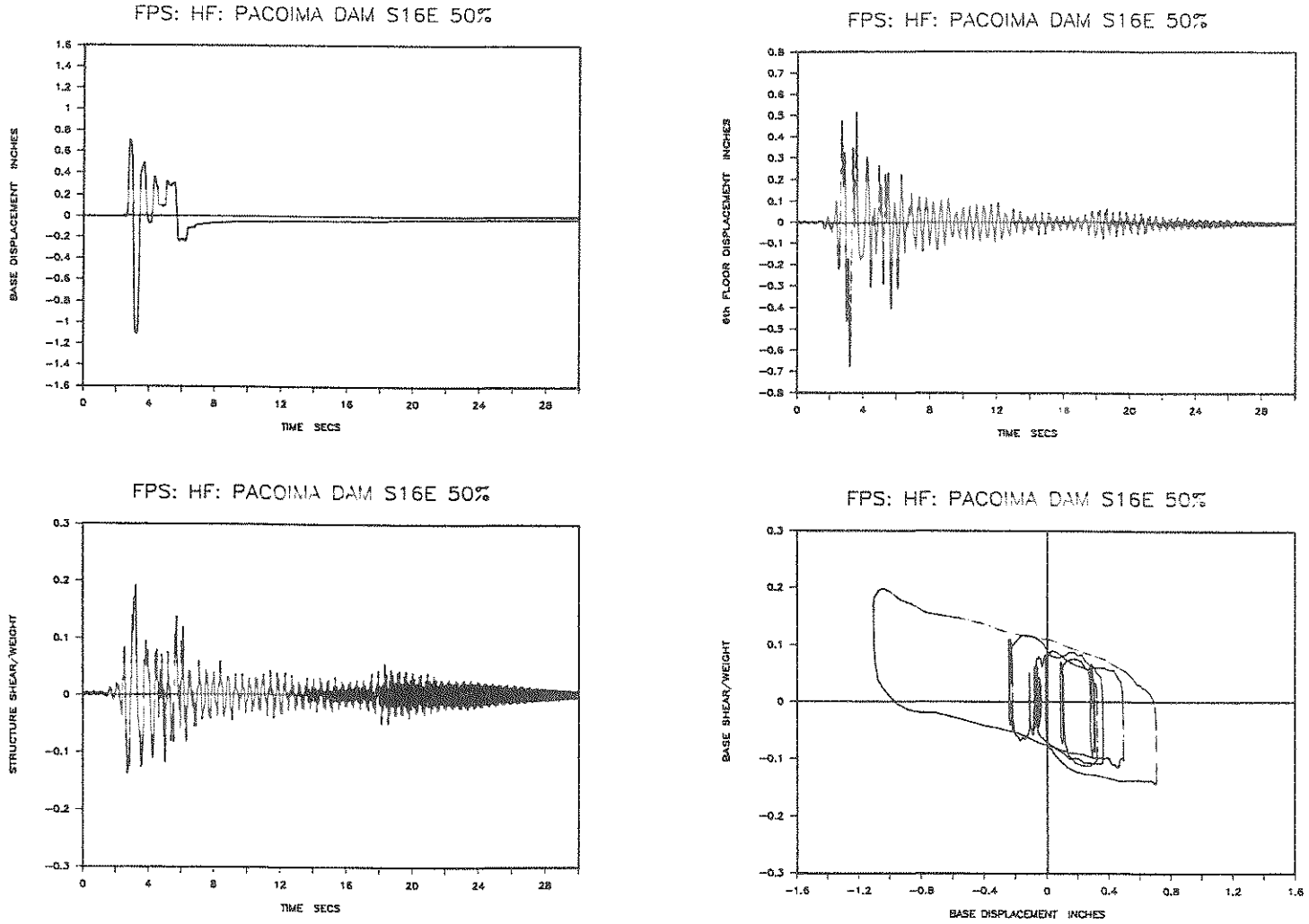

Figure 6-20 Experimental Time Histories of Base (Bearing) Displacement, Structure Shear and Sixth Floor Displacement with Respect to Base and Base Shear-Bearing Displacement Loop in Case of Techmet-B Material and for Pacoima S16E Input (0.56g peak table acceleration).

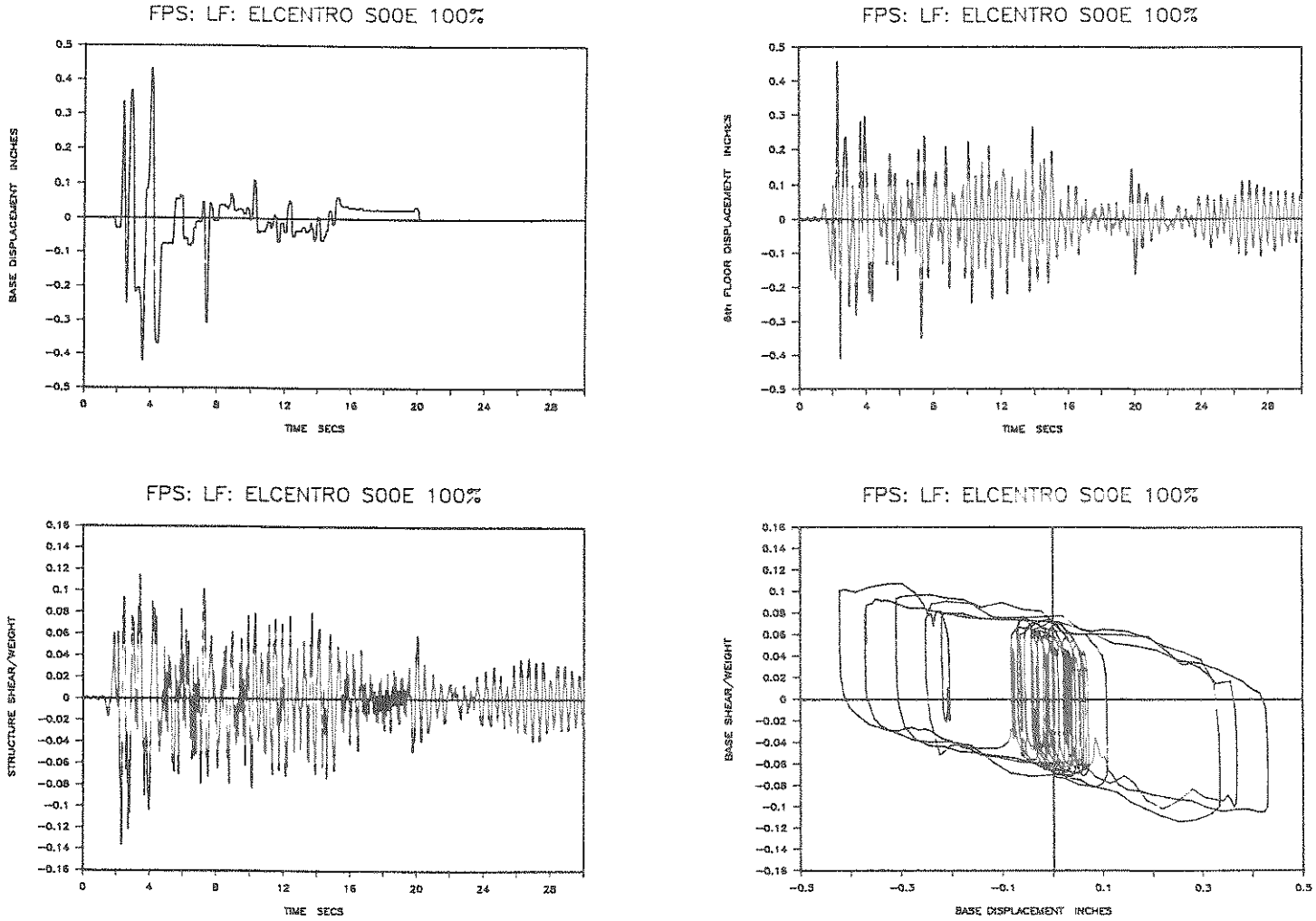

Figure 6-21 Experimental Time Histories of Base (Bearing) Displacement, Structure Shear and Sixth Floor Displacement with Respect to Base and Base Shear-Bearing Displacement Loop in Case of Woven Teflon Material and for El Centro Input (0.31g peak table acceleration).

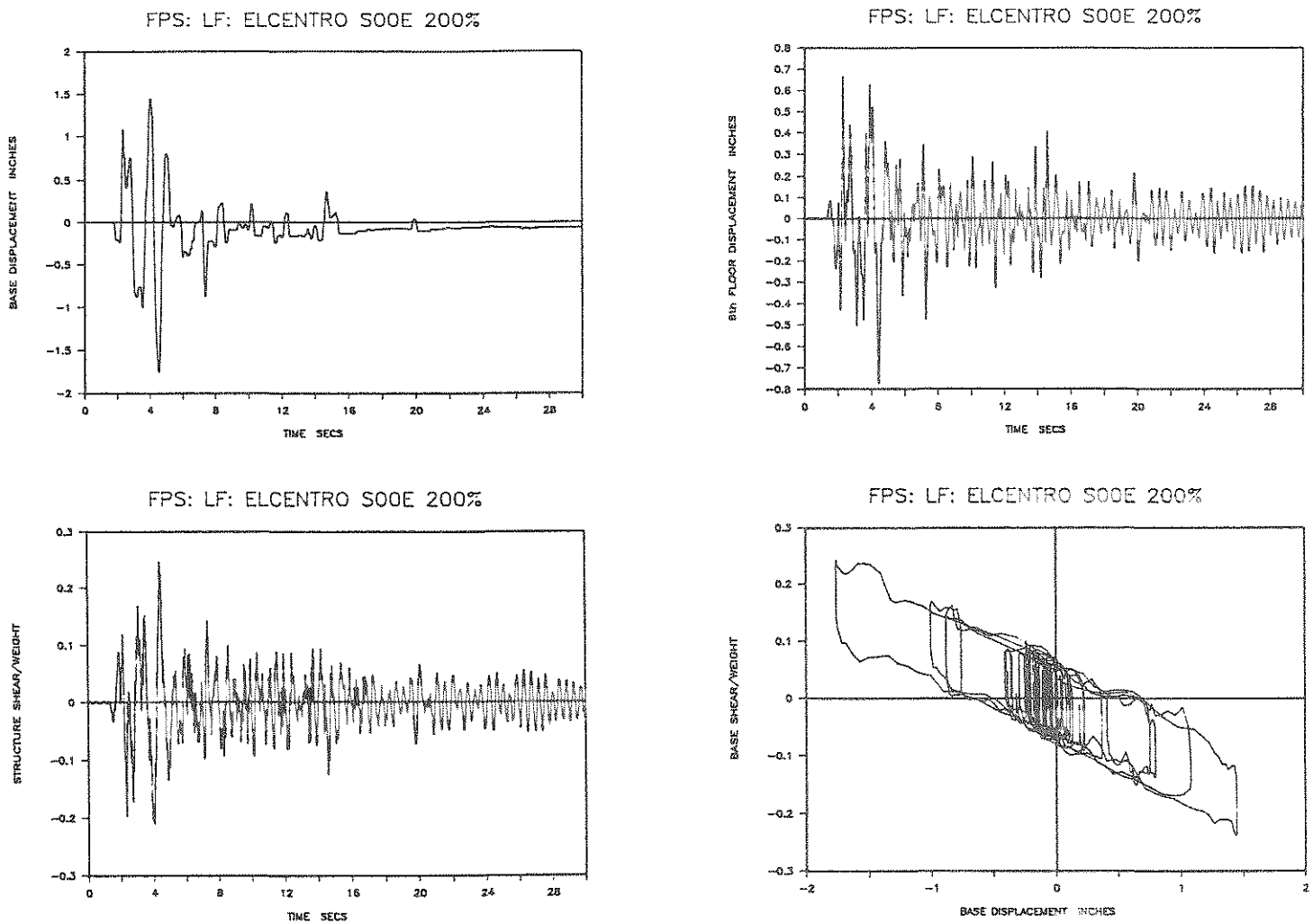

Figure 6-22 Experimental Time Histories of Base (Bearing) Displacement, Structure Shear and Sixth Floor Displacement with Respect to Base and Base Shear-Bearing Displacement Loop in Case of Woven Teflon Material and for El Centro Input (0.60g peak table acceleration).

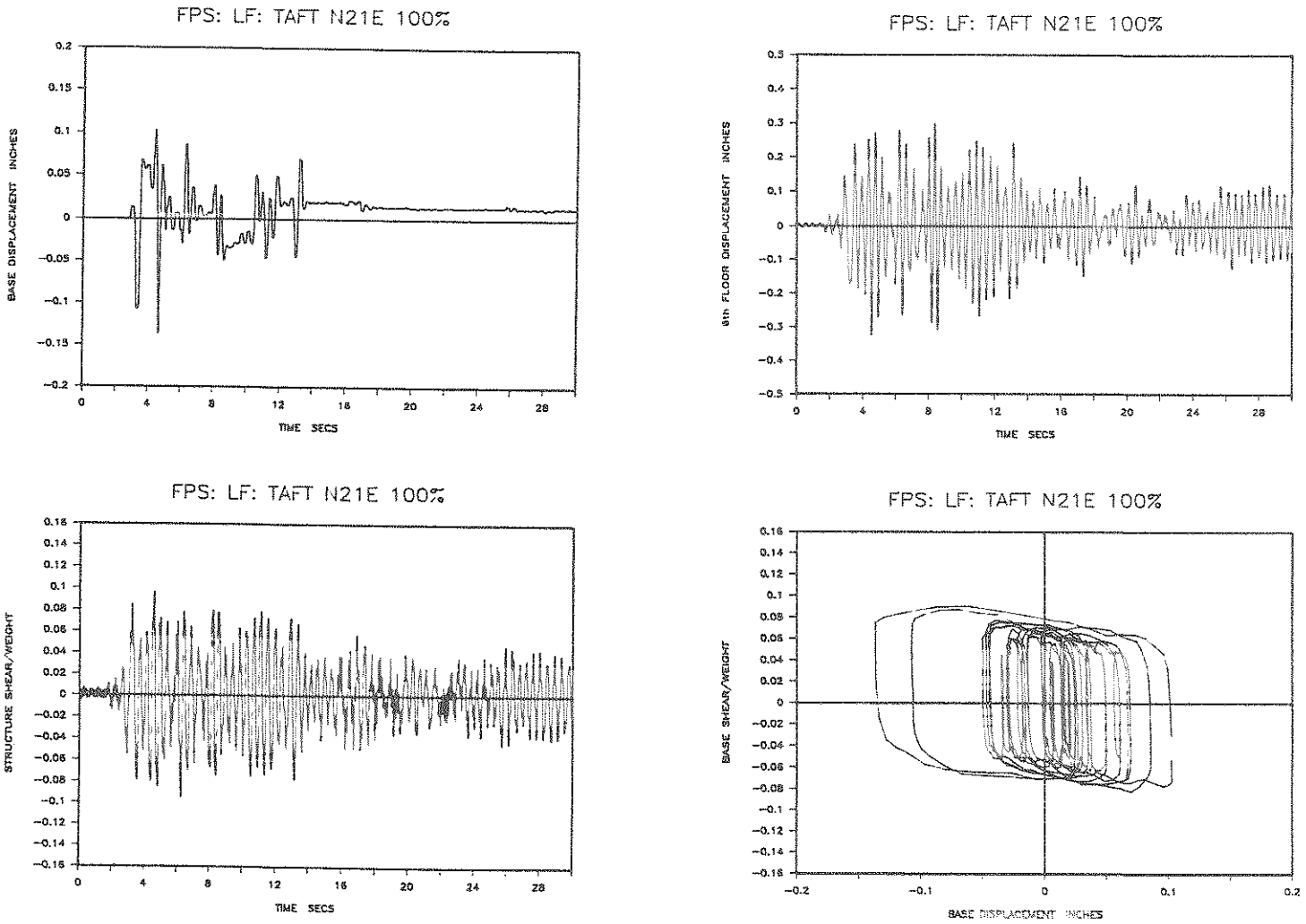

Figure 6-23 Experimental Time Histories of Base (Bearing) Displacement, Structure Shear and Sixth Floor Displacement with Respect to Base and Base Shear-Bearing Displacement Loop in Case of Woven Material and for Taft Input (0.17g peak table acceleration).

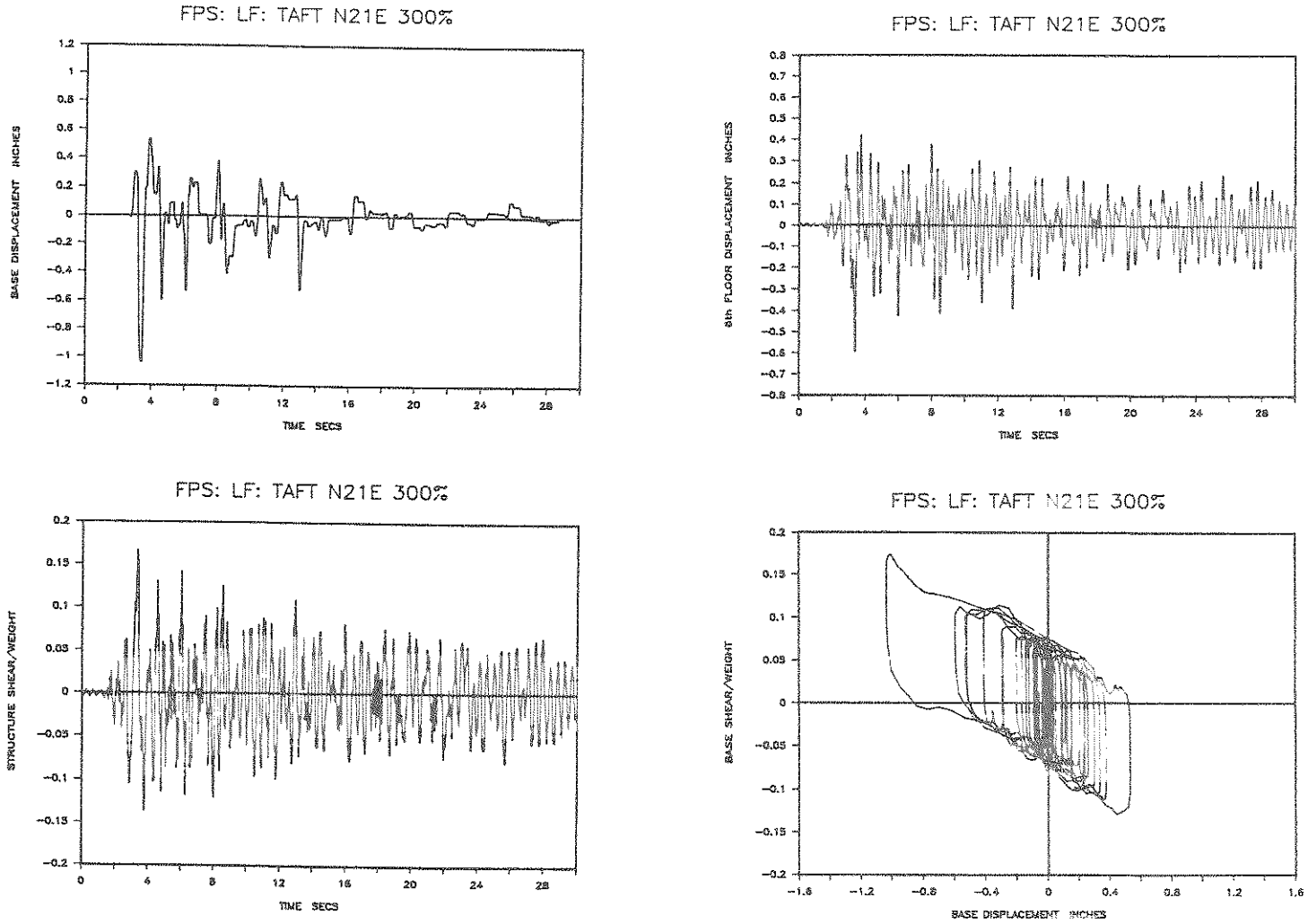

Figure 6-24 Experimental Time Histories of Base (Bearing) Displacement, Structure Shear and Sixth Floor Displacement with Respect to Base and Base Shear-Bearing Displacement Loop in Case of Woven Teflon Material and for Taft Input (0.55g peak table acceleration).

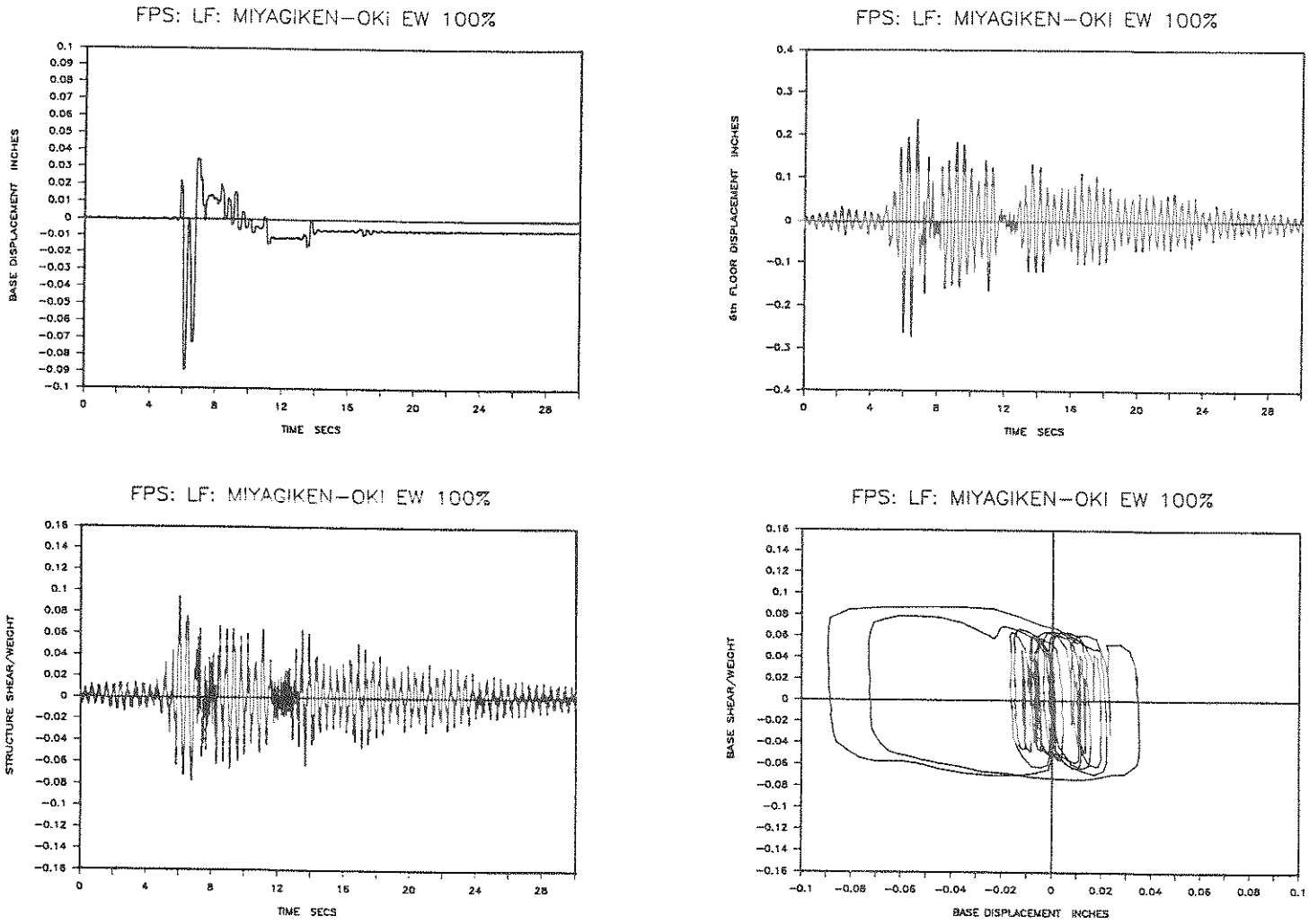

Figure 6-25 Experimental Time Histories of Base (Bearing) Displacement, Structure Shear and Sixth Floor Displacement with Respect to Base and Base Shear-Bearing Displacement Loop in Case of Woven Teflon Material and for Miyagiken-Oki Input (0.19g peak table acceleration).

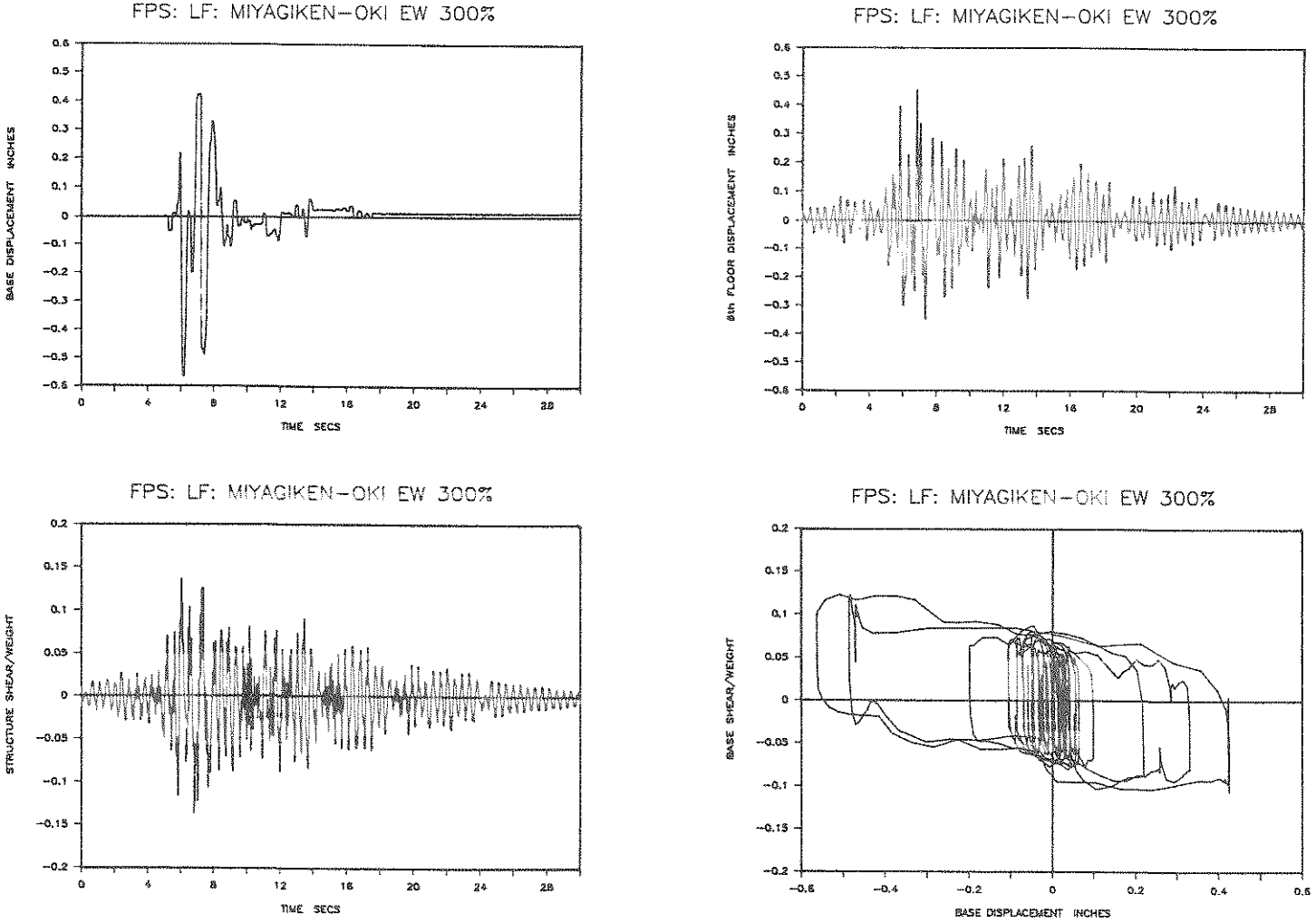

Figure 6-26 Experimental Time Histories of Base (Bearing) Displacement, Structure Shear and Sixth Floor Displacement with Respect to Base and Base Shear-Bearing Displacement Loop in Case of Woven Teflon Material and for Miyagiken-Oki Input (0.56g peak table acceleration).

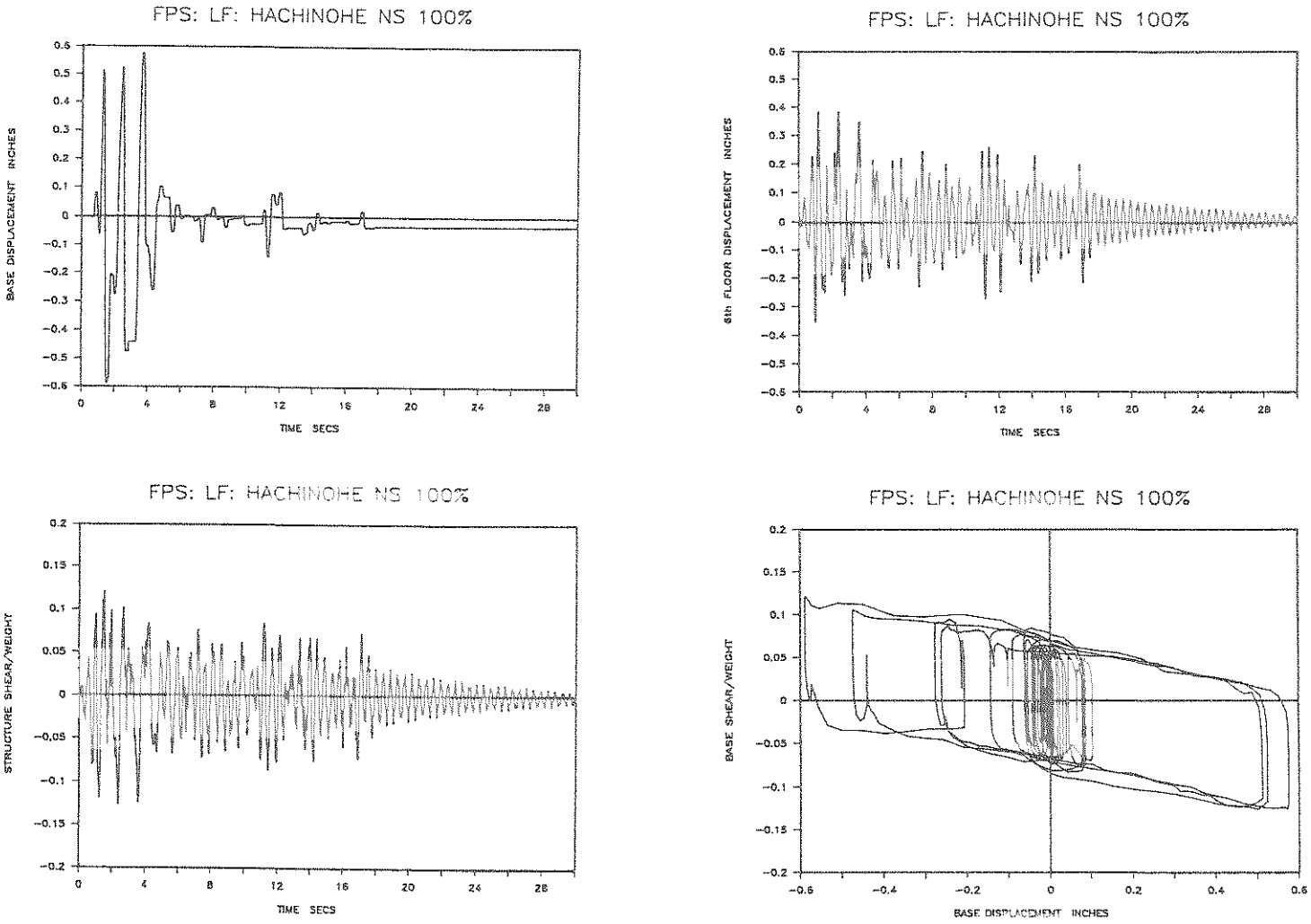

Figure 6-27 Experimental Time Histories of Base (Bearing) Displacement, Structure Shear and Sixth Floor Displacement with Respect to Base and Base Shear-Bearing Displacement Loop in Case of Woven Teflon Material and for Hachinohe Input (0.22g Peak table acceleration).

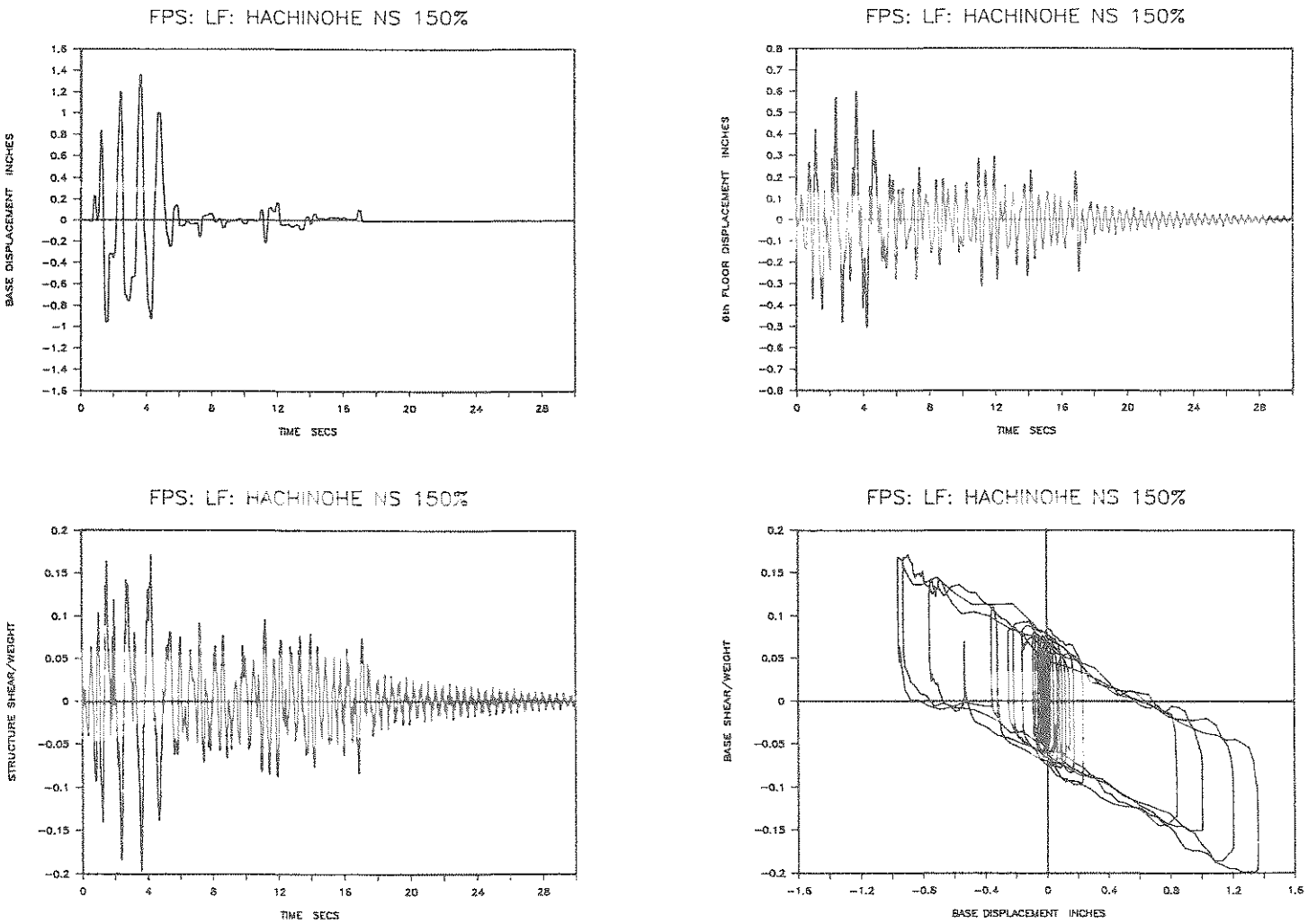

Figure 6-28 Experimental Time Histories of Base (Bearing) Displacement, Structure Shear and Sixth Floor Displacement with Respect to Base and Base Shear-Bearing Displacement Loop in Case of Woven Teflon Material and for Hachinohe Input (0.35g peak table acceleration).

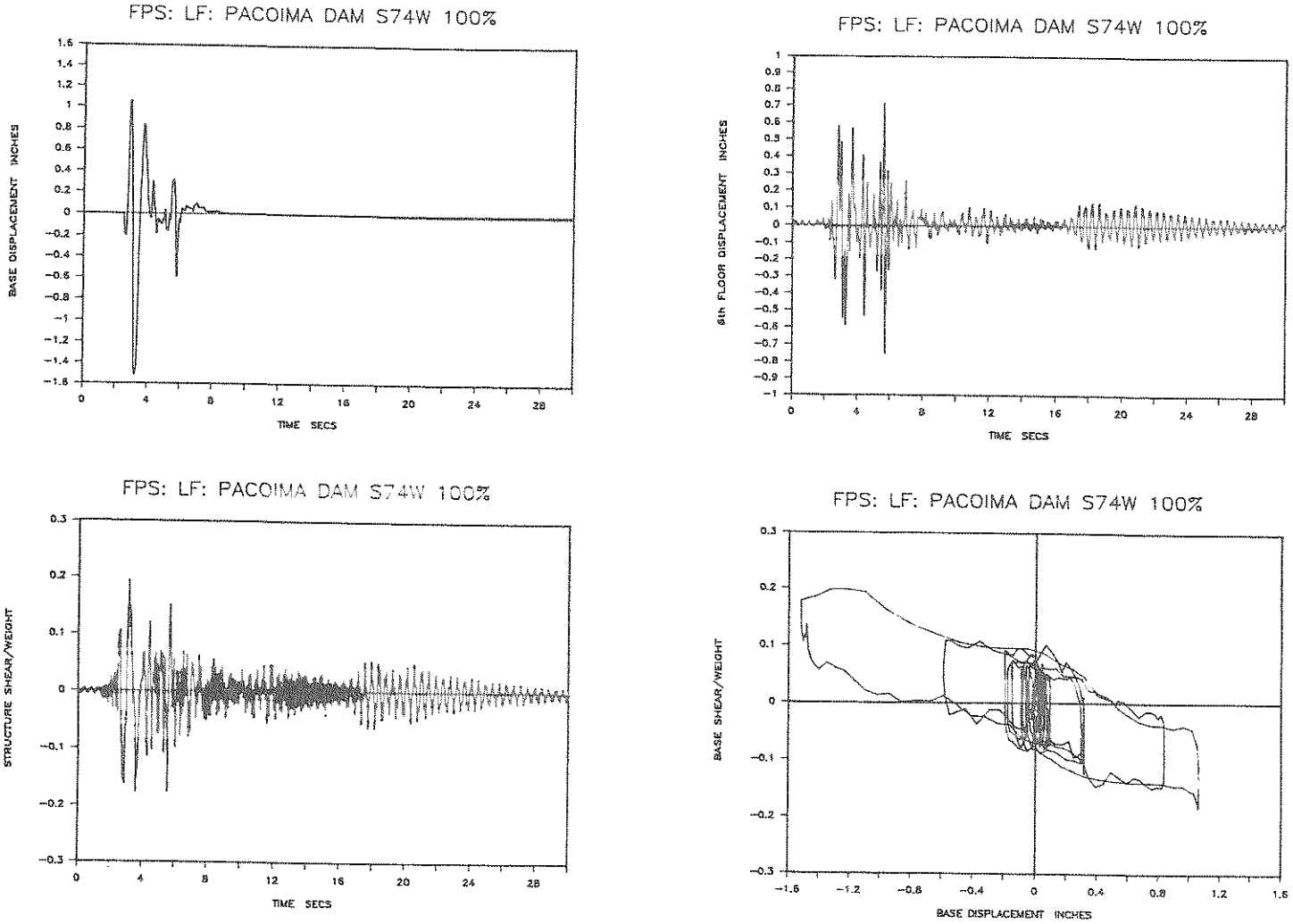

Figure 6-29 Experimental Time Histories of Base (Bearing) Displacement, Structure Shear and Sixth Floor Displacement with Respect to Base and Base Shear-Bearing Displacement Loop in Case of Woven Teflon Material and for Pacoima S74W Input (0.92g peak table acceleration).

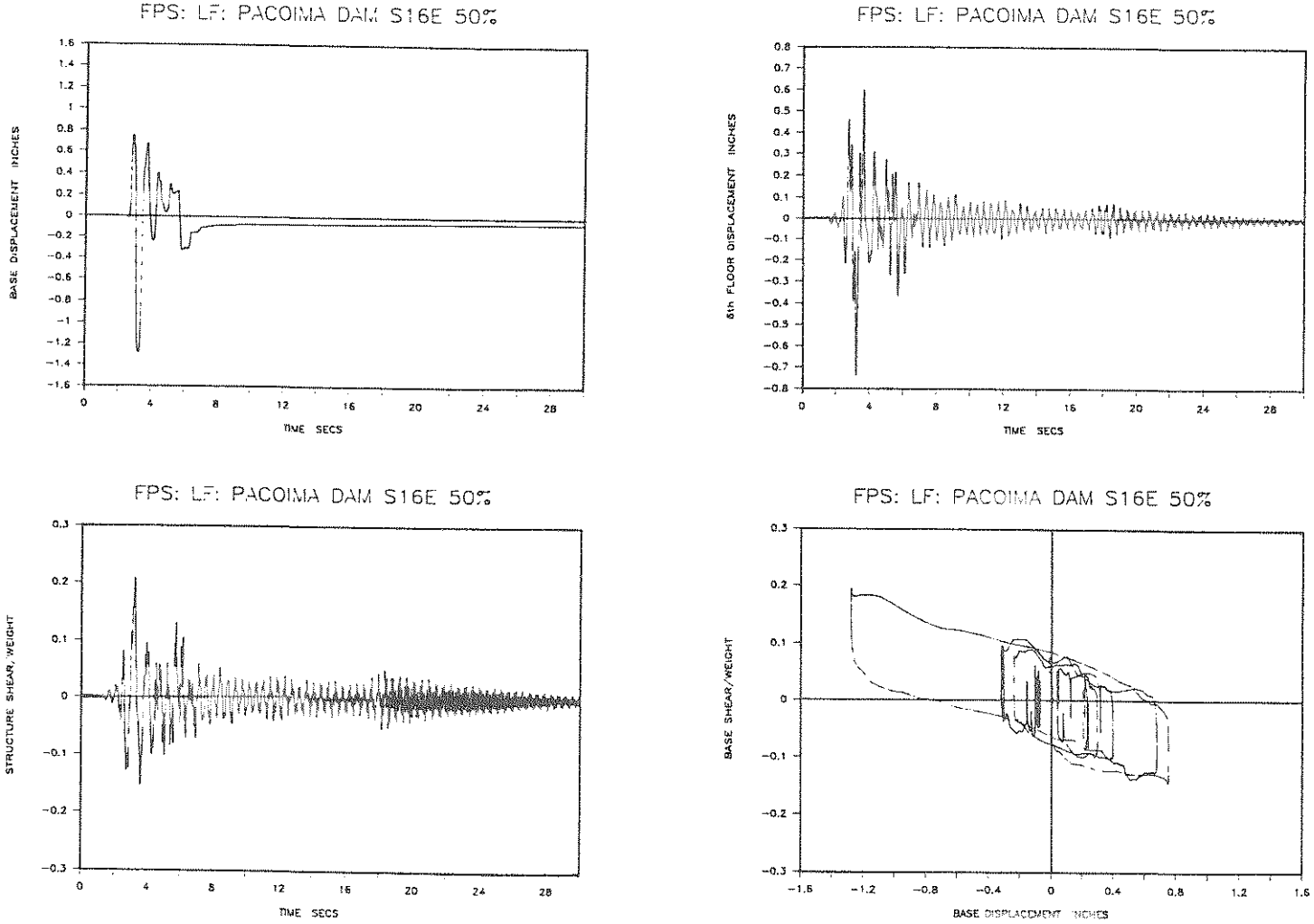

Figure 6-30 Experimental Time Histories of Base (Bearing) Displacement, Structure Shear and Sixth Floor Displacement with Respect to Base and Base Shear-Bearing Displacement Loop in Case of Woven Teflon Material and for Pacoima S16E Input (0.56g peak table acceleration).

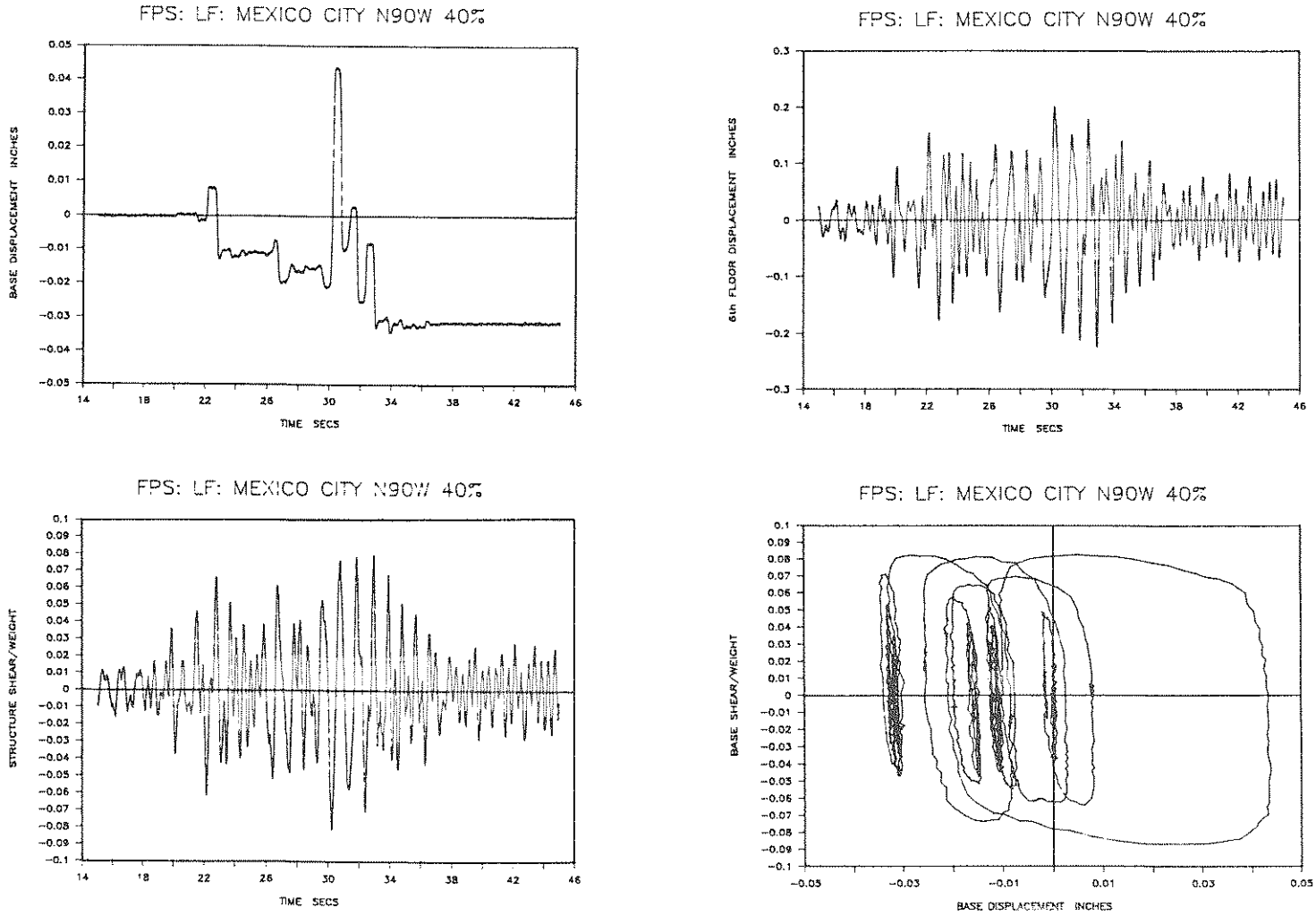

Figure 6-31 Experimental Time Histories of Base (Bearing) Displacement, Structure Shear and Sixth Floor Displacement with Respect to Base and Base Shear-Bearing Displacement Loop in Case of Woven Teflon Material and for Mexico City Input (0.07g peak table acceleration).

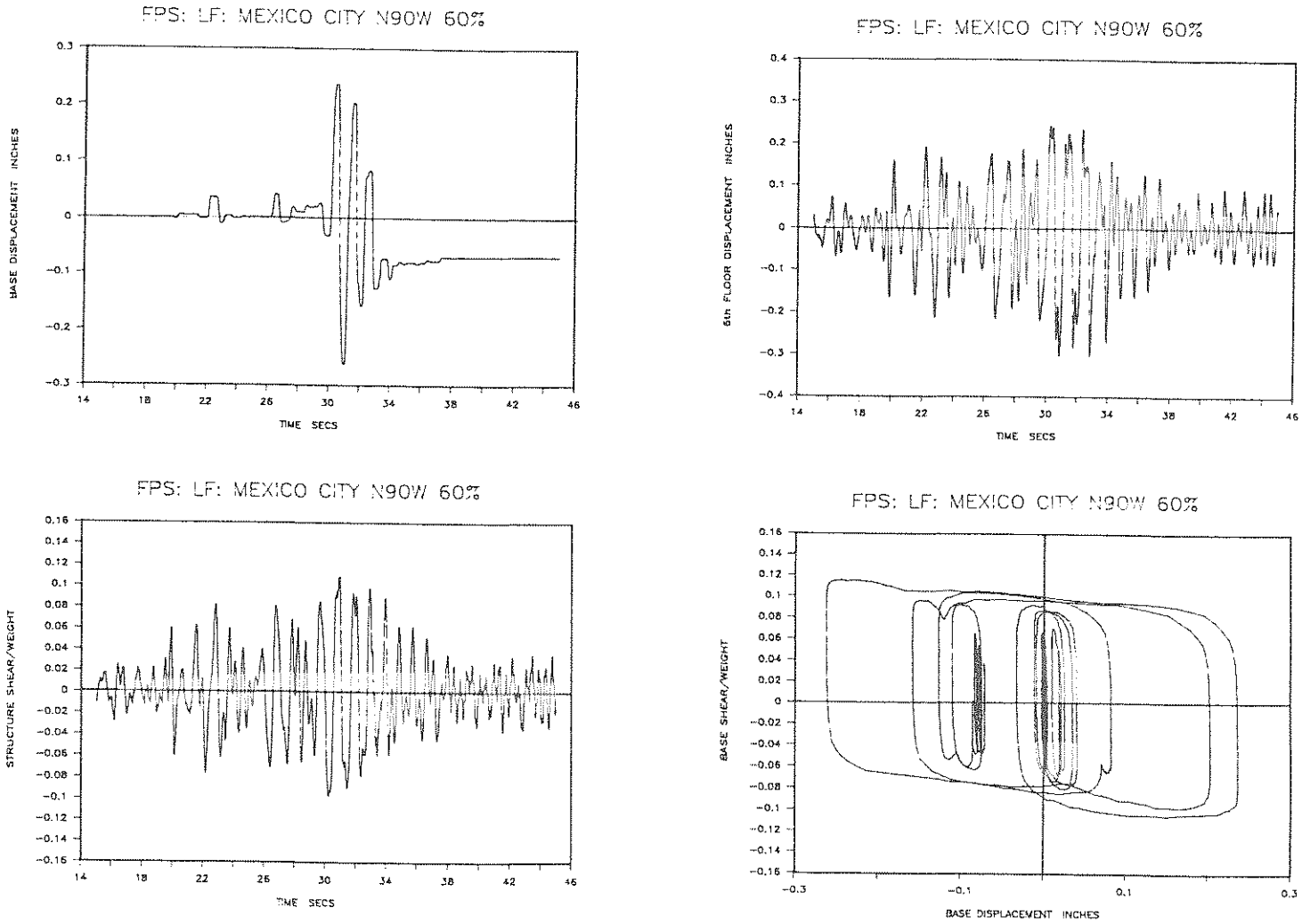

Figure 6-32 Experimental Time Histories of Base (Bearing) Displacement, Structure Shear and Sixth Floor Displacement with Respect to Base and Base Shear-Bearing Displacement Loop in Case of Woven Teflon Material and for Mexico City Input (0.11g peak table acceleration).

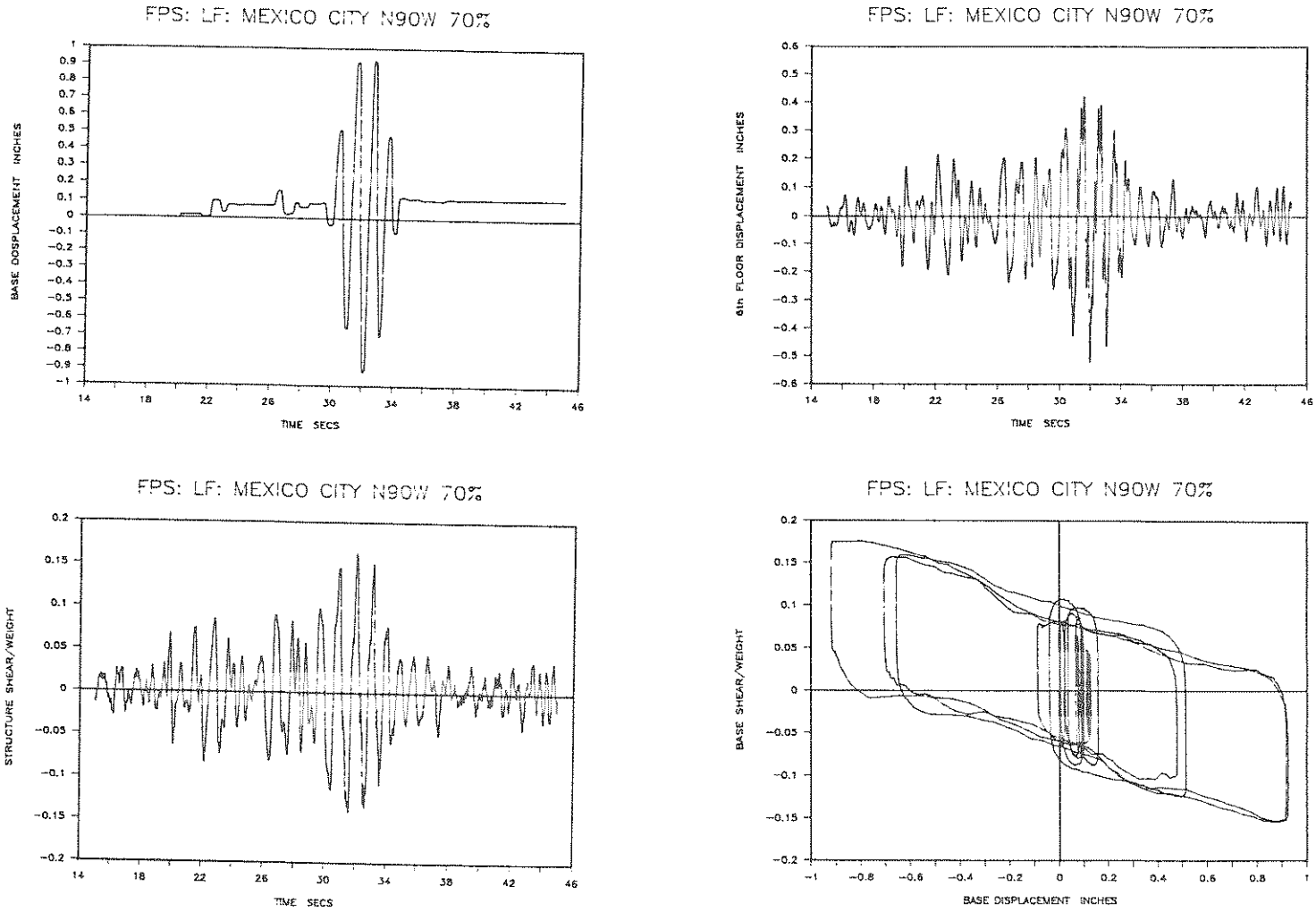

Figure 6-33 Experimental Time Histories of Base (Bearing) Displacement, Structure Shear and Sixth Floor Displacement with Respect to Base and Base Shear-Bearing Displacement Loop in Case of Woven Teflon Material and for Mexico City Input (0.12g peak table acceleration).

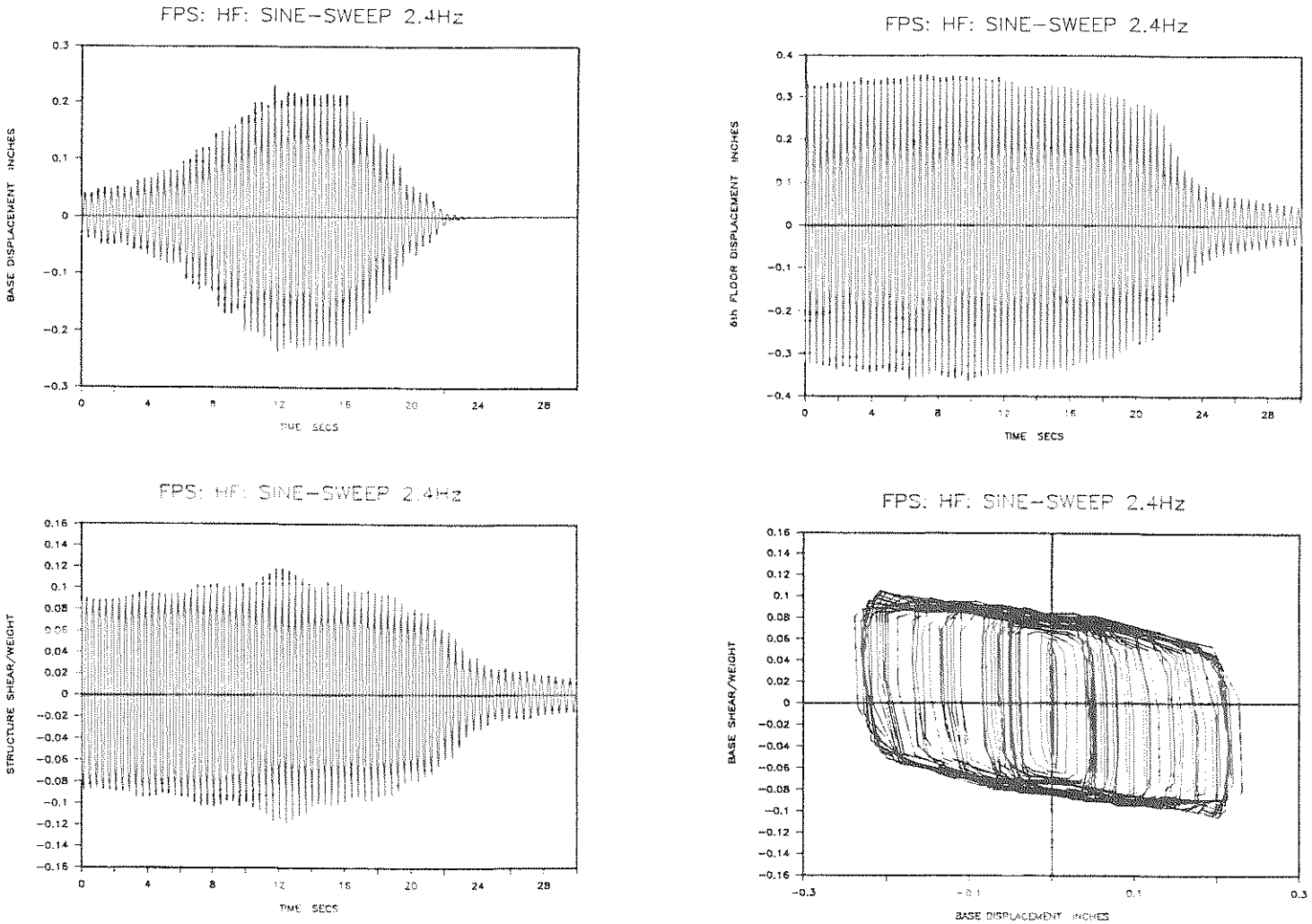

Figure 6-34 Experimental Time Histories of Base (Bearing) Displacement, Structure Shear and Sixth Floor Displacement with Respect to Base and Base Shear-Bearing Displacement Loop in Case of Techmet-B Material and for 2.4Hz Frequency Sinusoidal Input (0.17g peak table acceleration).

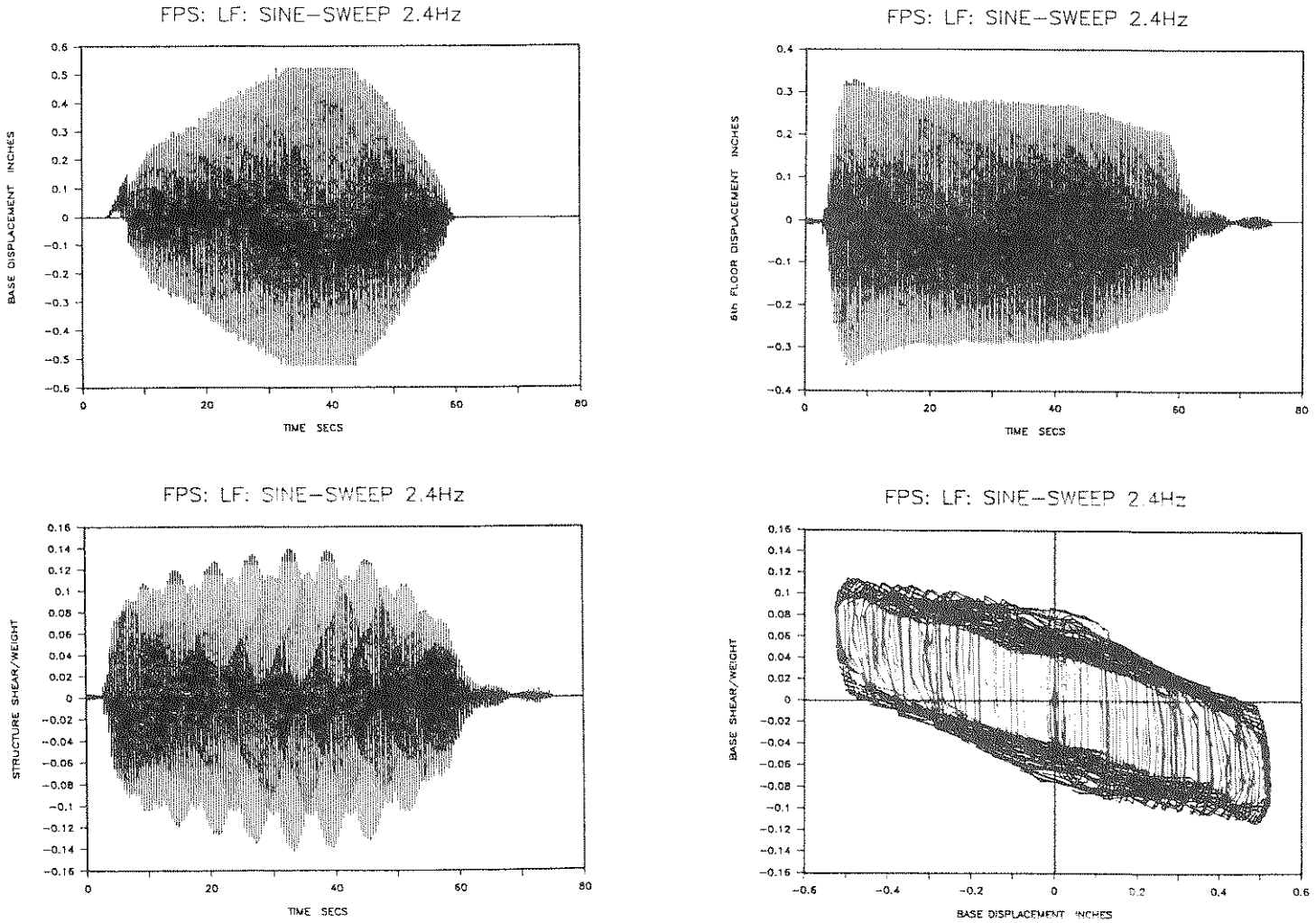

Figure 6-35 Experimental Time Histories of Base (Bearing) Displacement, Structure Shear and Sixth Floor Displacement with Respect to Base and Base Shear-Bearing Displacement Loop in Case of Woven Teflon Material and for 2.4Hz Frequency Sinusoidal Input (0.36g peak table acceleration).

SECTION 7
ANALYTICAL PREDICTION OF RESPONSE

The response of the tested structure was analyzed using a lumped mass model. The equations of motion of the six-story superstructure are:

$$[M]\{\ddot{U}\}+[C]\{\dot{U}\}+[K]\{U\}=-[M]\{1\}(\ddot{U}_g+\ddot{U}_b) \tag{7.1}$$

in which {U} is the vector of floor displacements with respect to the base, U_b is the base displacement with respect to the table and U_g is the table displacement (Figure 7-1). A dot denotes differentiation with respect to time. The mass matrix, [M], is diagonal. The stiffness matrix, [K], was determined by condensation of a stiffness matrix with 288 degrees of freedom which was constructed using a general purpose finite element program (GTSTRUDL). The damping matrix, [C], was constructed from the analytically determined frequencies and mode shapes (see Table 2-I) and the experimentally determined damping ratios using a procedure described by Clough and Penzien, 1975.

The additional needed equation was determined from the dynamic equilibrium of the entire system in the horizontal direction:

$$\sum_{i=1}^{6} m_i(\ddot{U}_i+\ddot{U}_b+\ddot{U}_g)+m_b(\ddot{U}_b+\ddot{U}_g)+F_b=0 \tag{7.2}$$

in which m_i , i=1,..,6 are the floor masses, m_b is the base mass and F_b is the force mobilized at the isolation interface. This force is given by:

$$F_b=\left(\frac{W}{R}\right)U_b+\mu(\dot{U}_b)WZ \tag{7.3}$$

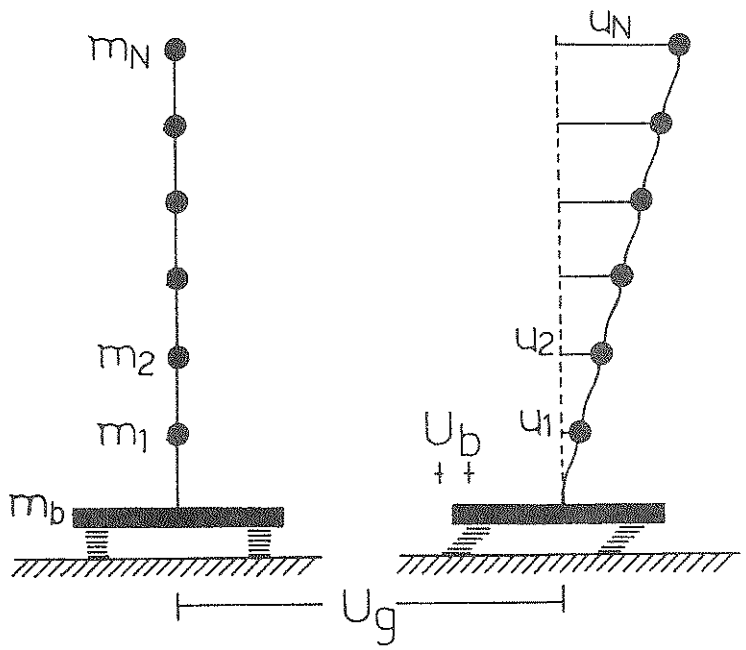

Figure 7-1 Mathematical Model of Test Structure.

in which μ is described by Eq. (4.3) with parameters f_{max} , Df and a determined experimentally as explained earlier. Z is a variable governed by the following differential equation (Constantinou et al, 1990):

$$Y\dot{Z} + \gamma|\dot{U}_b|Z|Z|^{+}\beta\dot{U}_b Z^2 - \dot{U}_b = 0 \tag{7.4}$$

in which Y = 0.005 inches (0.127 mm) and $\beta + \gamma = 1$. Z replaces the signum function in Eq. (4.1) and is used to account for the conditions of separation and reattachment.

The stiffness matrix of the superstructure could also be constructed from the frequencies, mode shapes and mass matrix by applying the procedure described below (Clough and Penzien, 1975). We let ω_i and $\{\phi_i\}$ be the ith frequency and corresponding mode shape of the superstructure. They satisfy the following eigenvalue equation:

$$\omega_i^2[M]\{\phi_i\} = [K]\{\phi_i\} \tag{7.5}$$

The diagonal generalized mass and stiffness matrices are defined as:

$$[M^*] = [\phi]^T[M][\phi] \tag{7.6}$$

$$[K^*] = [\phi]^T[K][\phi] \tag{7.7}$$

where $[\phi]$ is a matrix having as columns the mode shapes $\{\phi_i\}$. It may be easily shown that:

$$[\phi]^{-1} = [M^*]^{-1}[\phi]^T[M] \tag{7.8}$$

Equation (7.7) is solved for [K] and using Eq. (7.8) we arrive at the following:

$$[K] = [M][\phi][M^*]^{-1}[K^*][M^*]^{-1}[\phi]^T[M] \tag{7.9}$$

Noting that matrix [M*] is diagonal with elements m_i^*:

$$m_i^* = \{\phi_i\}^T[M]\{\phi_i\} \tag{7.10}$$

we rewrite Eq. (7.9) in the following convenient form:

$$[K]=[M]\left(\sum_{i=1}^{L}\frac{\omega_i^2}{m_i^*}\{\phi_i\}\{\phi_i\}^T\right)[M] \tag{7.11}$$

in which L is the number of modes to be maintained in the construction of the stiffness matrix.

A similar procedure results in the following equation for the damping matrix of the superstructure:

$$[C]=[M]\left(\sum_{i=1}^{L}\frac{2\xi_i\omega_i}{m_i^*}\{\phi_i\}\{\phi_i\}^T\right)[M] \tag{7.12}$$

where ξ_i is the damping ratio corresponding to mode i. Equation (7.12) has been used in the construction of matrix [C] with ξ_i being the experimental values in Table 2-I and ω_i , $\{\phi_i\}$ being the analytical frequencies and mode shapes which are also given in Table 2-I. The mass matrix used in the construction of the damping matrix and in Eq. (7.1) is diagonal with elements corresponding to the floor weight as used in the calculation of the base and structural shear from acceleration records: 7.65 Kips for the sixth floor and 7.84 Kips for floors fifth to first. The base mass, m_b, used in Eq. (7.2) corresponds to the base weight of 4.56 Kips.

Equations (7.11) and (7.12) could be used in the construction of matrices [K] and [C] using experimental values of frequencies, damping ratios and mode shapes.

Equations (4.3) to (7.4) are reduced to a system of first order differential equations and numerically integrated using an adaptive integration technique with truncation error control which is appropriate for stiff differential equations (Gear, 1971). Figures 7-2 to 7-7 present analytically determined responses of the model structure for conditions identical to those which resulted in the experimental responses of Figures 6-12, 6-18, 6-19, 6-22, 6-28, and 6-29, respectively. A comparison of the two sets of figures shows a very good agreement between analytical and exper-

imental results. It should be noted that the analytical prediction is not restricted to only peak response values but is capable of reproducing almost every detail of the observed response.

Evidently, analytical techniques are available for the prediction of the response of sliding isolation systems.

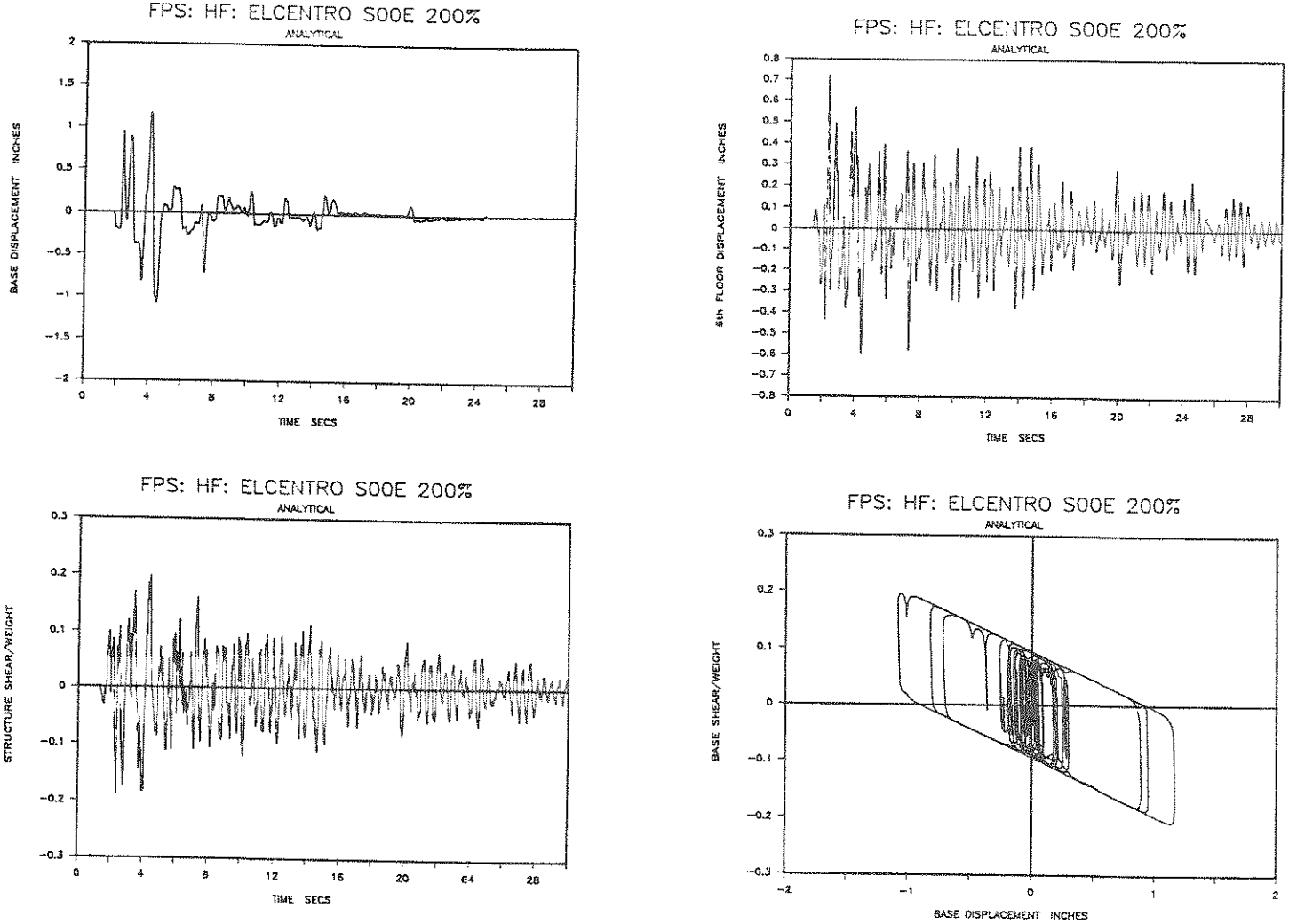

Figure 7-2 Analytical Time Histories of Base (Bearing) Displacement, Structure Shear and Sixth Floor Displacement with Respect to Base and Base Shear-Bearing Displacement Loop in Case of Techmet-B Material and for El Centro Input (0.78g Peak Acceleration). Compare With Figure 6-12.

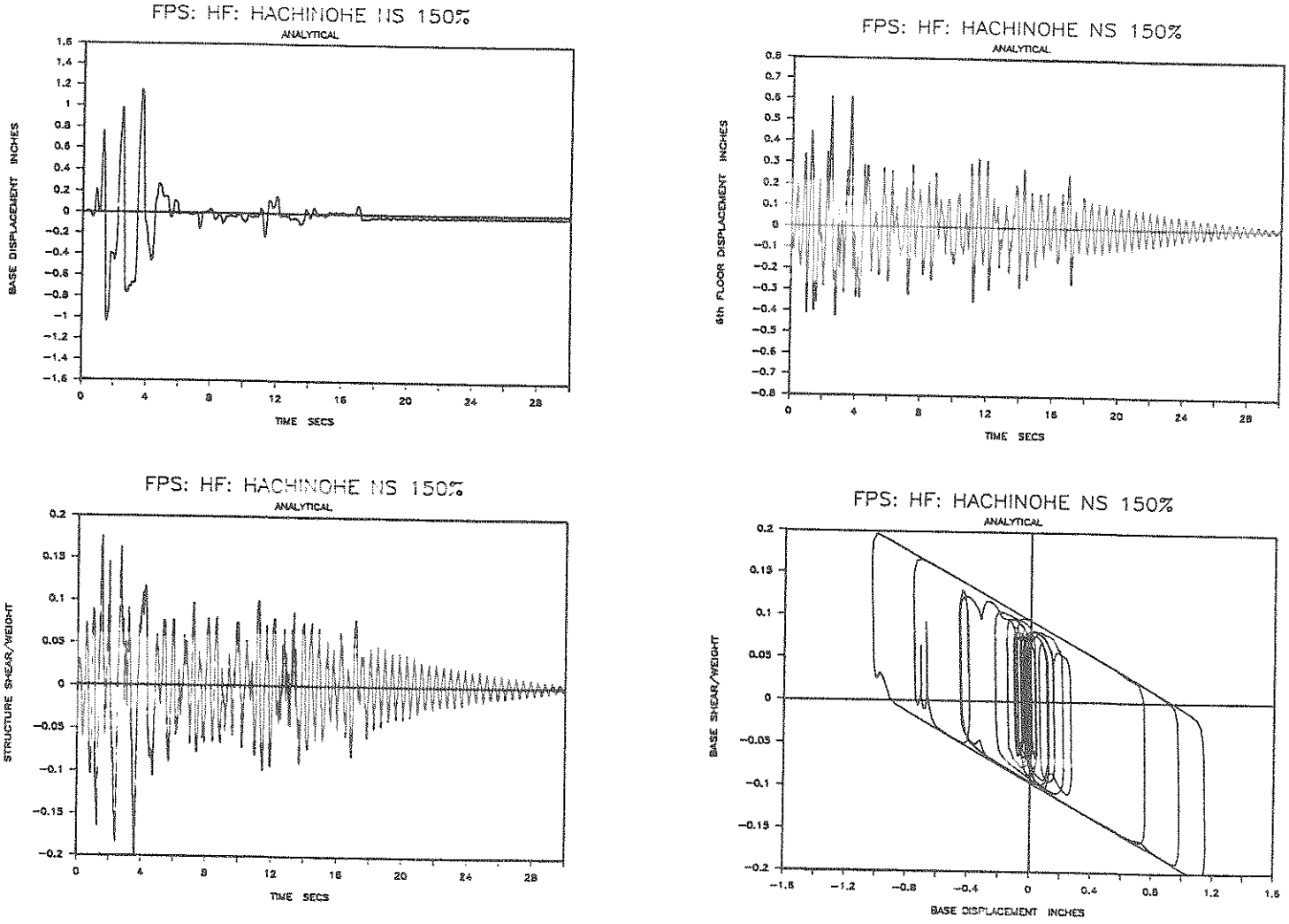

Figure 7-3 Analytical Time Histories of Base (Bearing) Displacement, Structure Shear and Sixth Floor Displacement with Respect to Base and Base Shear-Bearing Displacement Loop in Case of Techmet-B Material and for Hachinohe Input (0.36g Peak Acceleration). Compare With Figure 6-18.

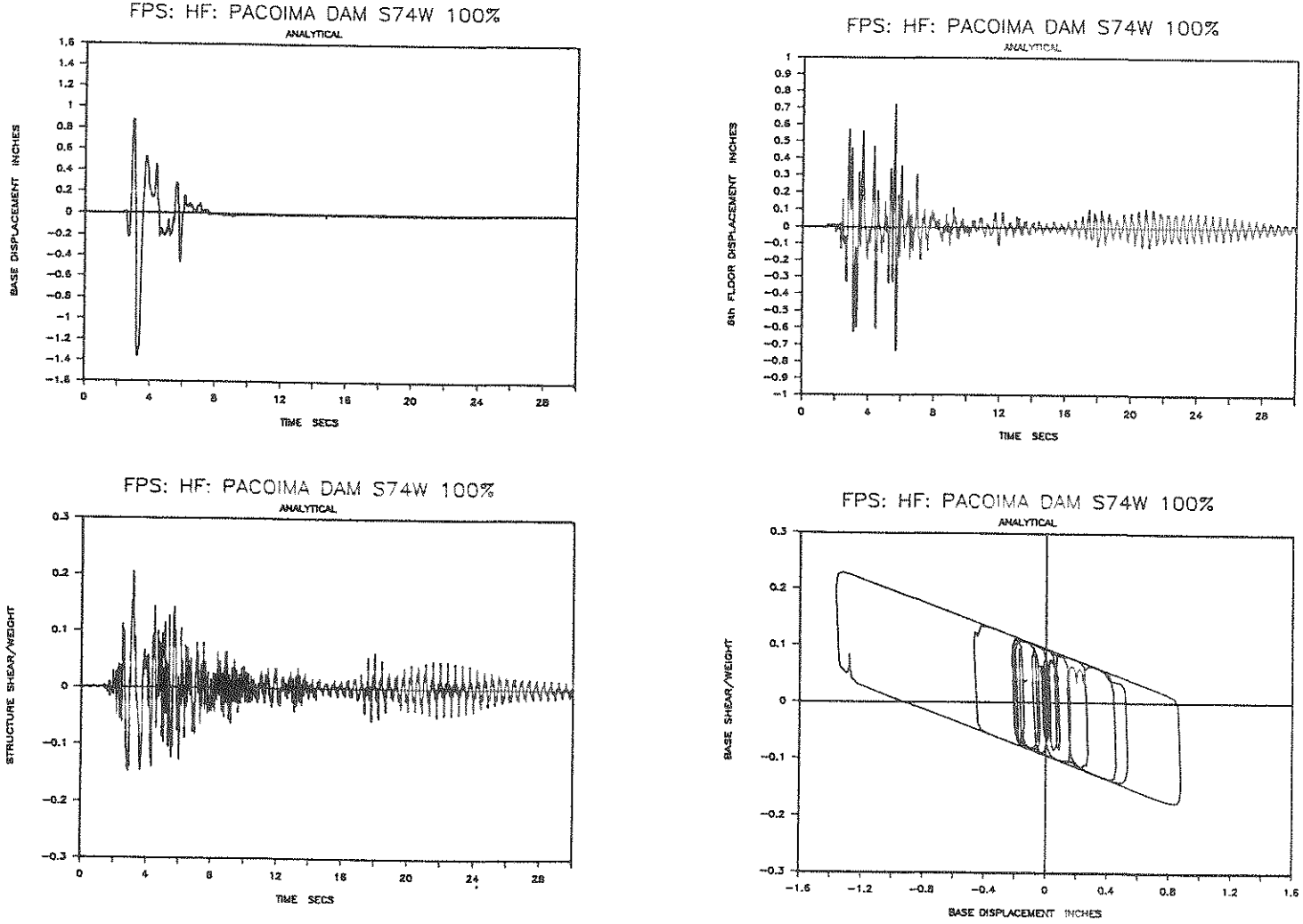

Figure 7-4 Analytical Time Histories of Base (Bearing) Displacement, Structure Shear and Sixth Floor Displacement with Respect to Base and Base Shear-Bearing Displacement Loop in Case of Techmet-B Material and for Pacoima S74W Input (0.92g Peak Acceleration). Compare With Figure 6-19.

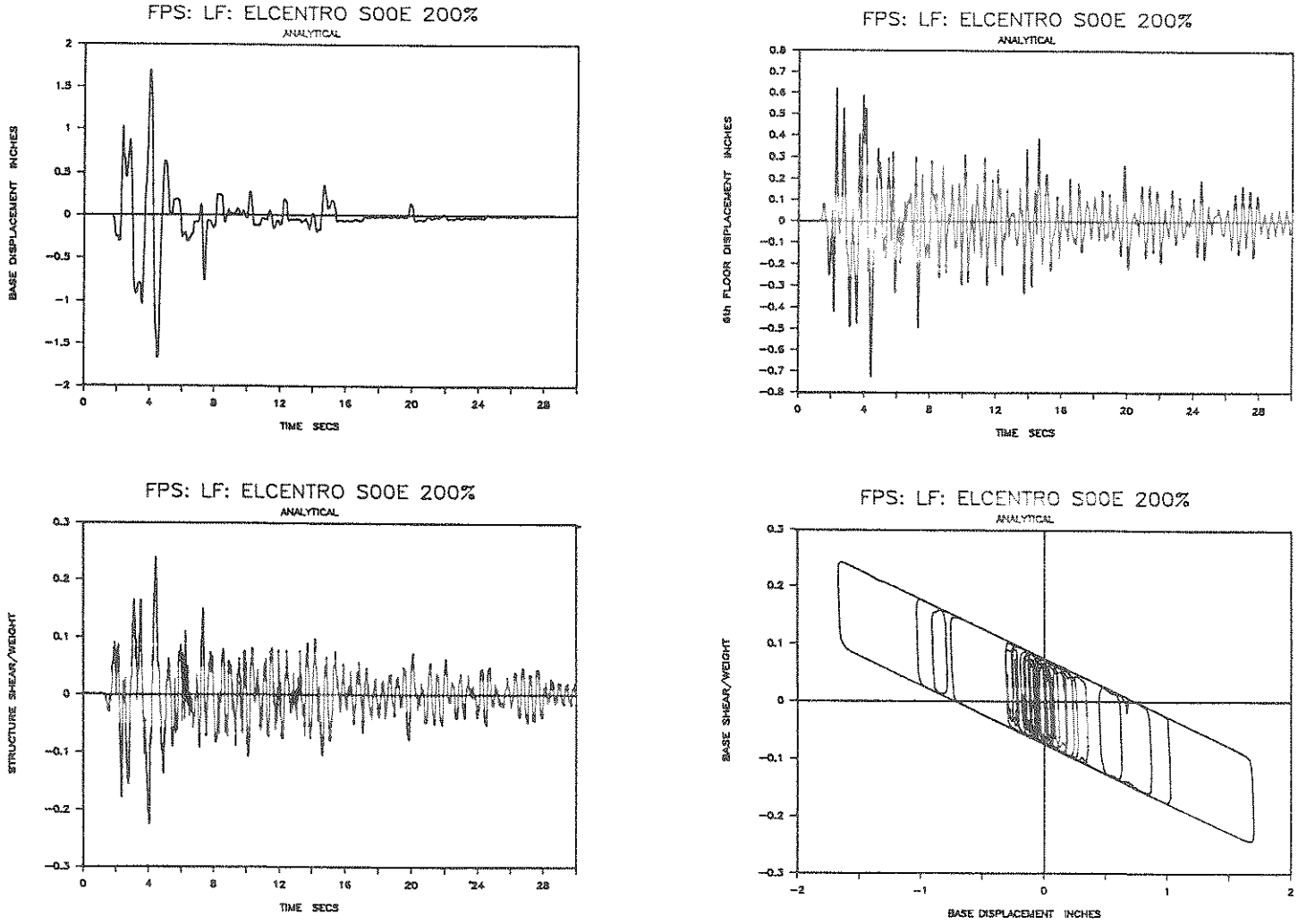

Figure 7-5 Analytical Time Histories of Base (Bearing) Displacement, Structure Shear and Sixth Floor Displacement with Respect to Base and Base Shear-Bearing Displacement Loop in Case of Woven Teflon Material and for El Centro Input (0.60g Peak Acceleration). Compare With Figure 6-22.

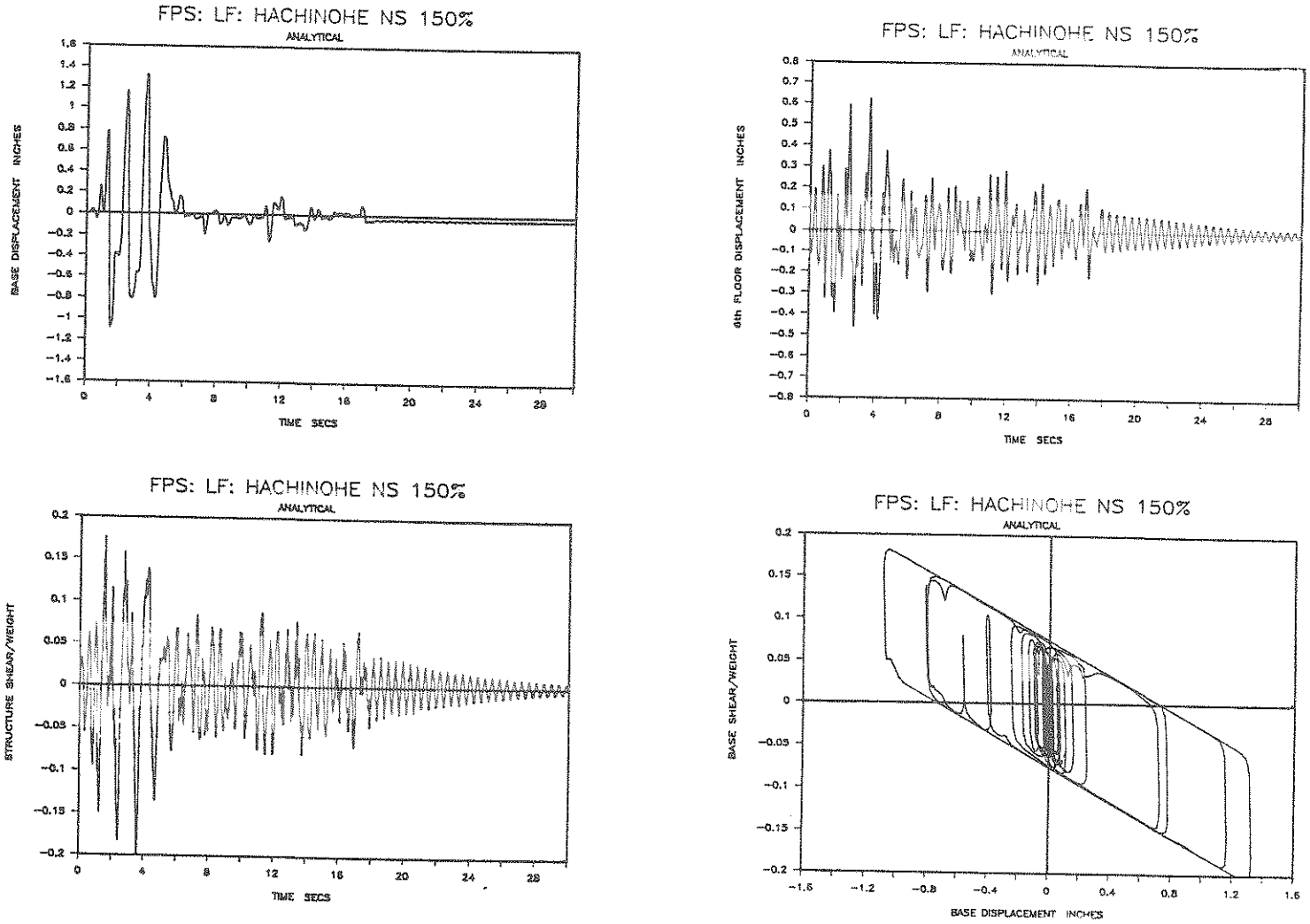

Figure 7-6 Analytical Time Histories of Base (Bearing) Displacement, Structure Shear and Sixth Floor Displacement with Respect to Base and Base Shear-Bearing Displacement Loop in Case of Woven Teflon Material and for Hachinohe Input (0.35g Peak Acceleration). Compare With Figure 6-28.

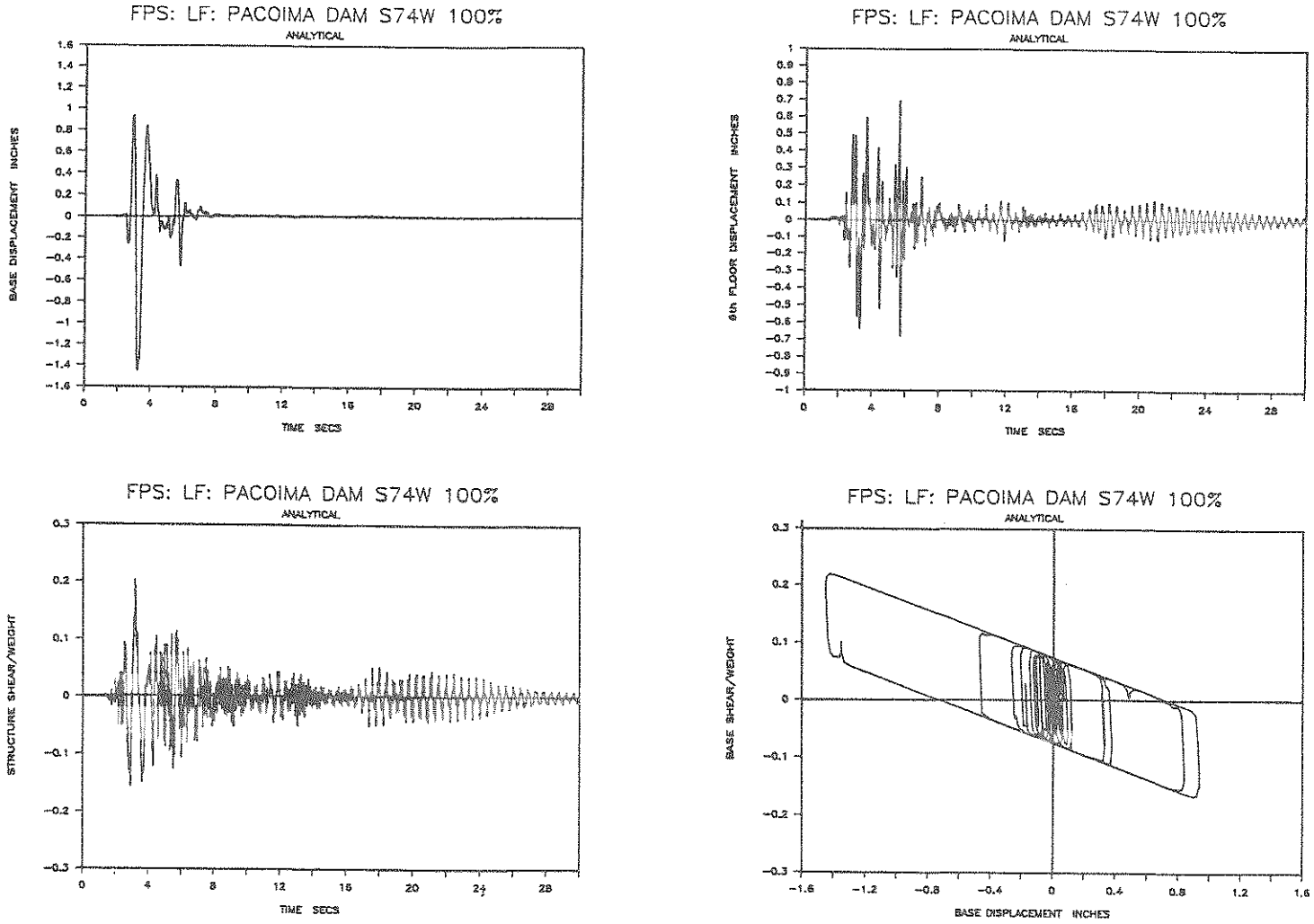

Figure 7-7 Analytical Time Histories of Base (Bearing) Displacement, Structure Shear and Sixth Floor Displacement with Respect to Base and Base Shear-Bearing Displacement Loop in Case of Woven Teflon Material and for Pacoima S74W Input (0.92g Peak Acceleration). Compare With Figure 6-29.

SECTION 8
CONCLUSIONS

Shake table tests have been performed to evaluate the behavior of the Friction Pendulum System installed in a tall flexible structure with large aspect ratio. The results show that:

(1) The isolation system is effective in protecting the structural system from extreme seismic loading conditions with significantly different frequency content. In all tests (some of which had a peak table acceleration of almost 1g) the model remained elastic.

(2) The maximum recorded permanent displacement at the bearings was very small and in particular less than six percent of the bearing design displacement.

(3) No bearing uplift occurred despite the model's large aspect ratio.

(4) High frequency response at the second and third modes of vibration of the six-story model with peak model acceleration larger than the table acceleration was observed. Owing, however, to the higher mode response the floor accelerations point to opposing directions leading to reduced story shear, overturning moment and drift.

(5) In tests with the El Centro motion it was shown that the isolated structure could sustain, while elastic, a peak table acceleration of six to eight times larger than that it could sustain under fixed-base conditions.

(6) The system has quantifiable properties and analysis techniques are available for the reliable prediction of its response.

SECTION 9

REFERENCES

1. Buckle, I. (1986). "Development and Application of Base Isolation and Passive Energy Dissipation: A World Overview." Proceeding of ATC-17 Seminar on Base Isolation and Passive Energy Dissipation, Applied Technology Council, Palo Alto, Calif., 153-174.

2. Clough, R.W. and Penzien, J. (1975). Dynamics of Structures. McGraw-Hill, Inc., New York, N.Y.

3. Constantinou, M.C., Mokha, A. and Reinhorn, A.M. (1990). "Teflon Bearings in Base Isolation II: Modeling," J. Structural Engng, ASCE, 116(2), 455-474.

4. Den Hartog, J.P. (1931). "Forced Vibration with Combined Coulomb and Viscous Friction," Trans. of ASME, 53 APM-53-9, 107-115.

5. Gear, C.W. (1971). "The Automatic Integration of Ordinary Differential Equations," Numerical Mathematics, Communications of ACM, 14(3), 176-190.

6. Griffith, M.C., Aiken, T.D. and Kelly,J.M. (1988). "Experimental Evaluation of Seismic Isolation of a nine-story Braced Steel Frame Subject to Uplift," Report No. UCB/EERC-88/05, Earthquake Engineering Research Center, University of California, Berkeley, Calif., May.

7. Kelly, J.M. (1988). "Base Isolation in Japan, 1988". Report No. UCB/EERC-88/20, Earthquake Engineering Research Center, University of California, Berkeley, Calif., December.

8. Makris N. (1989). "Analysis of Motion of Harmonically Excited Sliding Isolation Systems," thesis presented to the State University of New York, at Buffalo, N.Y., in partial fulfillment of the requirements for the degree of Master of Science.

9. Mokha, A. Constantinou, M.C. and Reinhorn, A.M. (1988). "Teflon Bearings in Aseismic Base Isolation. Experimental Studies and Mathematical Modeling." Report No. NCEER-88-0038, National Center for Earthquake Engineering Research, State University of New York, Buffalo, N.Y.

10. Mokha, A., Constantinou and Reinhorn, A.M. (1990). "Teflon Bearings in Base Isolation I: Testing." J. Structural Engng., ASCE, 116(2), 438-454.

11. Mostaghel, N. and Khodaverdian, M. (1987). "Dynamics of Resilient Friction Base Isolator (R-FBI)." Earthquake Engineering and Structural Dynamics, 15(3), 379-390.

12. Reinhorn, A. M. et al (1989). "1:4 Scale Model Studies of Active Tendons Systems and Active Mass Dampers for Aseismic Protection." Report No. NCEER-890026, National Center for Earthquake Engineering Research, State University of New York, Buffalo, N.Y.

13. Su, L., Ahmadi, G. and Tadjbakhsh, I. (1989). "A Comparative Study of Performance of Various Base Isolation Systems, Part I: Shear Beam Structures." Earthquake Engineering and Structural Dynamics, 18(1), 11-32.

14. Zayas, V., Low, S.S. and Mahin, S.A. (1987). "The FPS Earthquake Resisting System, Experimental Report." Report No. UCB/EERC-87/01, Earthquake Engineering Research Center, University of California, Berkeley, Calif., June.

NATIONAL CENTER FOR EARTHQUAKE ENGINEERING RESEARCH
LIST OF TECHNICAL REPORTS

The National Center for Earthquake Engineering Research (NCEER) publishes technical reports on a variety of subjects related to earthquake engineering written by authors funded through NCEER. These reports are available from both NCEER's Publications Department and the National Technical Information Service (NTIS). Requests for reports should be directed to the Publications Department, National Center for Earthquake Engineering Research, State University of New York at Buffalo, Red Jacket Quadrangle, Buffalo, New York 14261. Reports can also be requested through NTIS, 5285 Port Royal Road, Springfield, Virginia 22161. NTIS accession numbers are shown in parenthesis, if available.

NCEER-87-0001 "First-Year Program in Research, Education and Technology Transfer," 3/5/87, (PB88-134275/AS).

NCEER-87-0002 "Experimental Evaluation of Instantaneous Optimal Algorithms for Structural Control," by R.C. Lin, T.T. Soong and A.M. Reinhorn, 4/20/87, (PB88-134341/AS).

NCEER-87-0003 "Experimentation Using the Earthquake Simulation Facilities at University at Buffalo," by A.M. Reinhorn and R.L. Ketter, to be published.

NCEER-87-0004 "The System Characteristics and Performance of a Shaking Table," by J.S. Hwang, K.C. Chang and G.C. Lee, 6/1/87, (PB88-134259/AS). This report is available only through NTIS (see address given above).

NCEER-87-0005 "A Finite Element Formulation for Nonlinear Viscoplastic Material Using a Q Model," by O. Gyebi and G. Dasgupta, 11/2/87, (PB88-213764/AS).

NCEER-87-0006 "Symbolic Manipulation Program (SMP) - Algebraic Codes for Two and Three Dimensional Finite Element Formulations," by X. Lee and G. Dasgupta, 11/9/87, (PB88-219522/AS).

NCEER-87-0007 "Instantaneous Optimal Control Laws for Tall Buildings Under Seismic Excitations," by J.N. Yang, A. Akbarpour and P. Ghaemmaghami, 6/10/87, (PB88-134333/AS).

NCEER-87-0008 "IDARC: Inelastic Damage Analysis of Reinforced Concrete Frame - Shear-Wall Structures," by Y.J. Park, A.M. Reinhorn and S.K. Kunnath, 7/20/87, (PB88-134325/AS).

NCEER-87-0009 "Liquefaction Potential for New York State: A Preliminary Report on Sites in Manhattan and Buffalo," by M. Budhu, V. Vijayakumar, R.F. Giese and L. Baumgras, 8/31/87, (PB88-163704/AS). This report is available only through NTIS (see address given above).

NCEER-87-0010 "Vertical and Torsional Vibration of Foundations in Inhomogeneous Media," by A.S. Veletsos and K.W. Dotson, 6/1/87, (PB88-134291/AS).

NCEER-87-0011 "Seismic Probabilistic Risk Assessment and Seismic Margins Studies for Nuclear Power Plants," by Howard H.M. Hwang, 6/15/87, (PB88-134267/AS).

NCEER-87-0012 "Parametric Studies of Frequency Response of Secondary Systems Under Ground-Acceleration Excitations," by Y. Yong and Y.K. Lin, 6/10/87, (PB88-134309/AS).

NCEER-87-0013 "Frequency Response of Secondary Systems Under Seismic Excitation," by J.A. HoLung, J. Cai and Y.K. Lin, 7/31/87, (PB88-134317/AS).

NCEER-87-0014 "Modelling Earthquake Ground Motions in Seismically Active Regions Using Parametric Time Series Methods," by G.W. Ellis and A.S. Cakmak, 8/25/87, (PB88-134283/AS).

NCEER-87-0015 "Detection and Assessment of Seismic Structural Damage," by E. DiPasquale and A.S. Cakmak, 8/25/87, (PB88-163712/AS).

NCEER-87-0016 "Pipeline Experiment at Parkfield, California," by J. Isenberg and E. Richardson, 9/15/87, (PB88-163720/AS). This report is available only through NTIS (see address given above).

NCEER-87-0017 "Digital Simulation of Seismic Ground Motion," by M. Shinozuka, G. Deodatis and T. Harada, 8/31/87, (PB88-155197/AS). This report is available only through NTIS (see address given above).

NCEER-87-0018 "Practical Considerations for Structural Control: System Uncertainty, System Time Delay and Truncation of Small Control Forces," J.N. Yang and A. Akbarpour, 8/10/87, (PB88-163738/AS).

NCEER-87-0019 "Modal Analysis of Nonclassically Damped Structural Systems Using Canonical Transformation," by J.N. Yang, S. Sarkani and F.X. Long, 9/27/87, (PB88-187851/AS).

NCEER-87-0020 "A Nonstationary Solution in Random Vibration Theory," by J.R. Red-Horse and P.D. Spanos, 11/3/87, (PB88-163746/AS).

NCEER-87-0021 "Horizontal Impedances for Radially Inhomogeneous Viscoelastic Soil Layers," by A.S. Veletsos and K.W. Dotson, 10/15/87, (PB88-150859/AS).

NCEER-87-0022 "Seismic Damage Assessment of Reinforced Concrete Members," by Y.S. Chung, C. Meyer and M. Shinozuka, 10/9/87, (PB88-150867/AS). This report is available only through NTIS (see address given above).

NCEER-87-0023 "Active Structural Control in Civil Engineering," by T.T. Soong, 11/11/87, (PB88-187778/AS).

NCEER-87-0024 Vertical and Torsional Impedances for Radially Inhomogeneous Viscoelastic Soil Layers," by K.W. Dotson and A.S. Veletsos, 12/87, (PB88-187786/AS).

NCEER-87-0025 "Proceedings from the Symposium on Seismic Hazards, Ground Motions, Soil-Liquefaction and Engineering Practice in Eastern North America," October 20-22, 1987, edited by K.H. Jacob, 12/87, (PB88-188115/AS).

NCEER-87-0026 "Report on the Whittier-Narrows, California, Earthquake of October 1, 1987," by J. Pantelic and A. Reinhorn, 11/87, (PB88-187752/AS). This report is available only through NTIS (see address given above).

NCEER-87-0027 "Design of a Modular Program for Transient Nonlinear Analysis of Large 3-D Building Structures," by S. Srivastav and J.F. Abel, 12/30/87, (PB88-187950/AS).

NCEER-87-0028 "Second-Year Program in Research, Education and Technology Transfer," 3/8/88, (PB88-219480/AS).

NCEER-88-0001 "Workshop on Seismic Computer Analysis and Design of Buildings With Interactive Graphics," by W. McGuire, J.F. Abel and C.H. Conley, 1/18/88, (PB88-187760/AS).

NCEER-88-0002 "Optimal Control of Nonlinear Flexible Structures," by J.N. Yang, F.X. Long and D. Wong, 1/22/88, (PB88-213772/AS).

NCEER-88-0003 "Substructuring Techniques in the Time Domain for Primary-Secondary Structural Systems," by G.D. Manolis and G. Juhn, 2/10/88, (PB88-213780/AS).

NCEER-88-0004 "Iterative Seismic Analysis of Primary-Secondary Systems," by A. Singhal, L.D. Lutes and P.D. Spanos, 2/23/88, (PB88-213798/AS).

NCEER-88-0005 "Stochastic Finite Element Expansion for Random Media," by P.D. Spanos and R. Ghanem, 3/14/88, (PB88-213806/AS).

NCEER-88-0006 "Combining Structural Optimization and Structural Control," by F.Y. Cheng and C.P. Pantelides, 1/10/88, (PB88-213814/AS).

NCEER-88-0007 "Seismic Performance Assessment of Code-Designed Structures," by H.H-M. Hwang, J-W. Jaw and H-J. Shau, 3/20/88, (PB88-219423/AS).

NCEER-88-0008 "Reliability Analysis of Code-Designed Structures Under Natural Hazards," by H.H-M. Hwang, H. Ushiba and M. Shinozuka, 2/29/88, (PB88-229471/AS).

NCEER-88-0009 "Seismic Fragility Analysis of Shear Wall Structures," by J-W Jaw and H.H-M. Hwang, 4/30/88, (PB89-102867/AS).

NCEER-88-0010 "Base Isolation of a Multi-Story Building Under a Harmonic Ground Motion - A Comparison of Performances of Various Systems," by F-G Fan, G. Ahmadi and I.G. Tadjbakhsh, 5/18/88, (PB89-122238/AS).

NCEER-88-0011 "Seismic Floor Response Spectra for a Combined System by Green's Functions," by F.M. Lavelle, L.A. Bergman and P.D. Spanos, 5/1/88, (PB89-102875/AS).

NCEER-88-0012 "A New Solution Technique for Randomly Excited Hysteretic Structures," by G.Q. Cai and Y.K. Lin, 5/16/88, (PB89-102883/AS).

NCEER-88-0013 "A Study of Radiation Damping and Soil-Structure Interaction Effects in the Centrifuge," by K. Weissman, supervised by J.H. Prevost, 5/24/88, (PB89-144703/AS).

NCEER-88-0014 "Parameter Identification and Implementation of a Kinematic Plasticity Model for Frictional Soils," by J.H. Prevost and D.V. Griffiths, to be published.

NCEER-88-0015 "Two- and Three- Dimensional Dynamic Finite Element Analyses of the Long Valley Dam," by D.V. Griffiths and J.H. Prevost, 6/17/88, (PB89-144711/AS).

NCEER-88-0016 "Damage Assessment of Reinforced Concrete Structures in Eastern United States," by A.M. Reinhorn, M.J. Seidel, S.K. Kunnath and Y.J. Park, 6/15/88, (PB89-122220/AS).

NCEER-88-0017 "Dynamic Compliance of Vertically Loaded Strip Foundations in Multilayered Viscoelastic Soils," by S. Ahmad and A.S.M. Israil, 6/17/88, (PB89-102891/AS).

NCEER-88-0018 "An Experimental Study of Seismic Structural Response With Added Viscoelastic Dampers," by R.C. Lin, Z. Liang, T.T. Soong and R.H. Zhang, 6/30/88, (PB89-122212/AS).

NCEER-88-0019 "Experimental Investigation of Primary - Secondary System Interaction," by G.D. Manolis, G. Juhn and A.M. Reinhorn, 5/27/88, (PB89-122204/AS).

NCEER-88-0020 "A Response Spectrum Approach For Analysis of Nonclassically Damped Structures," by J.N. Yang, S. Sarkani and F.X. Long, 4/22/88, (PB89-102909/AS).

NCEER-88-0021 "Seismic Interaction of Structures and Soils: Stochastic Approach," by A.S. Veletsos and A.M. Prasad, 7/21/88, (PB89-122196/AS).

NCEER-88-0022 "Identification of the Serviceability Limit State and Detection of Seismic Structural Damage," by E. DiPasquale and A.S. Cakmak, 6/15/88, (PB89-122188/AS).

NCEER-88-0023 "Multi-Hazard Risk Analysis: Case of a Simple Offshore Structure," by B.K. Bhartia and E.H. Vanmarcke, 7/21/88, (PB89-145213/AS).

NCEER-88-0024 "Automated Seismic Design of Reinforced Concrete Buildings," by Y.S. Chung, C. Meyer and M. Shinozuka, 7/5/88, (PB89-122170/AS).

NCEER-88-0025 "Experimental Study of Active Control of MDOF Structures Under Seismic Excitations," by L.L. Chung, R.C. Lin, T.T. Soong and A.M. Reinhorn, 7/10/88, (PB89-122600/AS).

NCEER-88-0026 "Earthquake Simulation Tests of a Low-Rise Metal Structure," by J.S. Hwang, K.C. Chang, G.C. Lee and R.L. Ketter, 8/1/88, (PB89-102917/AS).

NCEER-88-0027 "Systems Study of Urban Response and Reconstruction Due to Catastrophic Earthquakes," by F. Kozin and H.K. Zhou, 9/22/88, (PB90-162348/AS).

NCEER-88-0028 "Seismic Fragility Analysis of Plane Frame Structures," by H.H-M. Hwang and Y.K. Low, 7/31/88, (PB89-131445/AS).

NCEER-88-0029 "Response Analysis of Stochastic Structures," by A. Kardara, C. Bucher and M. Shinozuka, 9/22/88, (PB89-174429/AS).

NCEER-88-0030 "Nonnormal Accelerations Due to Yielding in a Primary Structure," by D.C.K. Chen and L.D. Lutes, 9/19/88, (PB89-131437/AS).

NCEER-88-0031 "Design Approaches for Soil-Structure Interaction," by A.S. Veletsos, A.M. Prasad and Y. Tang, 12/30/88, (PB89-174437/AS).

NCEER-88-0032 "A Re-evaluation of Design Spectra for Seismic Damage Control," by C.J. Turkstra and A.G. Tallin, 11/7/88, (PB89-145221/AS).

NCEER-88-0033 "The Behavior and Design of Noncontact Lap Splices Subjected to Repeated Inelastic Tensile Loading," by V.E. Sagan, P. Gergely and R.N. White, 12/8/88, (PB89-163737/AS).

NCEER-88-0034 "Seismic Response of Pile Foundations," by S.M. Mamoon, P.K. Banerjee and S. Ahmad, 11/1/88, (PB89-145239/AS).

NCEER-88-0035 "Modeling of R/C Building Structures With Flexible Floor Diaphragms (IDARC2)," by A.M. Reinhorn, S.K. Kunnath and N. Panahshahi, 9/7/88, (PB89-207153/AS).

NCEER-88-0036 "Solution of the Dam-Reservoir Interaction Problem Using a Combination of FEM, BEM with Particular Integrals, Modal Analysis, and Substructuring," by C-S. Tsai, G.C. Lee and R.L. Ketter, 12/31/88, (PB89-207146/AS).

NCEER-88-0037 "Optimal Placement of Actuators for Structural Control," by F.Y. Cheng and C.P. Pantelides, 8/15/88, (PB89-162846/AS).

NCEER-88-0038 "Teflon Bearings in Aseismic Base Isolation: Experimental Studies and Mathematical Modeling," by A. Mokha, M.C. Constantinou and A.M. Reinhorn, 12/5/88, (PB89-218457/AS).

NCEER-88-0039 "Seismic Behavior of Flat Slab High-Rise Buildings in the New York City Area," by P. Weidlinger and M. Ettouney, 10/15/88, (PB90-145681/AS).

NCEER-88-0040 "Evaluation of the Earthquake Resistance of Existing Buildings in New York City," by P. Weidlinger and M. Ettouney, 10/15/88, to be published.

NCEER-88-0041 "Small-Scale Modeling Techniques for Reinforced Concrete Structures Subjected to Seismic Loads," by W. Kim, A. El-Attar and R.N. White, 11/22/88, (PB89-189625/AS).

NCEER-88-0042 "Modeling Strong Ground Motion from Multiple Event Earthquakes," by G.W. Ellis and A.S. Cakmak, 10/15/88, (PB89-174445/AS).

NCEER-88-0043 "Nonstationary Models of Seismic Ground Acceleration," by M. Grigoriu, S.E. Ruiz and E. Rosenblueth, 7/15/88, (PB89-189617/AS).

NCEER-88-0044 "SARCF User's Guide: Seismic Analysis of Reinforced Concrete Frames," by Y.S. Chung, C. Meyer and M. Shinozuka, 11/9/88, (PB89-174452/AS).

NCEER-88-0045 "First Expert Panel Meeting on Disaster Research and Planning," edited by J. Pantelic and J. Stoyle, 9/15/88, (PB89-174460/AS).

NCEER-88-0046 "Preliminary Studies of the Effect of Degrading Infill Walls on the Nonlinear Seismic Response of Steel Frames," by C.Z. Chrysostomou, P. Gergely and J.F. Abel, 12/19/88, (PB89-208383/AS).

NCEER-88-0047 "Reinforced Concrete Frame Component Testing Facility - Design, Construction, Instrumentation and Operation," by S.P. Pessiki, C. Conley, T. Bond, P. Gergely and R.N. White, 12/16/88, (PB89-174478/AS).

NCEER-89-0001 "Effects of Protective Cushion and Soil Compliancy on the Response of Equipment Within a Seismically Excited Building," by J.A. HoLung, 2/16/89, (PB89-207179/AS).

NCEER-89-0002 "Statistical Evaluation of Response Modification Factors for Reinforced Concrete Structures," by H.H-M. Hwang and J-W. Jaw, 2/17/89, (PB89-207187/AS).

NCEER-89-0003 "Hysteretic Columns Under Random Excitation," by G-Q. Cai and Y.K. Lin, 1/9/89, (PB89-196513/AS).

NCEER-89-0004 "Experimental Study of 'Elephant Foot Bulge' Instability of Thin-Walled Metal Tanks," by Z-H. Jia and R.L. Ketter, 2/22/89, (PB89-207195/AS).

NCEER-89-0005 "Experiment on Performance of Buried Pipelines Across San Andreas Fault," by J. Isenberg, E. Richardson and T.D. O'Rourke, 3/10/89, (PB89-218440/AS).

NCEER-89-0006 "A Knowledge-Based Approach to Structural Design of Earthquake-Resistant Buildings," by M. Subramani, P. Gergely, C.H. Conley, J.F. Abel and A.H. Zaghw, 1/15/89, (PB89-218465/AS).

NCEER-89-0007 "Liquefaction Hazards and Their Effects on Buried Pipelines," by T.D. O'Rourke and P.A. Lane, 2/1/89, (PB89-218481).

NCEER-89-0008 "Fundamentals of System Identification in Structural Dynamics," by H. Imai, C-B. Yun, O. Maruyama and M. Shinozuka, 1/26/89, (PB89-207211/AS).

NCEER-89-0009 "Effects of the 1985 Michoacan Earthquake on Water Systems and Other Buried Lifelines in Mexico," by A.G. Ayala and M.J. O'Rourke, 3/8/89, (PB89-207229/AS).

NCEER-89-R010 "NCEER Bibliography of Earthquake Education Materials," by K.E.K. Ross, Second Revision, 9/1/89, (PB90-125352/AS).

NCEER-89-0011 "Inelastic Three-Dimensional Response Analysis of Reinforced Concrete Building Structures (IDARC-3D), Part I - Modeling," by S.K. Kunnath and A.M. Reinhorn, 4/17/89, (PB90-114612/AS).

NCEER-89-0012 "Recommended Modifications to ATC-14," by C.D. Poland and J.O. Malley, 4/12/89, (PB90-108648/AS).

NCEER-89-0013 "Repair and Strengthening of Beam-to-Column Connections Subjected to Earthquake Loading," by M. Corazao and A.J. Durrani, 2/28/89, (PB90-109885/AS).

NCEER-89-0014 "Program EXKAL2 for Identification of Structural Dynamic Systems," by O. Maruyama, C-B. Yun, M. Hoshiya and M. Shinozuka, 5/19/89, (PB90-109877/AS).

NCEER-89-0015 "Response of Frames With Bolted Semi-Rigid Connections, Part I - Experimental Study and Analytical Predictions," by P.J. DiCorso, A.M. Reinhorn, J.R. Dickerson, J.B. Radziminski and W.L. Harper, 6/1/89, to be published.

NCEER-89-0016 "ARMA Monte Carlo Simulation in Probabilistic Structural Analysis," by P.D. Spanos and M.P. Mignolet, 7/10/89, (PB90-109893/AS).

NCEER-89-P017 "Preliminary Proceedings from the Conference on Disaster Preparedness - The Place of Earthquake Education in Our Schools," Edited by K.E.K. Ross, 6/23/89.

NCEER-89-0017 "Proceedings from the Conference on Disaster Preparedness - The Place of Earthquake Education in Our Schools," Edited by K.E.K. Ross, 12/31/89, (PB90-207895).

NCEER-89-0018 "Multidimensional Models of Hysteretic Material Behavior for Vibration Analysis of Shape Memory Energy Absorbing Devices, by E.J. Graesser and F.A. Cozzarelli, 6/7/89, (PB90-164146/AS).

NCEER-89-0019 "Nonlinear Dynamic Analysis of Three-Dimensional Base Isolated Structures (3D-BASIS)," by S. Nagarajaiah, A.M. Reinhorn and M.C. Constantinou, 8/3/89, (PB90-161936/AS).

NCEER-89-0020 "Structural Control Considering Time-Rate of Control Forces and Control Rate Constraints," by F.Y. Cheng and C.P. Pantelides, 8/3/89, (PB90-120445/AS).

NCEER-89-0021 "Subsurface Conditions of Memphis and Shelby County," by K.W. Ng, T-S. Chang and H-H.M. Hwang, 7/26/89, (PB90-120437/AS).

NCEER-89-0022 "Seismic Wave Propagation Effects on Straight Jointed Buried Pipelines," by K. Elhmadi and M.J. O'Rourke, 8/24/89, (PB90-162322/AS).

NCEER-89-0023 "Workshop on Serviceability Analysis of Water Delivery Systems," edited by M. Grigoriu, 3/6/89, (PB90-127424/AS).

NCEER-89-0024 "Shaking Table Study of a 1/5 Scale Steel Frame Composed of Tapered Members," by K.C. Chang, J.S. Hwang and G.C. Lee, 9/18/89, (PB90-160169/AS).

NCEER-89-0025 "DYNA1D: A Computer Program for Nonlinear Seismic Site Response Analysis - Technical Documentation," by Jean H. Prevost, 9/14/89, (PB90-161944/AS).

NCEER-89-0026 "1:4 Scale Model Studies of Active Tendon Systems and Active Mass Dampers for Aseismic Protection," by A.M. Reinhorn, T.T. Soong, R.C. Lin, Y.P. Yang, Y. Fukao, H. Abe and M. Nakai, 9/15/89, (PB90-173246/AS).

NCEER-89-0027 "Scattering of Waves by Inclusions in a Nonhomogeneous Elastic Half Space Solved by Boundary Element Methods," by P.K. Hadley, A. Askar and A.S. Cakmak, 6/15/89, (PB90-145699/AS).

NCEER-89-0028 "Statistical Evaluation of Deflection Amplification Factors for Reinforced Concrete Structures," by H.H.M. Hwang, J-W. Jaw and A.L. Ch'ng, 8/31/89, (PB90-164633/AS).

NCEER-89-0029 "Bedrock Accelerations in Memphis Area Due to Large New Madrid Earthquakes," by H.H.M. Hwang, C.H.S. Chen and G. Yu, 11/7/89, (PB90-162330/AS).

NCEER-89-0030 "Seismic Behavior and Response Sensitivity of Secondary Structural Systems," by Y.Q. Chen and T.T. Soong, 10/23/89, (PB90-164658/AS).

NCEER-89-0031 "Random Vibration and Reliability Analysis of Primary-Secondary Structural Systems," by Y. Ibrahim, M. Grigoriu and T.T. Soong, 11/10/89, (PB90-161951/AS).

NCEER-89-0032 "Proceedings from the Second U.S. - Japan Workshop on Liquefaction, Large Ground Deformation and Their Effects on Lifelines, September 26-29, 1989," Edited by T.D. O'Rourke and M. Hamada, 12/1/89, (PB90-209388/AS).

NCEER-89-0033 "Deterministic Model for Seismic Damage Evaluation of Reinforced Concrete Structures," by J.M. Bracci, A.M. Reinhorn, J.B. Mander and S.K. Kunnath, 9/27/89.

NCEER-89-0034 "On the Relation Between Local and Global Damage Indices," by E. DiPasquale and A.S. Cakmak, 8/15/89, (PB90-173865).

NCEER-89-0035 "Cyclic Undrained Behavior of Nonplastic and Low Plasticity Silts," by A.J. Walker and H.E. Stewart, 7/26/89, (PB90-183518/AS).

NCEER-89-0036 "Liquefaction Potential of Surficial Deposits in the City of Buffalo, New York," by M. Budhu, R. Giese and L. Baumgrass, 1/17/89, (PB90-208455/AS).

NCEER-89-0037 "A Determinstic Assessment of Effects of Ground Motion Incoherence," by A.S. Veletsos and Y. Tang, 7/15/89, (PB90-164294/AS).

NCEER-89-0038 "Workshop on Ground Motion Parameters for Seismic Hazard Mapping," July 17-18, 1989, edited by R.V. Whitman, 12/1/89, (PB90-173923/AS).

NCEER-89-0039 "Seismic Effects on Elevated Transit Lines of the New York City Transit Authority," by C.J. Costantino, C.A. Miller and E. Heymsfield, 12/26/89, (PB90-207887/AS).

NCEER-89-0040 "Centrifugal Modeling of Dynamic Soil-Structure Interaction," by K. Weissman, Supervised by J.H. Prevost, 5/10/89, (PB90-207879/AS).

NCEER-89-0041 "Linearized Identification of Buildings With Cores for Seismic Vulnerability Assessment," by I-K. Ho and A.E. Aktan, 11/1/89.

NCEER-90-0001 "Geotechnical and Lifeline Aspects of the October 17, 1989 Loma Prieta Earthquake in San Francisco," by T.D. O'Rourke, H.E. Stewart, F.T. Blackburn and T.S. Dickerman, 1/90, (PB90-208596/AS).

NCEER-90-0002 "Nonnormal Secondary Response Due to Yielding in a Primary Structure," by D.C.K. Chen and L.D. Lutes, 2/28/90.

NCEER-90-0003 "Earthquake Education Materials for Grades K-12," by K.E.K. Ross, 4/16/90.

NCEER-90-0004 "Catalog of Strong Motion Stations in Eastern North America," by R.W. Busby, 4/3/90.

NCEER-90-0005 "NCEER Strong-Motion Data Base: A User Manuel for the GeoBase Release (Version 1.0 for the Sun3)," by P. Friberg and K. Jacob, 3/31/90.

NCEER-90-0006 "Seismic Hazard Along a Crude Oil Pipeline in the Event of an 1811-1812 Type New Madrid Earthquake," by H.H.M. Hwang and C-H.S. Chen, 4/16/90.

NCEER-90-0007 "Site-Specific Response Spectra for Memphis Sheahan Pumping Station," by H.H.M. Hwang and C.S. Lee, 5/15/90.

NCEER-90-0008 "Pilot Study on Seismic Vulnerability of Crude Oil Transmission Systems," by T. Ariman, R. Dobry, M. Grigoriu, F. Kozin, M. O'Rourke, T. O'Rourke and M. Shinozuka, 5/25/90.

NCEER-90-0009 "A Program to Generate Site Dependent Time Histories: EQGEN," by G.W. Ellis, M. Srinivasan and A.S. Cakmak, 1/30/90.

NCEER-90-0010 "Active Isolation for Seismic Protection of Operating Rooms," by M.E. Talbott, Supervised by M. Shinozuka, 6/8/9.

NCEER-90-0011 "Program LINEARID for Identification of Linear Structural Dynamic Systems," by C-B. Yun and M. Shinozuka, 6/25/90.

NCEER-90-0012 "Two-Dimensional Two-Phase Elasto-Plastic Seismic Response of Earth Dams," by A.N. Yiagos, Supervised by J.H. Prevost, 6/20/90.

NCEER-90-0013 "Secondary Systems in Base-Isolated Structures: Experimental Investigation, Stochastic Response and Stochastic Sensitivity," by G.D. Manolis, G. Juhn, M.C. Constantinou and A.M. Reinhorn, 7/1/90.

NCEER-90-0014 "Seismic Behavior of Lightly-Reinforced Concrete Column and Beam-Column Joint Details," by S.P. Pessiki, C.H. Conley, P. Gergely and R.N. White, 8/22/90.

NCEER-90-0015 "Two Hybrid Control Systems for Building Structures Under Strong Earthquakes," by J.N. Yang and A. Danielians, 6/29/90.

NCEER-90-0016 "Instantaneous Optimal Control with Acceleration and Velocity Feedback," by J.N. Yang and Z. Li, 6/29/90.

NCEER-90-0017 "Reconnaissance Report on the Northern Iran Earthquake of June 21, 1990," by M. Mehrain, 10/4/90.

NCEER-90-0018 "Evaluation of Liquefaction Potential in Memphis and Shelby County," by T.S. Chang, P.S. Tang, C.S. Lee and H. Hwang, 8/10/90.

NCEER-90-0019 "Experimental and Analytical Study of a Combined Sliding Disc Bearing and Helical Steel Spring Isolation System," by M.C. Constantinou, A.S. Mokha and A.M. Reinhorn, 10/4/90.

NCEER-90-0020 "Experimental Study and Analytical Prediction of Earthquake Response of a Sliding Isolation System with a Spherical Surface," by A.S. Mokha, M.C. Constantinou and A.M. Reinhorn, 10/11/90.